NASA Technical Memorandum 4429

Pressure Distribution for the Wing of the YAV-8B Airplane; With and Without Pylons

(NASA-TM-4429) PRESSURE DISTRIBUTION FOR THE WING OF THE YAV-8B AIRPLANE; WITH AND WITHOUT PYLONS (NASA) 139 p

N93-14451

Unclas

H1/02 0133994

Edwin J. Saltzman
PRC Inc.
Edwards, California

John H. Del Frate, Catherine M. Sabsay, and Jill M. Yarger
Dryden Flight Research Facility
Edwards, California

National Aeronautics and Space Administration

Office of Management

Scientific and Technical Information Program

1992

CONTENTS

PRECEDING PAGE BLANK NOT FILMED

ii INTENTIONALLY BLANK

LIST OF FIGURES

ABSTRACT

Pressure distribution data have been obtained in flight at four span stations on the wing panel of the YAV-8B airplane. Data obtained for the supercritical profiled wing, with and without pylons installed, ranged from Mach 0.46 to 0.88. The altitude ranged from approximately 20,000 to 40,000 ft and the resultant Reynolds numbers varied from approximately 7.2 million to 28.7 million based on the mean aerodynamic chord.

Pressure distribution data and flow visualization results show that the full-scale flight wing performance is compromised because the lower surface cusp region experiences flow separation for some important transonic flight conditions. This condition is aggravated when local shocks occur on the lower surface of the wing (mostly between 20- and 35-percent chord) when the pylons are installed for Mach 0.8 and above. There is evidence that convex fairings, which cover the pylon attachment flanges, cause these local shocks. Pressure coefficients significantly more negative than those for sonic flow also occur farther aft on the lower surface (near 60-percent chord) whether or not the pylons are installed for Mach numbers ≥ 0.8. These negative pressure coefficient peaks and associated local shocks would be expected to cause increasing wave and separation drag as transonic Mach number increases.

NOMENCLATURE

A	wing aspect ratio, $\frac{b^2}{S}$
a/c	aircraft
b	total wing span, ft or in.
C_D	drag coefficient, $\frac{D}{\bar{q} \cdot S}$
C_L	lift coefficient, $\frac{L}{\bar{q} \cdot S}$
C_{L_α}	slope of lift coefficient with respect to α, $\frac{dC_L}{d\alpha}$, $\deg^{-1}$
C_N	wing panel normal force coefficient, $\int_{0.185}^{1.0} c_n \frac{c}{c_{av}} d_\eta$, normal to wing panel
$C_{N'}$	wing panel normal force coefficient, $\cos\varepsilon \int_{0.185}^{1.0} c_n \frac{c}{c_{av}} d_\eta$, normal with respect to aircraft reference axis system, (accounts for negative dihedral)
C_{N_α}	slope of panel normal force coefficient with respect to α, $\frac{dC_N}{d\alpha}$, $\deg^{-1}$
C_p(CP)	local pressure coefficient, $\frac{(p-p_\infty)}{\bar{q}}$
C_p^*	critical pressure coefficient for sonic velocity
c (C)	local wing chord, in.
$\bar{c}$	mean aerodynamic chord, in., $\frac{2}{S}\int_0^{\frac{b}{2}} c^2 dy$
c_{av}	average chord of wing panel, in.
c_m	section pitching moment coefficient about 0.25 c, $\int_0^1 \Delta C_p (0.25-\frac{x}{c})\, d\frac{x}{c}$
c_n	section normal force coefficient, $\int_0^1 \Delta C_p\, d\frac{x}{c}$
D	drag, lb
F	plan form parameter, $A[\frac{\sqrt{1-(M\cos\Lambda')^2}}{0.9\ \cos\Lambda'}]$

hp(HP)	pressure altitude, ft
L	lift, lb
LERX	leading-edge root extension
$\frac{L}{D}$max	maximum lift-drag ratio
M(MINF)	free-stream Mach number
N	panel normal force coefficient slope parameter, $10\ C_{N_\alpha} [\frac{\sqrt{1-(M\cos\Lambda')^2}}{\cos\Lambda'}]$
p	local absolute static pressure $p_l + p_r$, lb/ft^2
p_l	local differential static pressure, lb/ft^2
p_r	reference pressure, lb/ft^2
p_∞(PSINF)	ambient static pressure, lb/ft^2
$\bar{q}$(QBAR)	free-stream dynamic pressure, $0.7M^2 \cdot p_\infty$, lb/ft^2
S	wing reference area, ft^2
THEO	theoretical
T.P.	test point
t	local airfoil thickness, in.
V/STOL	vertical short takeoff and landing
x(X)	distance along chord from leading edge, in.
y	distance outboard from aircraft centerline, in.
z'	distance above and below wing chord line normal to the wing panel, in.
α(ALPHA)	angle of attack, deg
ΔC_p	Cp lower - Cp upper, at same value of $\frac{x}{c}$
$\Delta t/c$	ratio of increase in section thickness (from addition of strip tubing) to the section cord
ε	negative dihedral angle, per panel, deg
η	semi-span fraction, $y/\frac{b}{2}$
Λ	leading-edge sweep angle, deg
$\Lambda\frac{c}{4}$	sweep angle of quarter chord, deg
Λ'	effective angle of sweep, deg (as defined in ref. 14), $\Lambda\frac{c}{4} - \frac{25}{A}$
λ	taper ratio

INTRODUCTION

Development of a prototype vertical short takeoff and landing (V/STOL) tactical fighter known as the Hawker Siddeley Kestrel (designated the P.1127), was begun in the United Kingdom in 1957. From this beginning evolved the Harrier, whose mission was close support and armed reconnaissance (approximately 1966, (ref. 1)). In 1971, the first Harriers, with modifications to suit customers' specifications, were delivered to the United States Marine Corps (USMC) under the designation AV-8A.

During the mid-1970's, the USMC issued requirements for an advanced version of the Harrier, the AV-8B, which was intended to have a significantly increased range–payload radius. The increased performance was to be obtained through structural, propulsion, and aerodynamic improvements. The aerodynamics improvements have several sources, but the primary elements of aerodynamics improvement were to be the inclusion of an advanced supercritical airfoil and a planform of greater area and span.

Before the AV-8B was in production, McDonnell-Douglas (St. Louis, MO) and the USMC modified two AV-8A aircraft (designated as YAV-8B) to serve as prototype configurations for the follow-on AV-8B aircraft (ref. 2). One of the YAV-8B aircraft was loaned to the National Aeronautics and Space Administration (NASA) for special in-flight evaluation.

Early flight experience with the YAV-8B revealed inadequate level flight acceleration. From the standpoint of aerodynamics, the YAV-8B wing was designed without regard for pylons. However, the aircraft was to be flown operationally with six underwing pylons, and there was concern that these items might preclude efficient lower surface flow. In addition, when the aircraft was loaned to NASA it was considered appropriate to define the range of flight conditions (Mach number (M) and angle of attack (α)) that would provide efficient supercritical chordwise pressure profiles over the wing upper surface. Consequently, NASA performed an in-flight wing pressure distribution and flow visualization evaluation with and without the underwing pylons. Taken together, the pressure data and flow visualization results were expected to define the performance of the wing, show the effects of the pylons, and reveal any regions of poor flow conditions over the wing surface.

The NASA Ames Research Center in Moffett Field, CA, completed these flight tests during the spring and summer of 1986, with analysis done by the NASA Dryden Flight Research Facility at Edwards, CA. The data are shown mainly as wing surface pressure coefficients (plotted as a function of local chord station), section normal force coefficients, and panel normal force coefficient. Data were obtained from four rows of wing surface orifices aligned parallel to the aircraft centerline at discrete span stations. Mach numbers ranged from approximately 0.46 to 0.88, and altitude varied from 20,000 to 40,000 ft. This provided Reynolds numbers between 7.2×10^6 and 28.7×10^6 based on the wing mean aerodynamic chord.

AIRCRAFT

General Physical Features

The YAV-8B is a single-seat, transonic light attack V/STOL aircraft powered by a single turbofan engine (fig. 1). The YAV-8B aircraft is a derivative of the AV-8A aircraft. It retains the characteristic appearance of the AV-8A while incorporating an improved inlet design, a larger wing with an advanced technology airfoil (the design was considered advanced during the mid-1970's), and other modifications (ref. 2). With this airfoil, the "design" Mach number was 0.85 and the Mach number for cruise was 0.815 (ref. 3).

ORIGINAL PAGE
BLACK AND WHITE PHOTOGRAPH

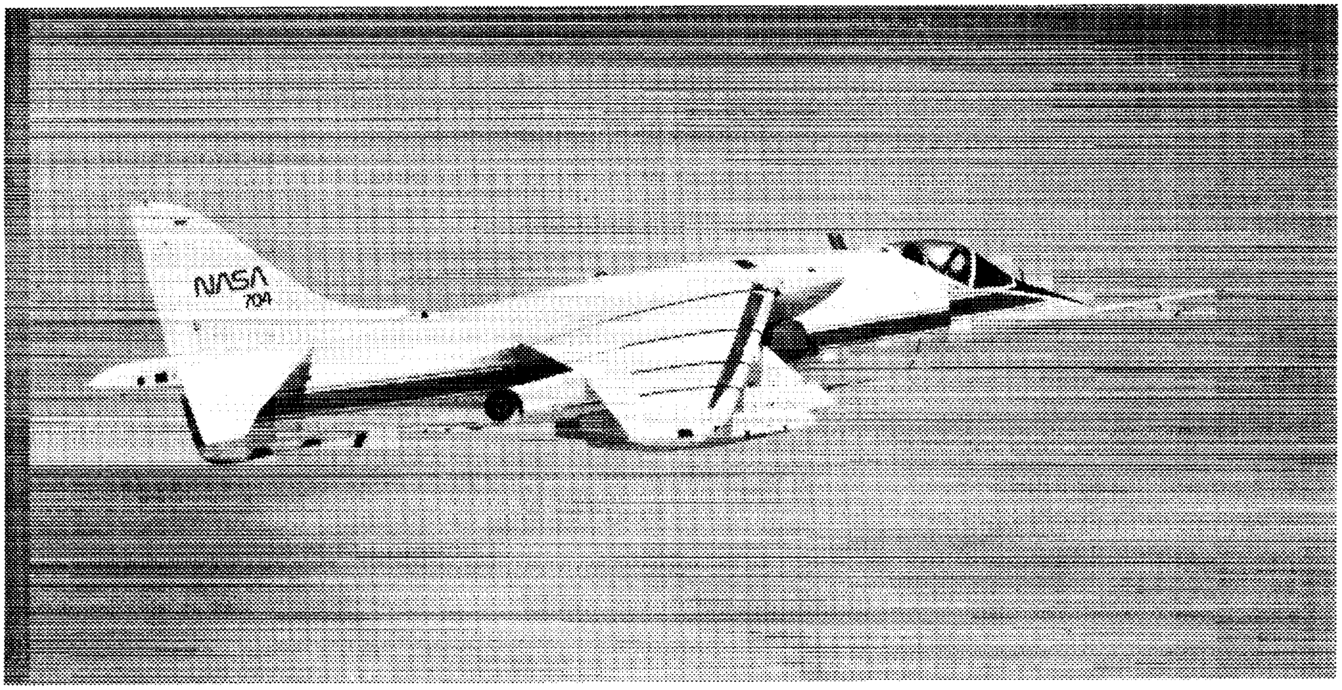

Figure 1. YAV-8B in wingborne flight; four chordwise rows of external (pressure orifice) tubing shown on right wing.

The YAV-8B has provisions for external store installations on six wing pylons. In addition, two gun pods can be attached to the fuselage. Figure 2(a) is a three-view of the YAV-8B. Figure 2(b) shows two of the four rotatable exhaust nozzles. Although these nozzles were rotated to exhaust to the rear for the wingborne flights in this report, they can rotate downward through 98° for V/STOL operations and transitional flight. The YAV-8B was flight tested using a removable leading-edge root extension (LERX) designed to increase the wingborne maneuverability. A version of the LERX was installed on the YAV-8B aircraft for the flights reported in this report, figures 1, 2(c), and other subsequent photographs.

Conventional aerodynamic controls are used in wingborne flight and engine bleed-air reaction controls are used in jetborne flight, with both systems operative during transition modes. A comprehensive listing of physical characteristics of the airplane and other details about the propulsion system, controls system, and the V/STOL phases of flight are found in references 4 and 5. A brief listing of physical dimensions is given in table 1.

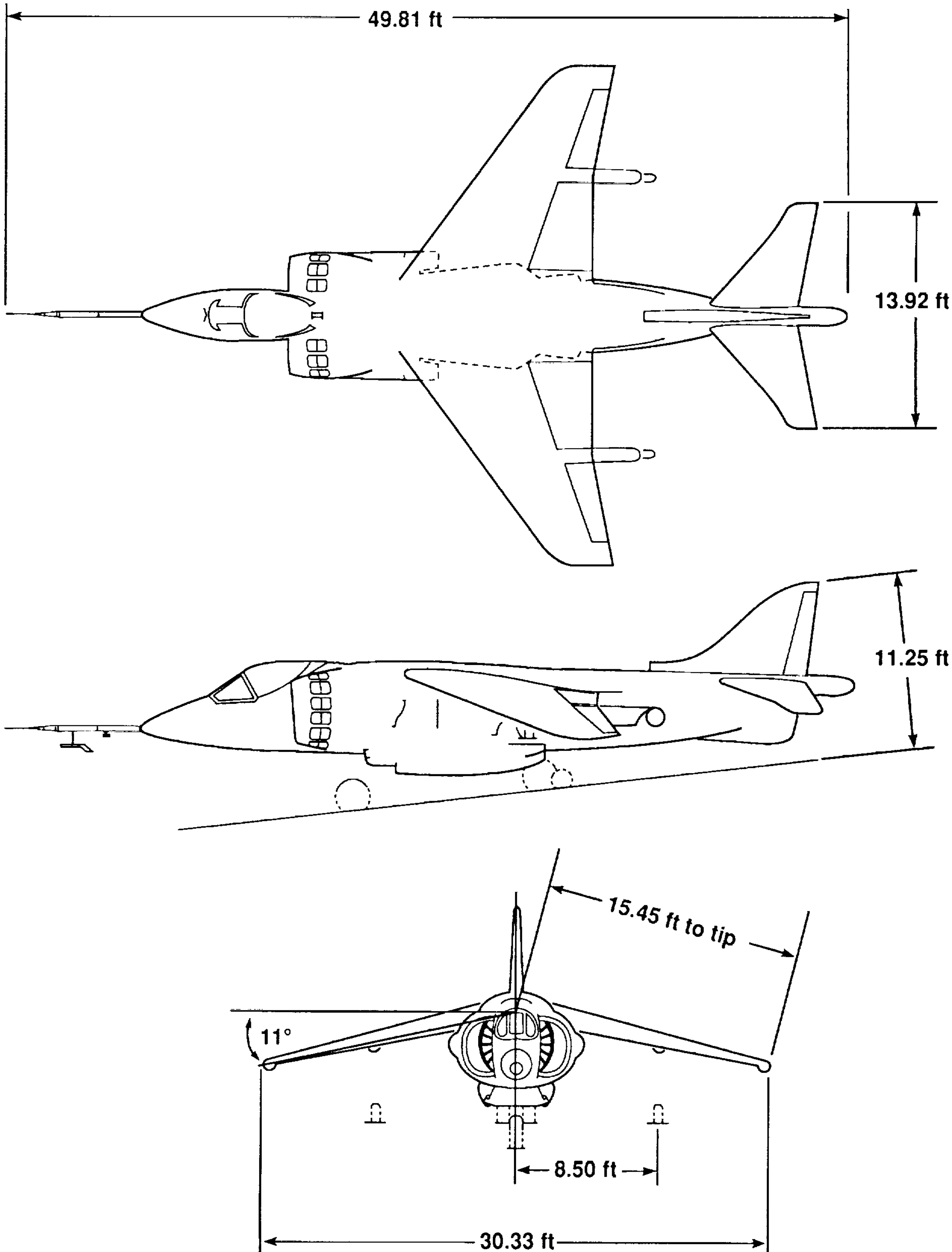

(a) Three view, dimensions in feet, without pylons or LERX.

Figure 2. YAV-8B airplane.

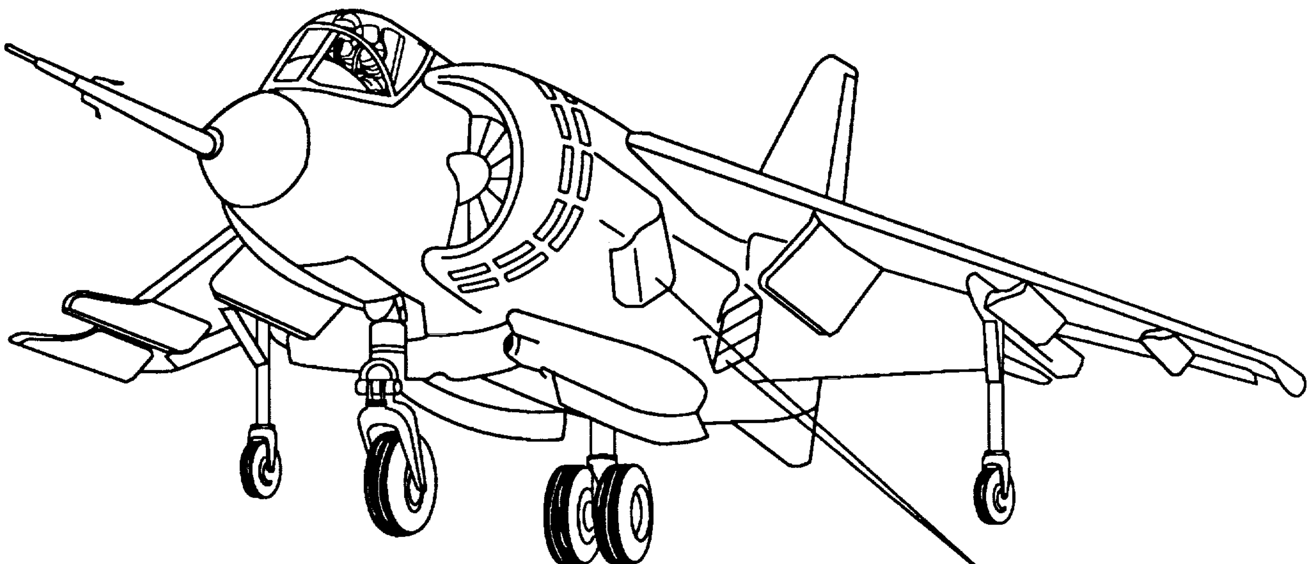

(b) View showing rotatable exhaust nozzles on left side, without LERX.

Figure 2. Continued.

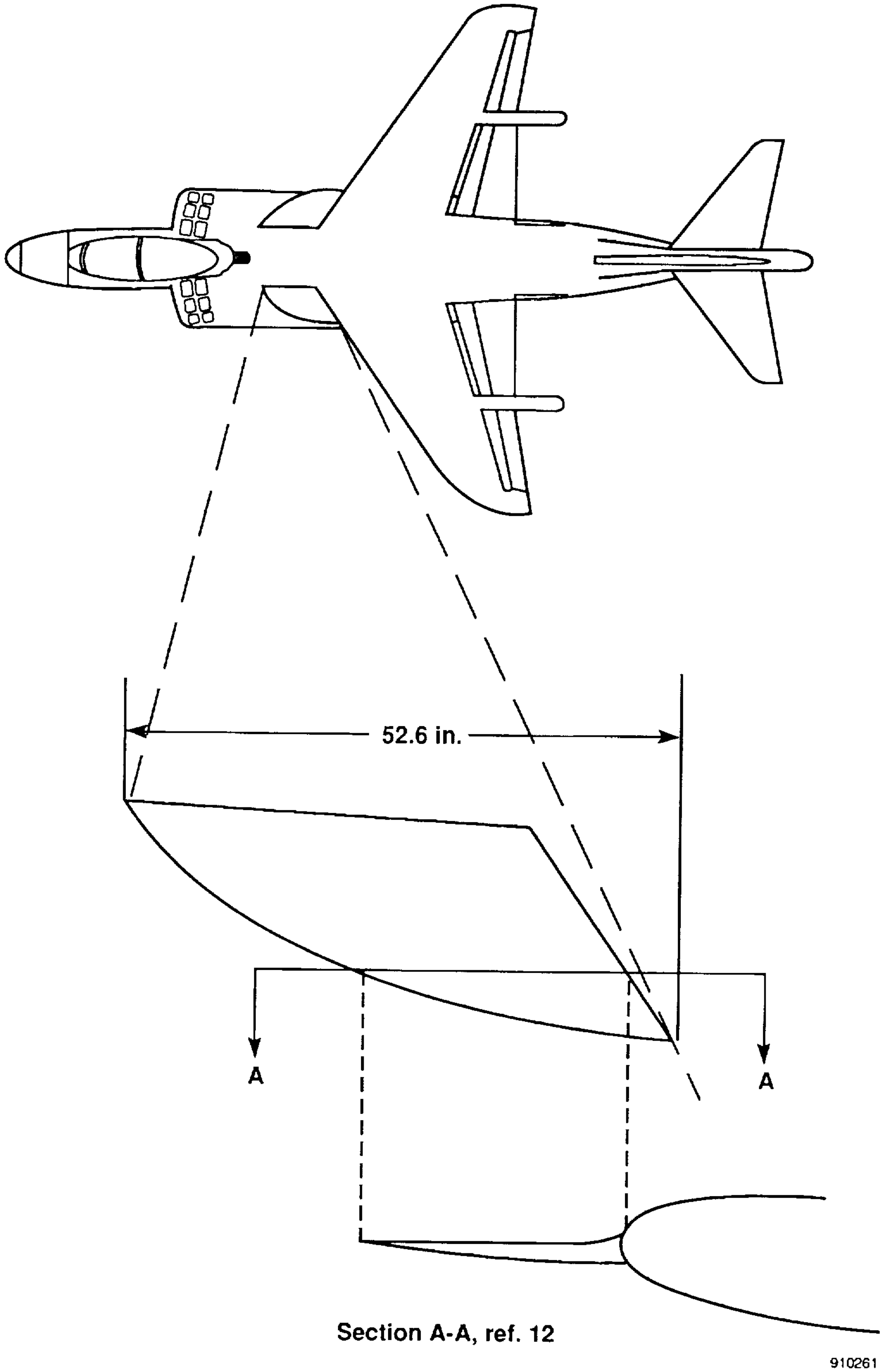

(c) Leading-edge root extension (LERX).

Figure 2. Concluded.

Wing Characteristics

Table 2(a) gives the section coordinates for the YAV-8B at the four semi-span stations from which pressures were obtained. Figure 3 is a diagram of one of the sections, and the variation of thickness ratio with respect to span station is shown in figure 4 (ref. 5). The variation of wing twist, leading-edge radius, and camber with span station is also found in reference 5.

Twelve vortex generators are located at approximately 29 percent of local chord on the upper surface of each wing from slightly outboard of the landing gear outriggers, from η = 0.58 to η = 0.87. The spacing of the vortex generators along the span is about 5.2 in., nearly 7 times the height (span) of each vortex generator. The vortex generators have a span of 0.75 in., a chord of 1.88 in., and are canted (leading-edge outboard) at an angle of 13° relative to free-stream flow. They are shown in figures 5 and 6 and will appear in another in-flight photograph to follow.

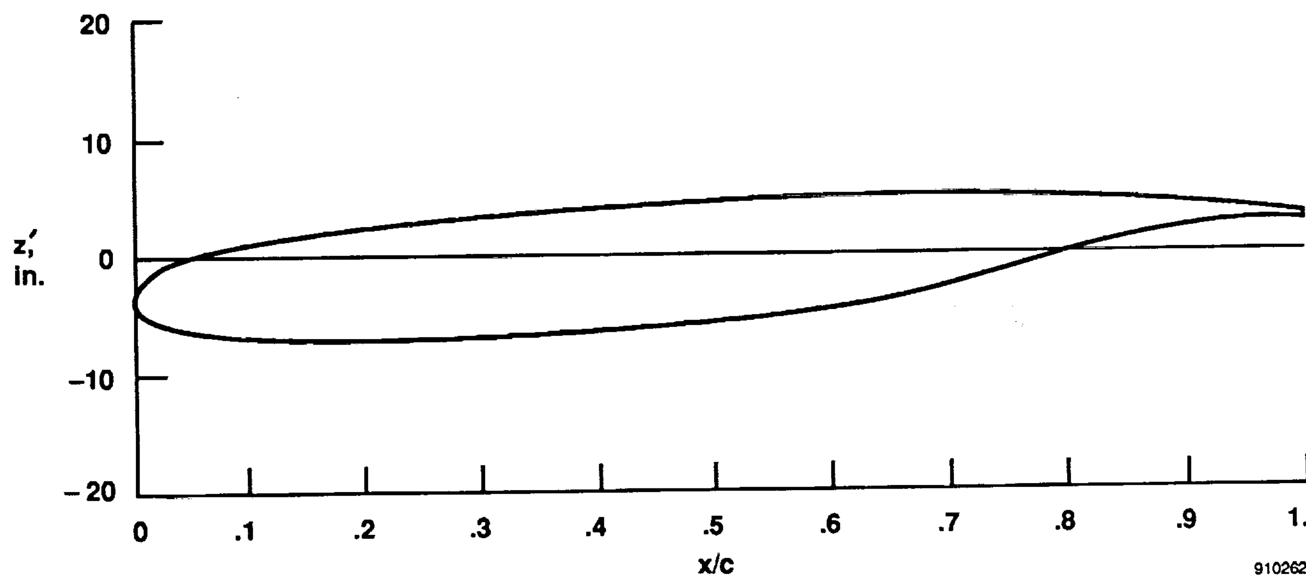

Figure 3. Airfoil of YAV-8B at η = 0.47. Ordinates for all four orifice row sections shown in table 2 (a).

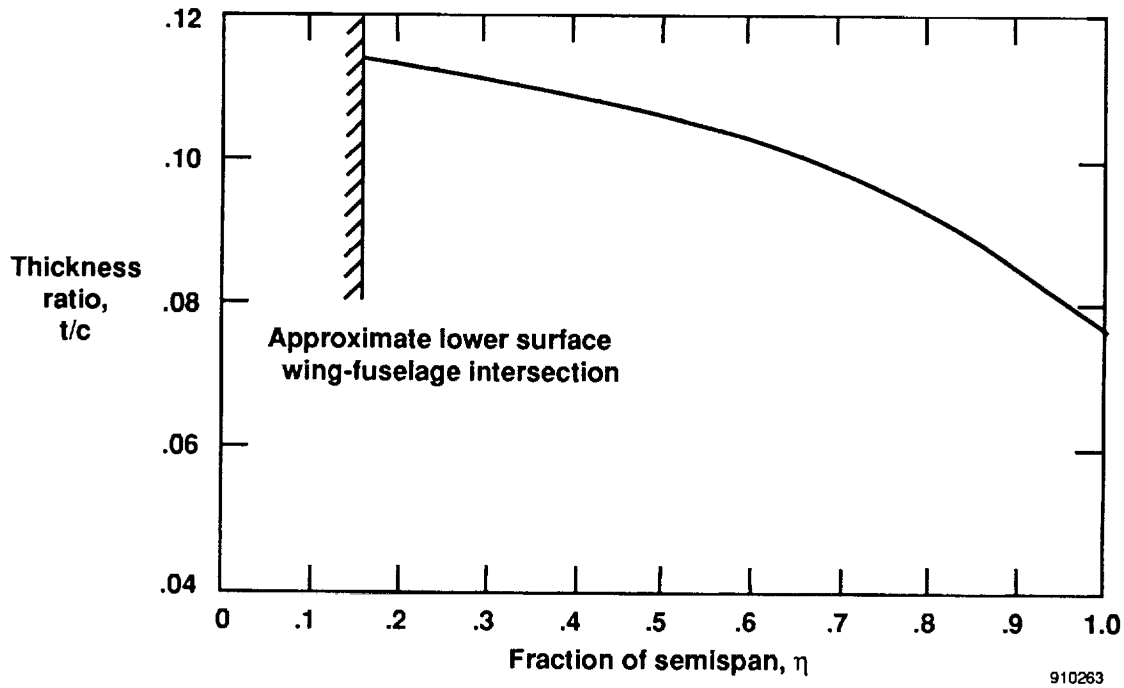

Figure 4. The variation of airfoil thickness ratio as a function of semi-span, reference 5.

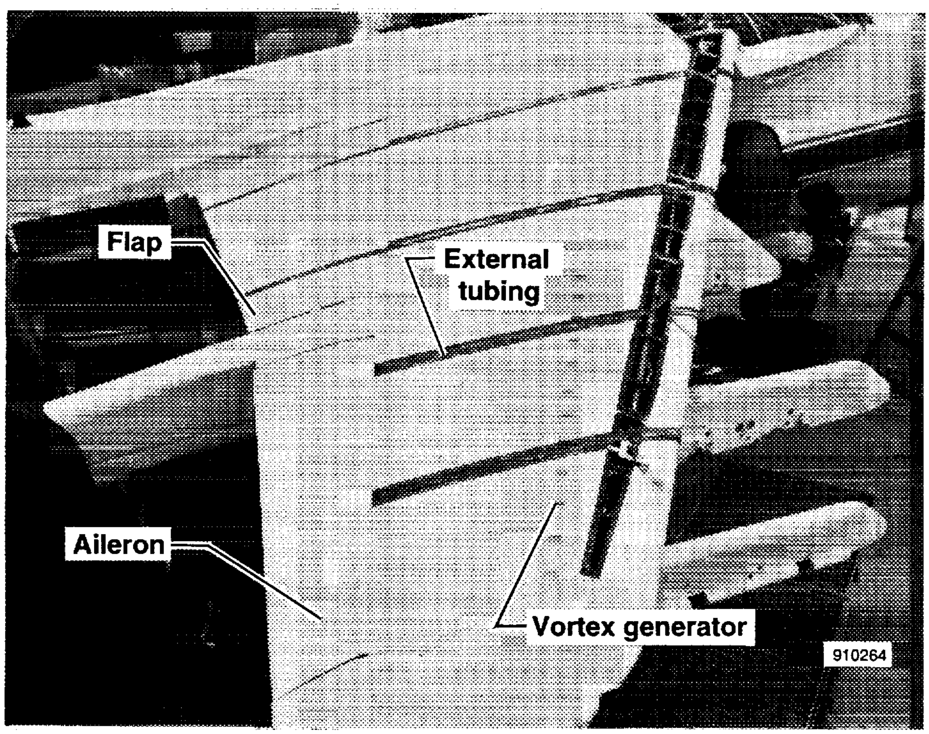

Figure 5. Four chordwise rows of external tubing, cover plate removed.

ORIGINAL PAGE
BLACK AND WHITE PHOTOGRAPH

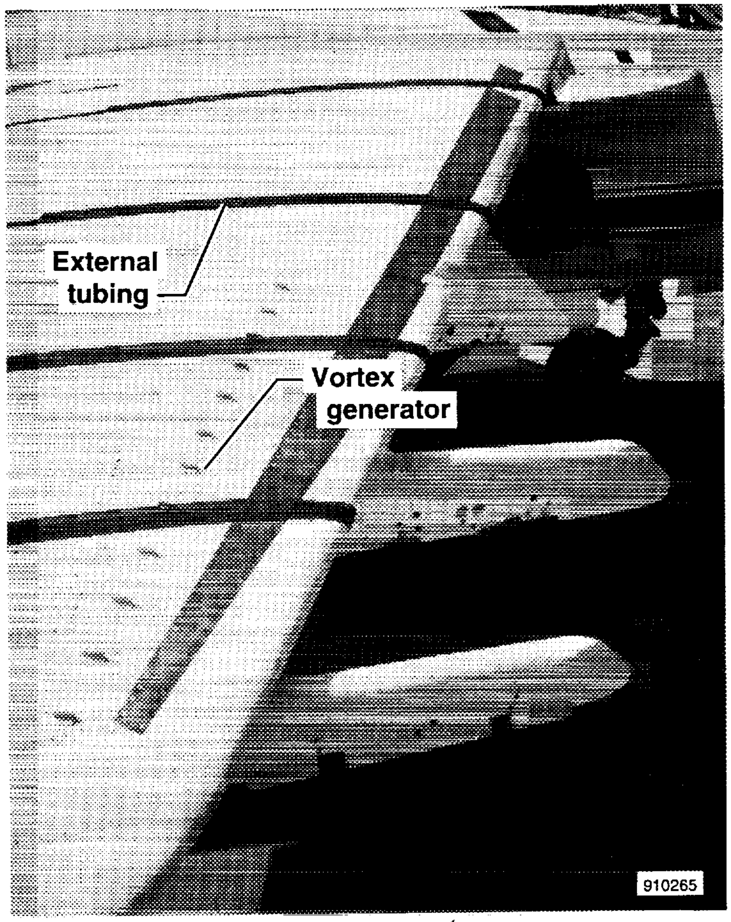

Figure 6. Four rows of flexible external tubing, cover plate in place.

Pylons

The wing surface pressure measurements of this report were made with pylons installed and with pylons removed. The three semispan locations of the pylons are shown in figures 1, 2(b), and in figure 7(a) in terms of the semispan fraction. Figure 7(a) also shows the pylon interface profile with the lower surface of the wing. The bulbous portions of these profiles are caused by convex fairings which cover mounting flanges and bolts. Photographs of the fairing and a part of the pylon for $\eta = 0.70$ (left wing) are shown in figures 7(b) and 7(c) to show the relative size and shape of these convex fairings. For flights without pylons these fairings, flanges, and bolts are absent and the wing lower surface is clean except for the outrigger fairings and control surface actuator fairings.

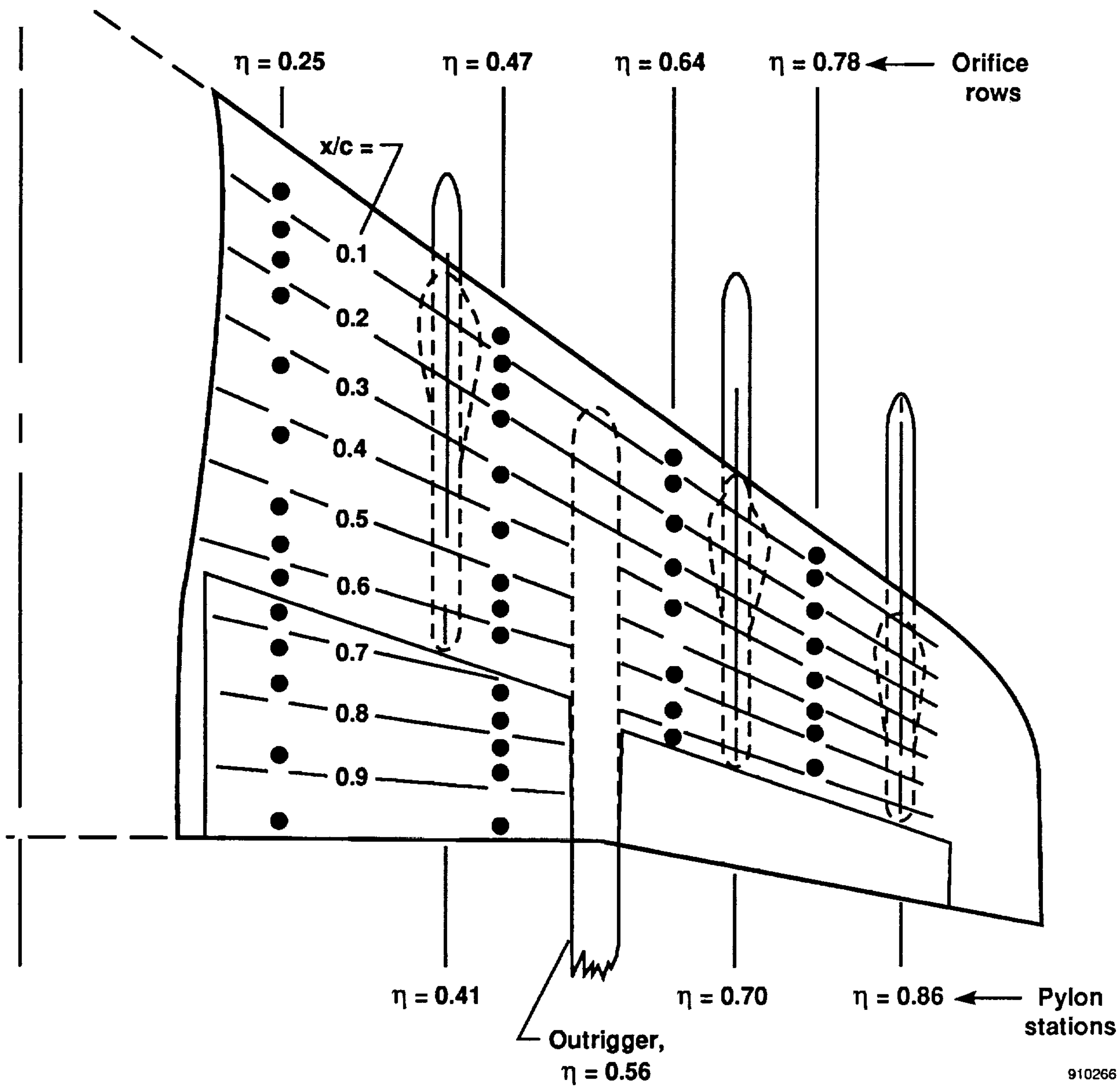

(a) Relative location of pylons, outrigger, and lower surface pressure orifices (as viewed from above the wing).

Figure 7. Interface of pylons and lower surface of wing.

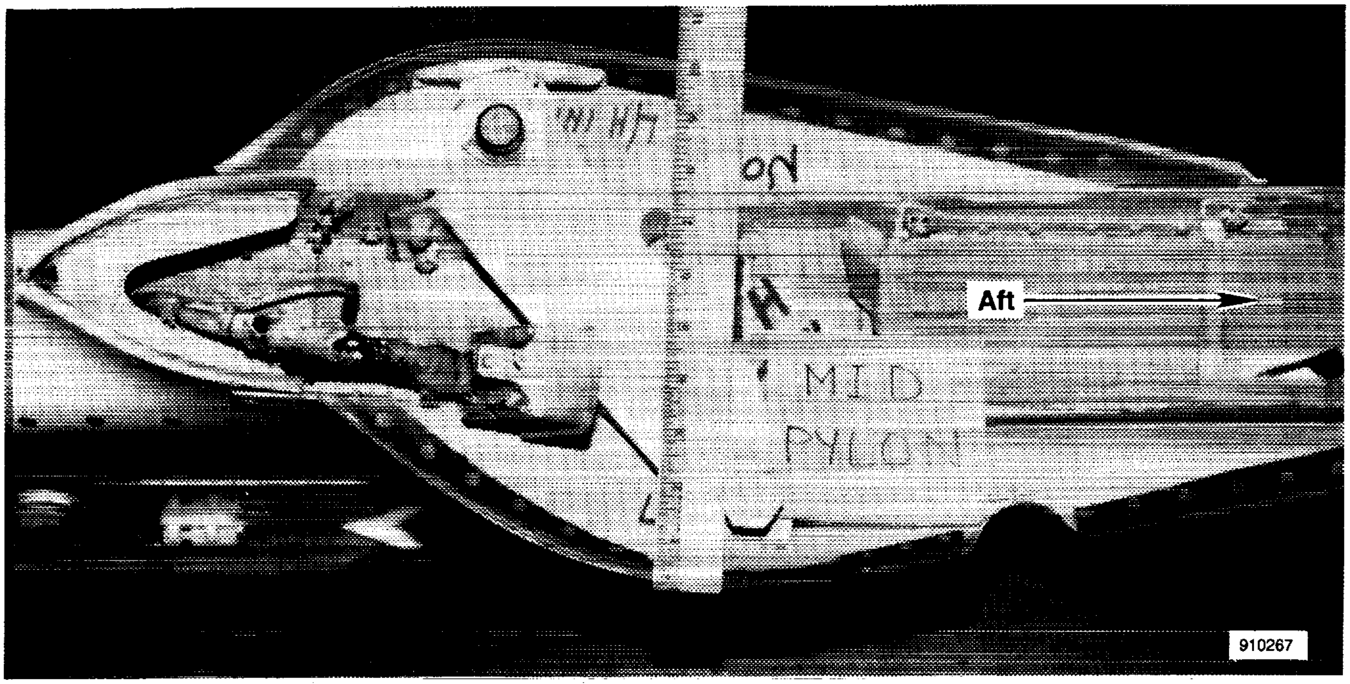

(b) Top view of intermediate pylon, η = 0.70, showing interface of pylon and wing lower surface in region of mounting flanges.

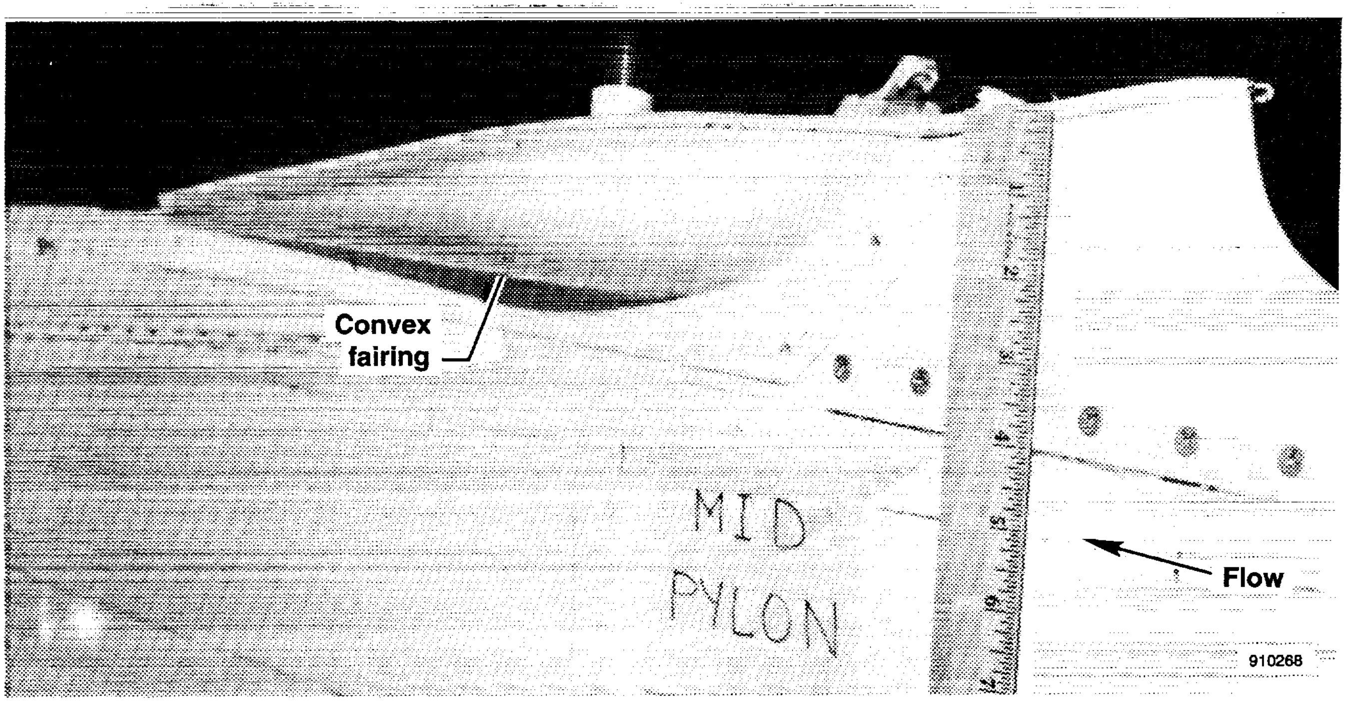

(c) Intermediate pylon, η = 0.70, viewed from 2 o'clock position.

Figure 7. Concluded.

Figure 8(a) shows an in-flight view of the pylons-on configuration. Note the location and relative size of the outrigger landing gear fairing, and the array of tufting (flow cones) which were used to identify regions of separated flow. Figure 8(b) shows the pylons-off configuration. When the pylons are installed (fig. 8(a)), the aft-most portions blend into the aileron actuator fairings, and the inboard pylon covers a major part of the flap actuator fairing.

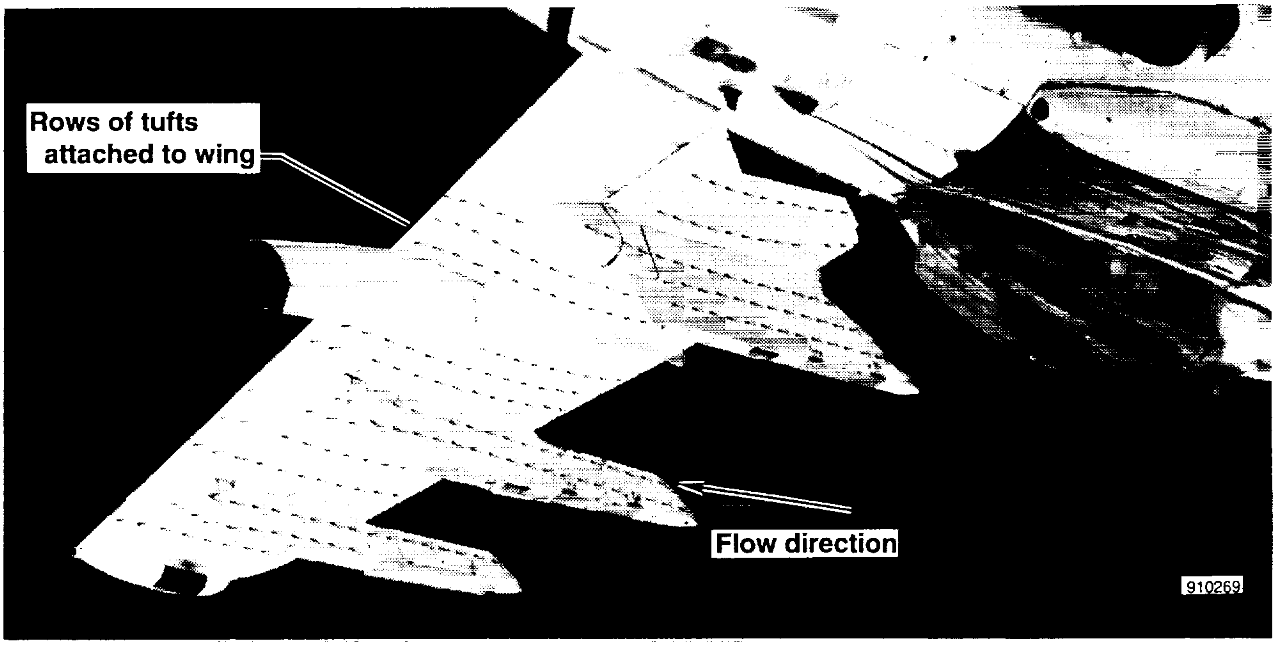

(a) Pylons on.

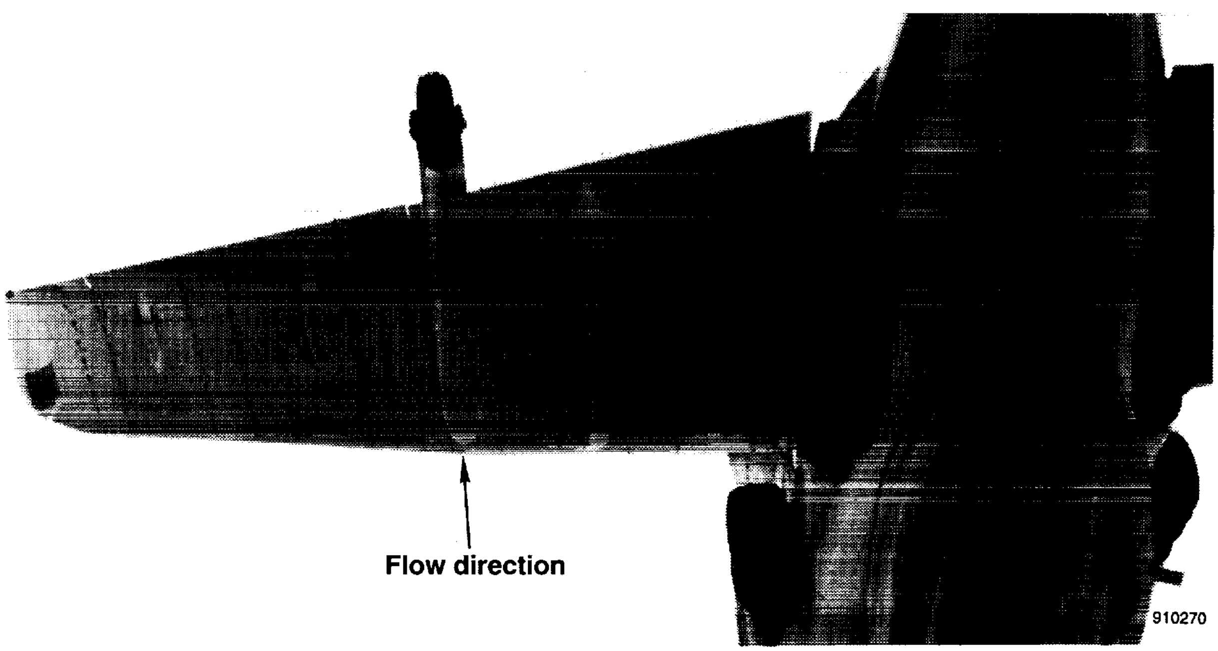

(b) Pylons off.

Figure 8. In-flight views of wing lower surface, $M \approx 0.64$, $\alpha \approx 5^{\circ}$.

INSTRUMENTATION AND DATA ACQUISITION

Wing Pressures

The in-flight surface pressures were measured on the upper and lower surfaces at four rows of orifices. These orifices were located in external flexible tubing which was installed parallel to the free-stream flow. The locations of these orifice rows over the span are shown in figure 7(a); the chordwise orifice locations for the lower surface are illustrated schematically in figure 7(a) and given explicitly in table 2(b). Figure 5 shows the flexible tubing during installation. The two inboard rows extend to the trailing edge (over the flaps), whereas the two outboard rows end where they intersect the aileron hinge line. In figure 5 near the leading edge of the wing surface, the cover plates have been removed to permit access for hook-up of the external flexible tubing to the pressure transducers. Figure 6 shows the installation after the flush cover plates had been installed, which provided a smooth, sealed profile.

The external flexible tubing was obtained in strips of multiple tubes and was bonded to the upper and lower surfaces of the wing with a potting compound. The same compound provided a faired ramp-like surface at the lateral edges of the tubing strip (fig. 9). Figure 9 also shows the inside and outside diameters of this tubing. Reference 6 contains details on the method of installation and examples of comparisons of pressure data obtained from external tubing and flush orifices, both for the same airplane.

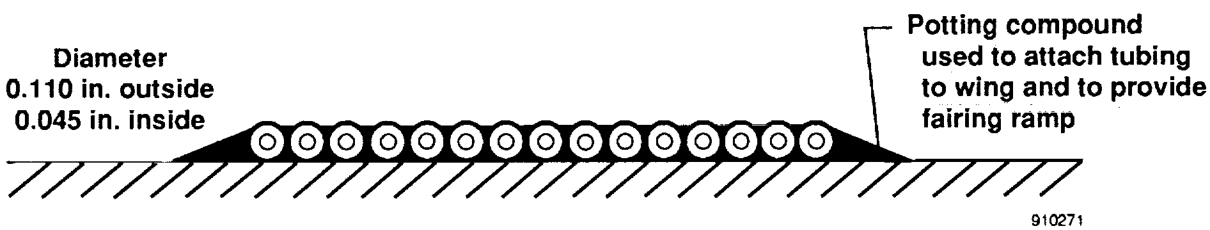

Figure 9. Cross-sectional view of external tubing.

Inside the wing, beneath the cover plates (fig. 6), the tubing from the individual orifices was connected to individual ports of a pressure transducer unit (one unit for each of the four orifice rows). The transducer units were 32-port electronically multiplexed differential devices which were referenced to a plenum (volume roughly 0.4 gal.) that provided a quasi-steady level of reference pressure. Heater blankets covered the transducer units to maintain a constant temperature throughout the test flights.

The reference pressure for the wing pressure transducer units, the reference plenum, originated from within the fuselage (vented to the outside atmosphere) aft of the wing. An absolute high-accuracy digital transducer measured the plenum reference pressure. It was not necessary to control the temperature of this transducer because it was located in the avionics bay which was maintained at a temperature near +22 °C.

Airdata System

Absolute high-accuracy digital transducers measured static pressure and total pressure for determining Mach number, dynamic pressure, and surface pressure coefficients. These transducers were also located in the temperature controlled avionics bay. Figure 10 shows the airdata head which senses static and total pressure. Static pressure was calibrated for position error by the pacer method (ref. 7). Calibrated vanes on the airdata head measured angle of attack and angle of sideslip.

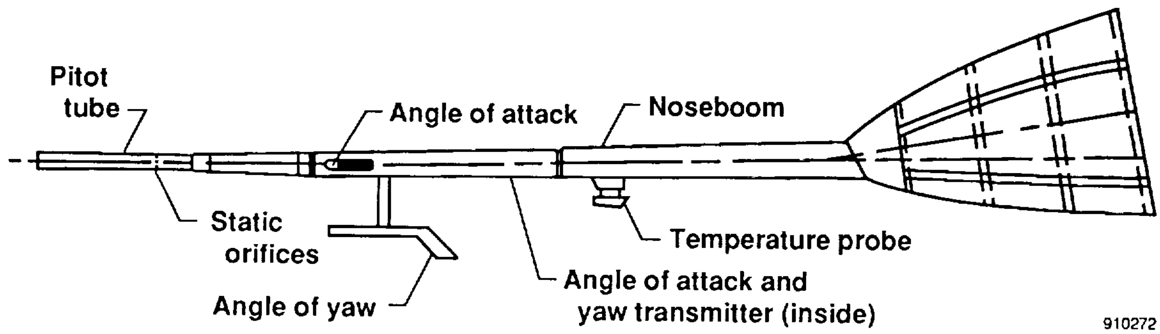

Figure 10. Airdata head and noseboom, reference 4.

Data Processing

Most of the flight-test program consisted of steady-state flight conditions where each condition was held for at least 30 sec. Because the data rate was 10 samples/sec, the data sets were approximately 300 samples for each parameter. Each data set was run through two sets of filters. The first filter removed telemetry dropouts and spikes, the second filter took out points which deviated significantly (more than ± 10 percent) from the mean. After the filtering, the data were averaged. The averaged pressure values were used to calculate local pressure coefficients for each orifice and these were the pressure coefficients analyzed and integrated to obtain section and panel normal force coefficients and pitching moments.

Flow Visualization

In-flight flow visualization was used as an aid in interpreting the wing surface pressure data. The visualization was achieved through the use of flow cones, which provide evidence similar to tufts (ref. 8), and in-flight photography from a nearby chase plane. The flow cones were attached with nylon filament reinforced tape in chordwise rows spaced throughout the span (approximately 10 in. apart) with a fore-to-aft spacing of about 5 in. The cones were applied to the upper and lower surfaces of the left wing and pylons (figs. 8 and 11). Figure 11(b) shows the flow cones as applied to the lower wing surface, outboard of the main landing gear, under static conditions. Though flow cones were used to achieve flow visualization, there are instances in this report where they are referred to as tufts.

ORIGINAL PAGE
BLACK AND WHITE PHOTOGRAPH

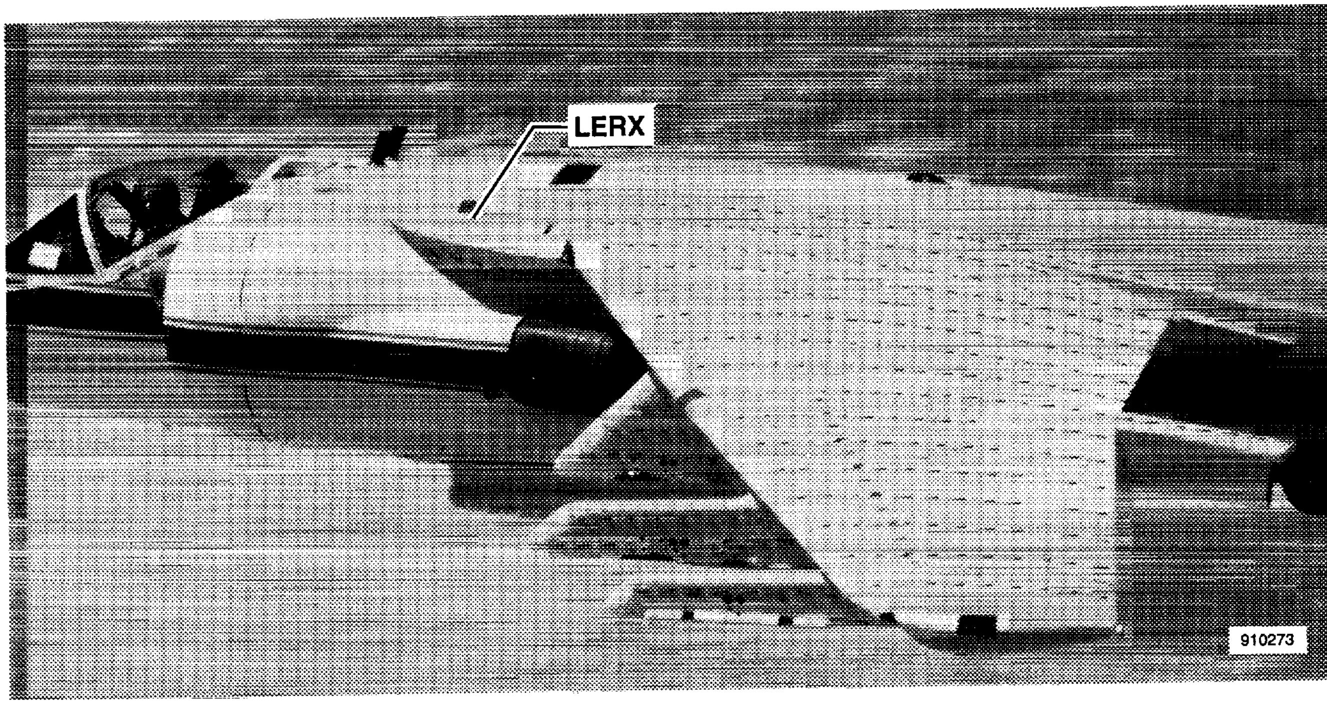

(a) Upper surface, flight conditions.

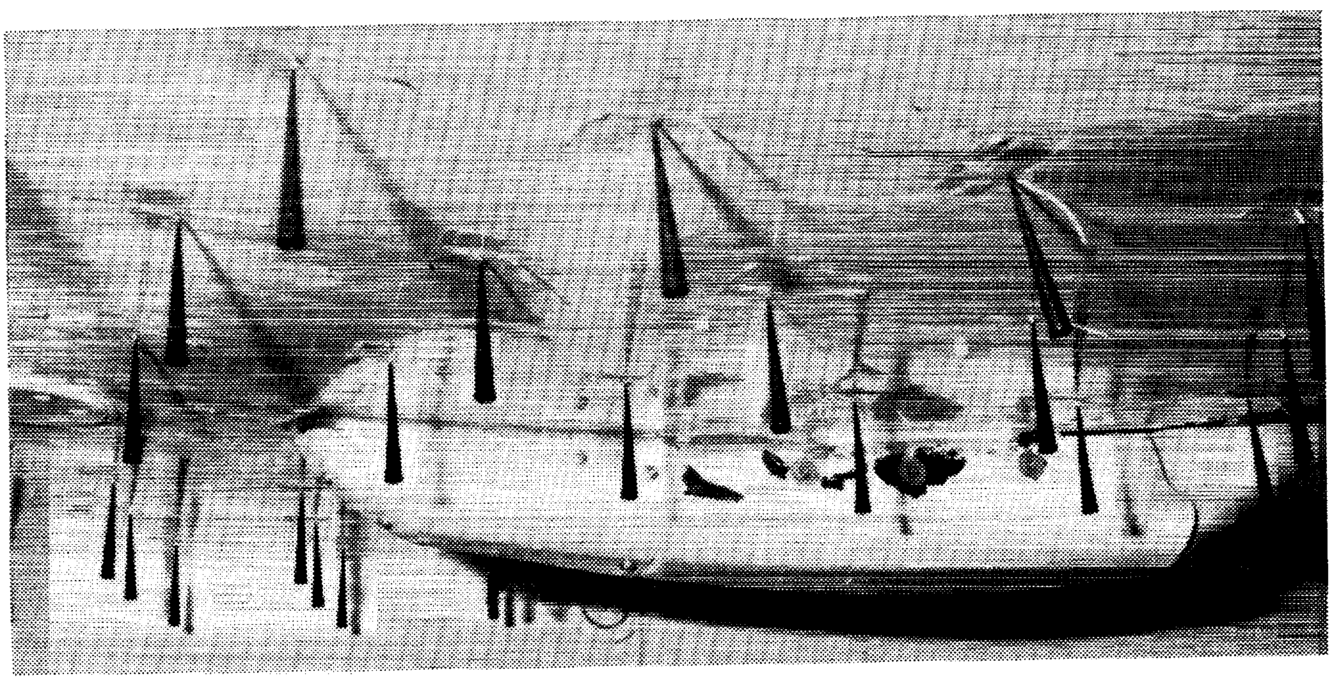

(b) Flow cones as applied to lower surface outboard of landing gear outrigger, static conditions.

Figure 11. Flow cones as applied to left wing and pylons of YAV-8B.

DATA UNCERTAINTY

Random Error

Random pressure errors are estimated to be within the following limits. These limitations are based on the characteristics of the various pressure transducers used to obtain the wing surface pressure coefficients, experience with similar sensor systems, and the airdata calibration (i.e., position error calibration of the research airspeed system).

Error source	Pressure error, lb/ft^2
p_∞	±3.9
p_r	±0.6
p_l	±4.0
q	±2.6

These errors are calculated for flight at $M = 0.85$, a pressure altitude of 30,000 ft, and an angle of attack of approximately 5°. This important combination of Mach number and angle of attack provides upper surface flow that is supercritical at near-design conditions. The random error limits for Mach number and angle of attack are approximately ±0.005° and ±0.3°, respectively.

A worst-case arrangement of the pressure errors, i.e., a case in which the errors are entirely additive, would produce a maximum random error in C_p of ±0.02. This occurrence would be statistically rare, however, and a representative average random error would be approximately ±0.01 in C_p.

Bias Error

External tubing was bonded to the wing surfaces longitudinally at four span stations to obtain wing pressure data. It was not practical to retrofit the wing panel with flush orifices and internally routed pressure tubing because the YAV-8B had a wet wing.

The probable bias in measured pressures caused by the external tubing (primarily near the leading edges) was acceptable because the wing pressure data were to be interpreted primarily on an incremental basis. That is, the main purpose of this investigation was to define the difference in wing pressures for the same flight condition, for pylons-on and pylons-off configurations. Thus, for this evaluation, random errors are of greater concern than are bias errors.

The bias in the data caused by the external tubing can be estimated through earlier experiments in which data were obtained on a high-aspect ratio supercritical wing (ref. 6). It was determined therein that the presence of a proportionally larger (thicker) strip of tubing caused an increase in section normal force coefficients of approximately 10 percent over those c_n values obtained from flush orifices. This increase in c_n was attributed to an apparent increase in local section thickness. The ratio of apparent local section thickness-to-chord length, t/c, for the YAV-8B was increased less than for the aircraft of reference 6, when the external tubing was applied (Δ t/c for YAV-8B was 40 percent of Δ t/c for ref. 6). Therefore, the expected increase in c_n caused by the external tubing on the YAV-8B was approximately 4 percent. This increase, however, would exist for pylons-on and pylons-off configurations.

A data anomaly not addressed in the previous paragraphs was discovered after all the flights were completed and after the data were processed. This problem affected pressure coefficients derived from two orifice locations between x/c = 0.65 and x/c = 0.80 for the upper surface at $\eta = 0.47$. Two different ports of the 32-port transducer devices may have been assigned the same parameter identification, or the controller card may have addressed the wrong transducer port on two occasions for every cycle through the 32 ports. Irrespective of which condition was the cause, because only two orifice locations experienced the problem, the impact on the affected section profiles is not major and the influence on the panel normal force coefficients is considered to be minor. The conclusions derived from the data are unaffected.

TEST CONDITIONS

Flight data were obtained from a range of approximately $M = 0.46$ to 0.88. Test altitudes varied from approximately 20,000 to 40,000 ft which provided a Reynolds number range extending from 7.2 million to 28.7 million based on the mean aerodynamic chord. Data were obtained over much of these stated ranges for pylons on and pylons off. Most of the test runs were constant Mach number–altitude, however, a few runs were made in which velocity was increased or decreased, or constant angle of attack turns were made at constant altitude.

The following table contains the number of test runs at which pressure distribution data were obtained for several combinations of nominal Mach number and pressure altitude.

Nominal Mach number	Nominal altitude, ft: 20,000, Pylons on	20,000, Pylons off	30,000, Pylons on	30,000, Pylons off	40,000, Pylons on	40,000, Pylons off
0.50	2	3	0	0	0	0
0.65	1	3	1	3	0	0
0.75	1	4	1	3	1	1
0.80	3	5	1	3	1	1
0.845	1	3	2	3	1	1
0.86	1	2	0	0	0	0
0.875	0	1	3	3	0	0

PRESENTATION OF THE DATA

Tables in Appendixes A through F contain tabulated local surface pressure coefficients derived from the pressure measurements for the YAV-8B airplane with pylons on and pylons off. The chordwise distribution of some of these pressure coefficients will be presented in support of the Results and Discussions section.

All other quantitative flight data to be presented in subsequent figures are integrated quantities which are derived from the basic data presented in Appendixes A through F and the various pressure distribution plots. The integrated section quantities, c_n and c_m, are listed in Appendixes G through L for all the flight conditions shown in the preceding table.

RESULTS AND DISCUSSION

General Remarks

Among the well-known features of supercritical airfoils is a significantly reduced upper surface curvature as compared with conventional airfoils. This lessened surface curvature provides reduced shock losses and, for the same lift, reduced wave drag and possibly diminished shock induced separation (refs. 9, 10). The design condition pressure distribution resulting from a supercritical airfoil is characterized by a flattened or plateau-like upper surface chordwise distribution of pressure and a high-pressure region under the aft, cusp, portion of the airfoil (fig. 12).

The preceding characteristics, which are somewhat typical for advanced supercritical airfoils, are noted to gauge qualitatively whether the YAV-8B wing provides the design (i.e., supercritical) upper surface plateau-like pressure distribution for important high-speed flight conditions. Of the many flight-test conditions recorded (Test Conditions section and Appendixes A through F), those displaced not more than 1° in angle of attack from the envelope of conditions for near maximum lift-drag ratio will be given the most attention.

The conditions evaluated in this series of flights, the specific combinations of Mach number and angle of attack, are shown in figure 13. In addition, shown in cross-hatch is the envelope for conditions near maximum lift-drag ratio. These conditions are the Mach number–angle-of-attack combinations which would be expected to provide near-maximum lift-drag ratios throughout the speed range, and Mach number–angle-of-attack combinations that would achieve wing pressure profiles displaying supercritical upper surface flow conditions at "design" transonic speeds. This envelope was derived from 15-percent scale model force tests (ref. 11) because the full-scale airplane was not instrumented to determine lift and drag in flight. Figure 13 shows that at the higher Mach numbers where compressibility is important, many of the flight-data runs were performed at angles of attack lower than those expected to produce the most efficient flight, based upon the model-derived envelope. The approximate design condition and the anticipated cruise condition are also shown in figure 13. Few of the many test points shown in figure 13 will be analyzed and discussed in detail; however, all the test points shown will become a part of the integrated force and moment coefficients and will be used to evaluate the relative efficiency of the entire wing panel.

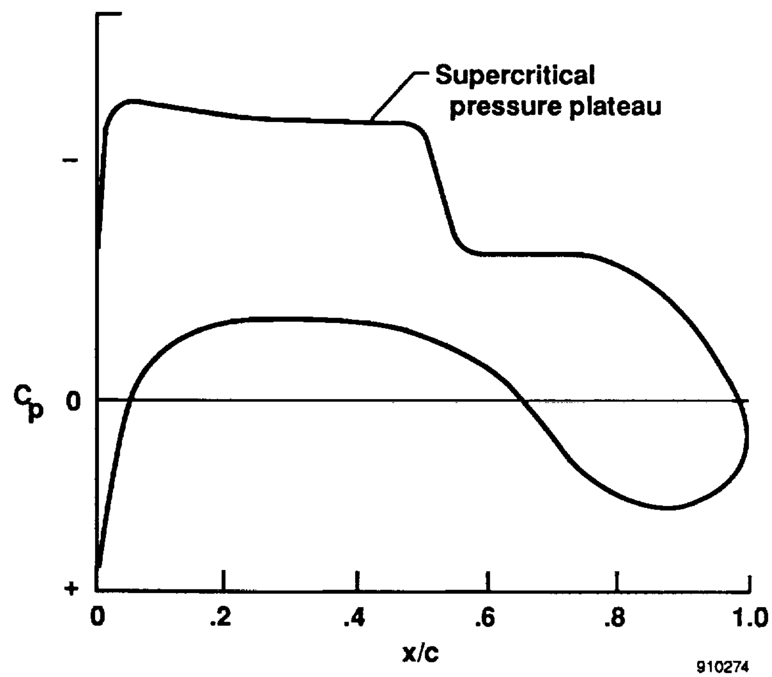

Figure 12. Schematic of chordwise pressure distribution for typical supercritical airfoil at design condition, i.e., at design Mach number and angle of attack.

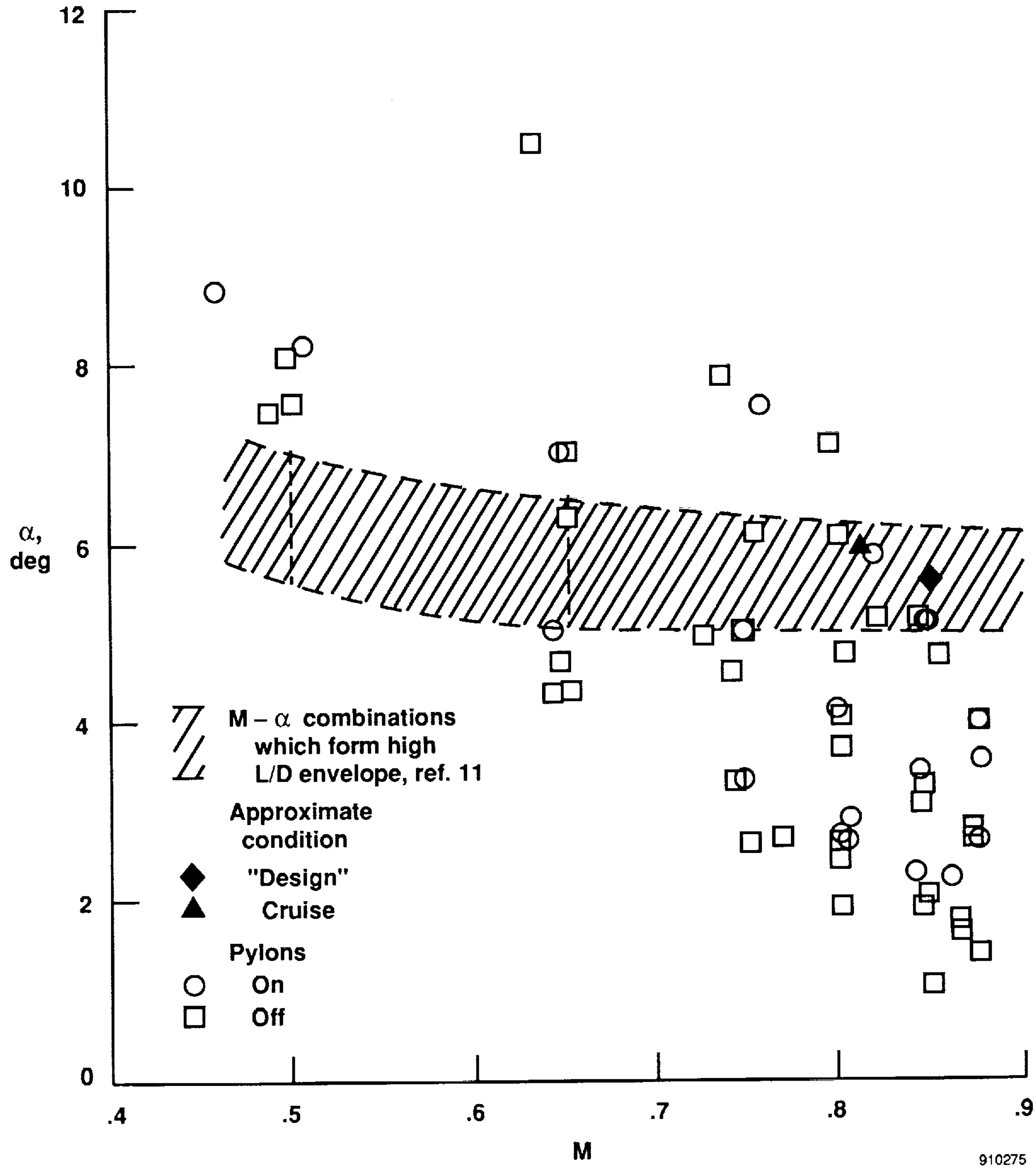

Figure 13. Mach number–angle-of-attack combinations for which wing pressure distribution data have been obtained in flight.

Chordwise Pressure Distribution, Pylons On and Pylons Off

Comparison at Off-Design Mach Number

Chordwise pressure distributions will be compared at a Mach number well below the region where the most significant compressibility effects occur. These data are presented for pylons on and pylons off in figures 14(a) and (b) respectively for $M \approx 0.64$ and $\alpha = 7°$. The flight conditions for these two configurations are closely matched, therefore differences in the pressures provide conclusive evidence of the effects of the pylons.

Careful orifice-by-orifice study of the data (i.e., comparison of pressure data at a given test chord for the same x/c location) in figures 14(a) and 14(b) reveals differences in pressure coefficients for some orifice rows. A less tedious observation is presented as figure 14(c), where the pressure coefficient data at $\eta = 0.78$ are shown for both configurations. The pylons-on configuration experiences a lower negative pressure coefficient (higher pressure) in the region of the most forward upper surface orifice x/c = 0.05. For the lower surface, the pylons cause somewhat lower pressures over most of the instrumented portion of the chord. These upper and lower surface pressure differences, between the two configurations, combine to reduce the section lift being produced when the pylons are mounted for a given angle of attack.

A closer orifice-by-orifice comparison for all orifice rows (figs. 14(a) and 14(b)) shows that for the lower surface, the pylons cause slightly lower pressure over much of the chord (approximately 40 percent) for $\eta = 0.25$ and a somewhat larger region of lower pressures at $\eta = 0.64$. These differences are in addition to the aforementioned greatest differences at $\eta = 0.78$. The net result is that the pylons cause pressure differences that are measurable which diminish lift in local areas at Mach numbers well below design or cruise conditions. The degree to which the entire wing panel loading is diminished by the pylons will be presented later in this report through the integrated pressures which will provide section and panel normal force coefficients.

Photographs of flow cones for $M \approx 0.64$ and $\alpha \approx 5°$ (fig. 8) show the lower surface flow to be attached, although there is evidence of some velocity decay in the aileron-cusp region. Flow cone photographs are not available for $\alpha = 7°$, the angle of attack for the data of figure 14; however, based upon experience at various angles of attack for other Mach numbers, it is believed that there would be less velocity decay at the conditions of figures 14(a) through 14(c) than at the $\alpha \approx 5°$ condition of figure 8.

Figure 11 (a) shows upper surface flow cone patterns for the pylons-on configuration. This photograph is typical of the results for all the Mach numbers and angles of attack reported herein; it is also representative of the pylons-off configuration. The upper surface flow is attached throughout. Though attached flow was always observed over the upper surfaces for these tests, it should be acknowledged that the angle-of-attack range of these tests was modest. The slight canting of cones in the third longitudinal row of flow cones outboard from the fuselage is assumed to be caused by a vortex from the LERX.

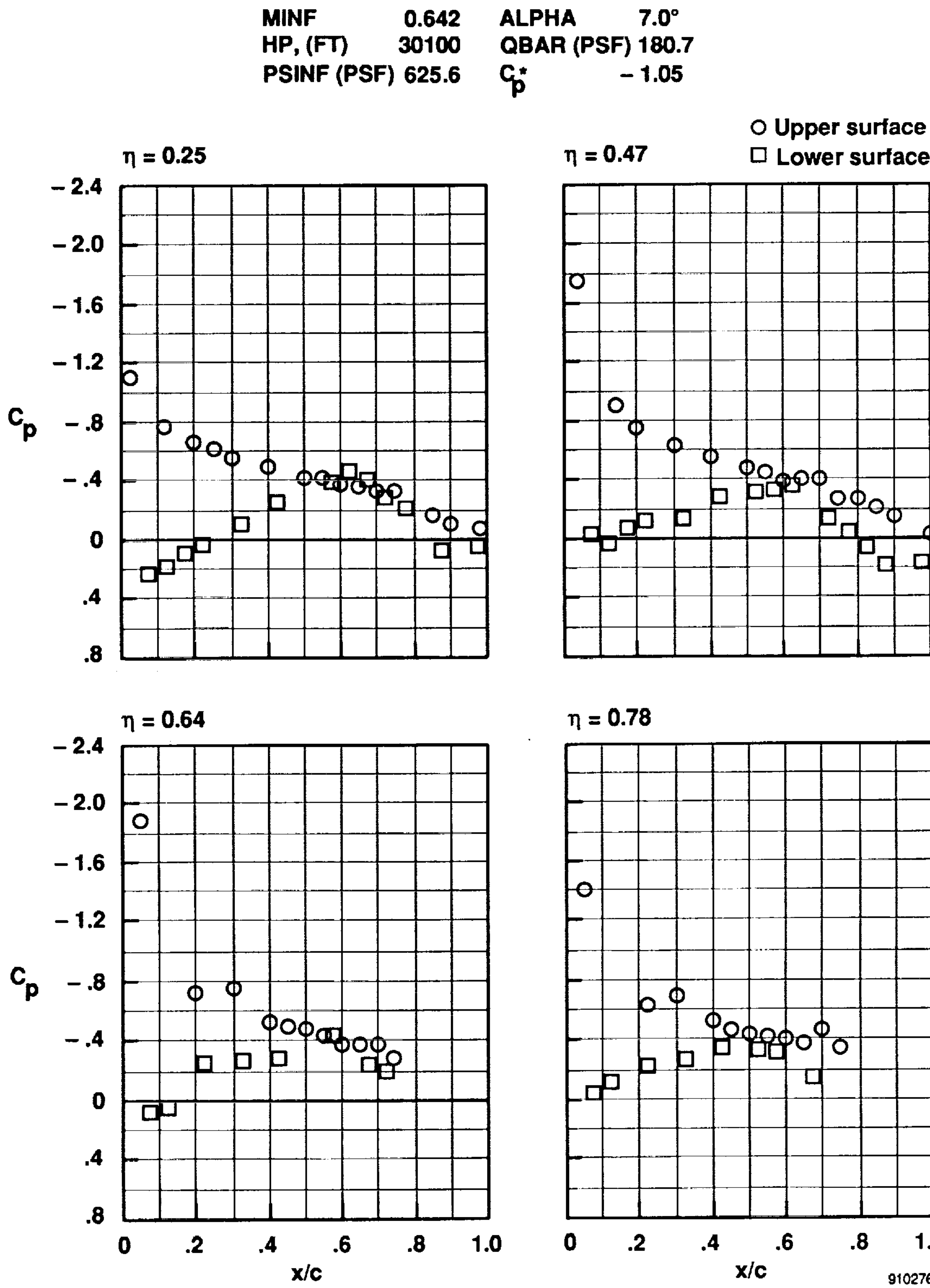

(a) Pylons on.

Figure 14. Chordwise distribution of pressure for $M = 0.64$, $\alpha = 7.0^\circ$.

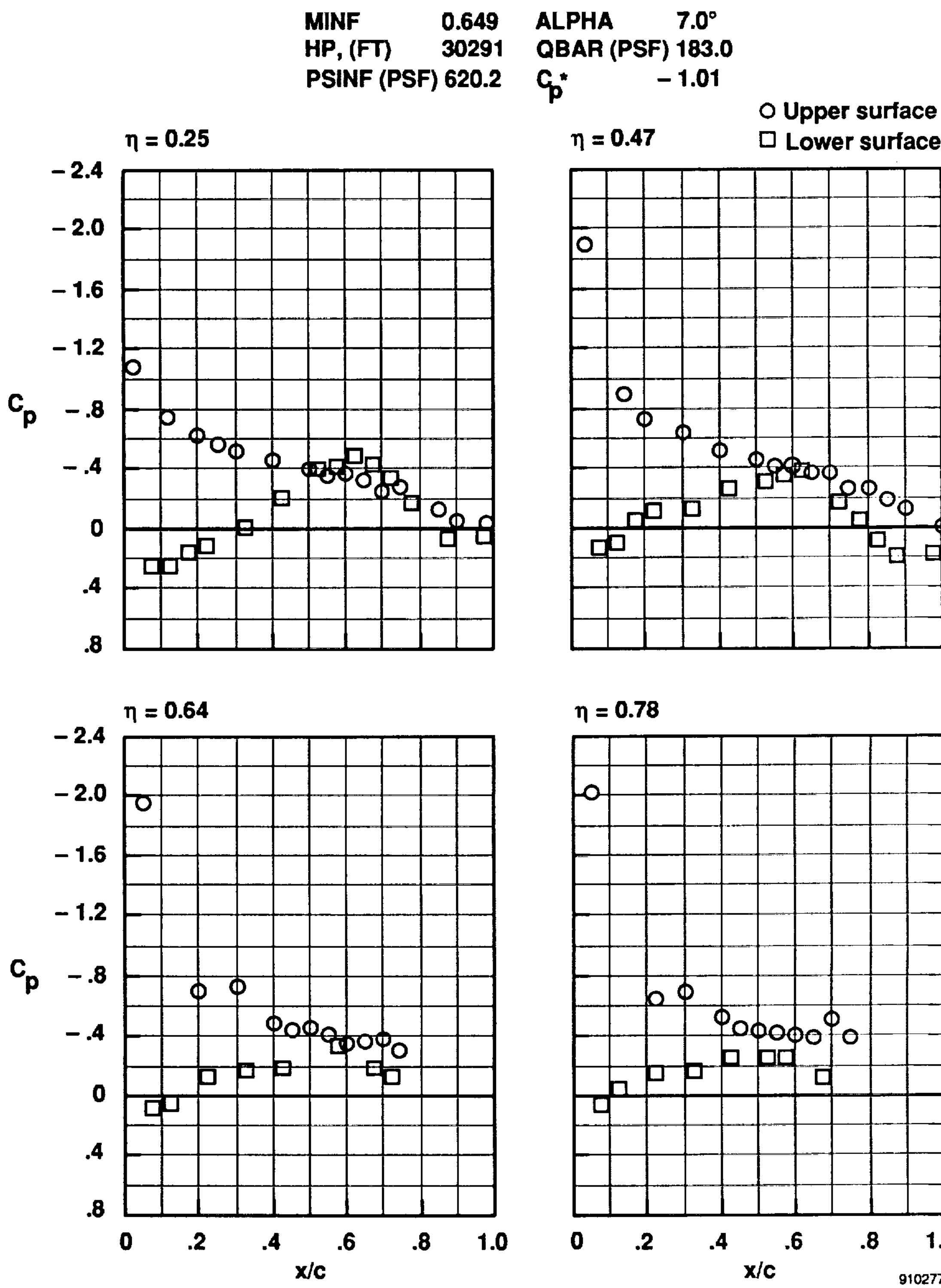

(b) Pylons off.

Figure 14. Continued.

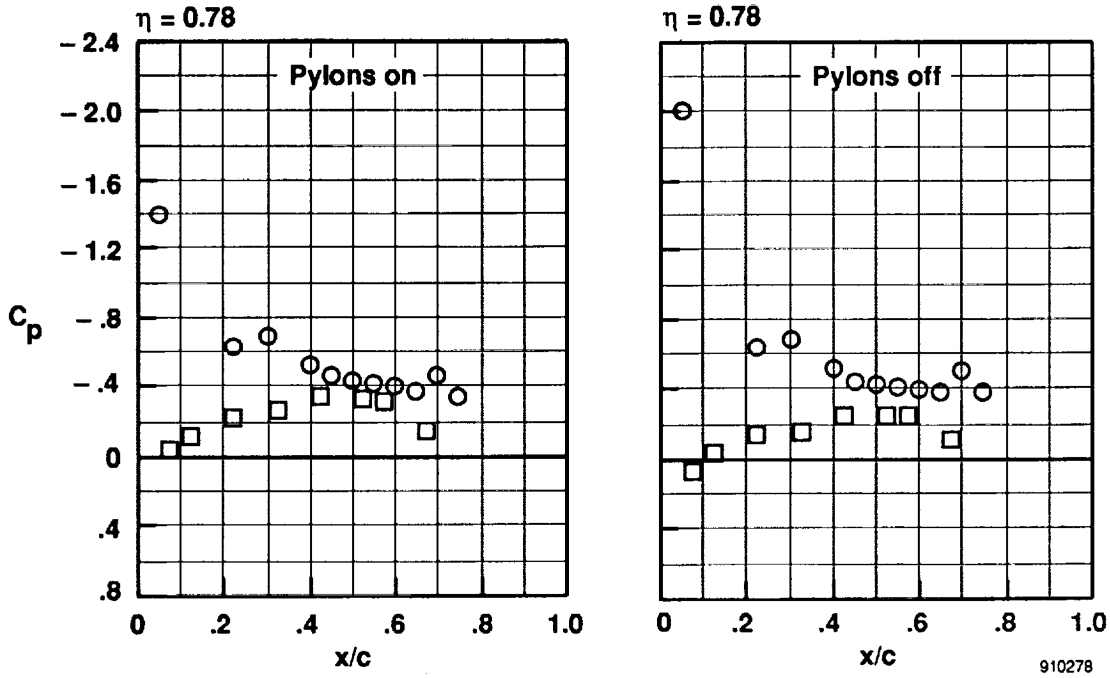

(c) Comparison for pylons on and pylons off at $\eta = 0.78$, $M \approx 0.64$, $\alpha = 7^{\circ}$.

Figure 14. Concluded.

Comparison at Angle of Attack Near 5° for Off-Design Mach Number and Near-Design Mach Number

Off-Design Mach Number, $\alpha \approx 5°$. Chordwise pressure distribution data are shown in figure 15 for both configurations at $M \approx 0.75$ and $\alpha \approx 5.0°$. The pylons-on and pylons-off data, figures 15(a) and 15(b) respectively, show peaked upper surface pressure profiles forward of 0.2 x/c for the three outboard orifice rows. This is typical for supercritical airfoils at Mach numbers below the design condition (ref. 9, 10). The pressure profiles for both configurations are characterized by very low upper surface-to-lower surface pressure differentials over the mid-chord region for all four η locations, orifice rows. Consequently, for this flight condition, whatever lift is being generated by the wing must come primarily from the regions toward the leading and trailing edges. Because external tubing was not bonded to the ailerons, the distribution of pressure over the aft 0.3 chord is not available from flight for the two outboard orifice rows, $\eta = 0.64$ and 0.78. Therefore, only at $\eta = 0.47$ is there evidence from flight data of significant amounts of lift (i.e., significant upper surface-to-lower surface pressure differentials) over the aft 0.3 chord.

Orifice-by-orifice comparison of upper surface pressures shows almost no influence from the pylons (figs. 15(a) and 15(b)). For the lower surfaces, at $M \approx 0.75$ and $\alpha \approx 5.0°$, the effect of the pylons is qualitatively similar to the effects seen earlier for $M \approx 0.64$. Thus, the pylons cause somewhat lower pressures throughout much of the under surface, resulting in diminished lift for a given angle of attack. The pressure data for the most forward lower surface orifice (x/c = 0.075) at $\eta = 0.47$, and for the x/c = 0.225 at $\eta = 0.64$, show the effects of the pylons, negative pressure coefficient peaks, which portend lower surface supersonic velocity regions and local shock losses at higher aircraft Mach numbers. These local effects are believed to be caused by the convex fairings mentioned in the description of the pylons in the Aircraft section of this report and illustrated in figure 7.

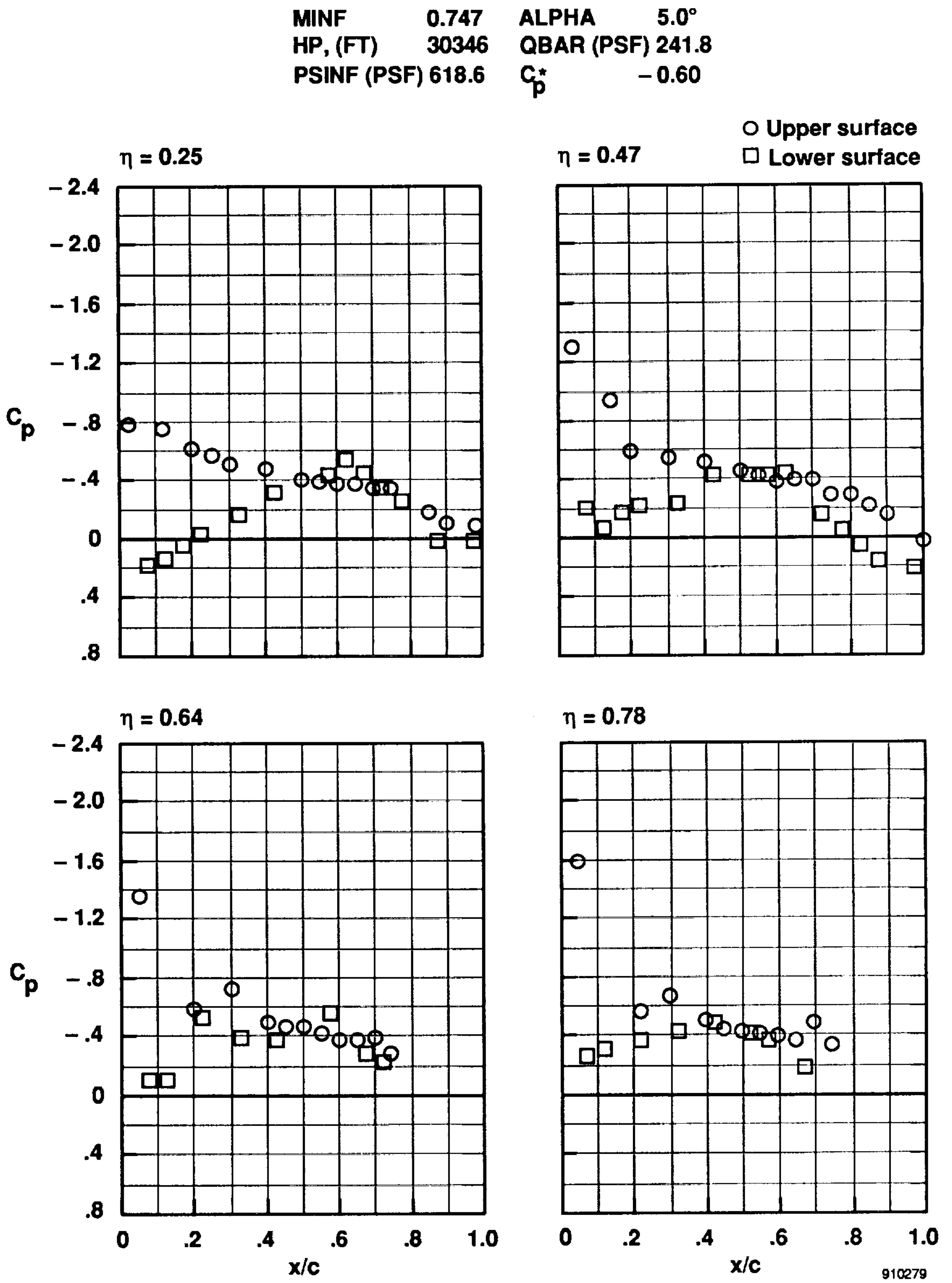

(a) Pylons on.

Figure 15. Chordwise distribution of pressure for $M \approx 0.75, \alpha \approx 5.0^\circ$.

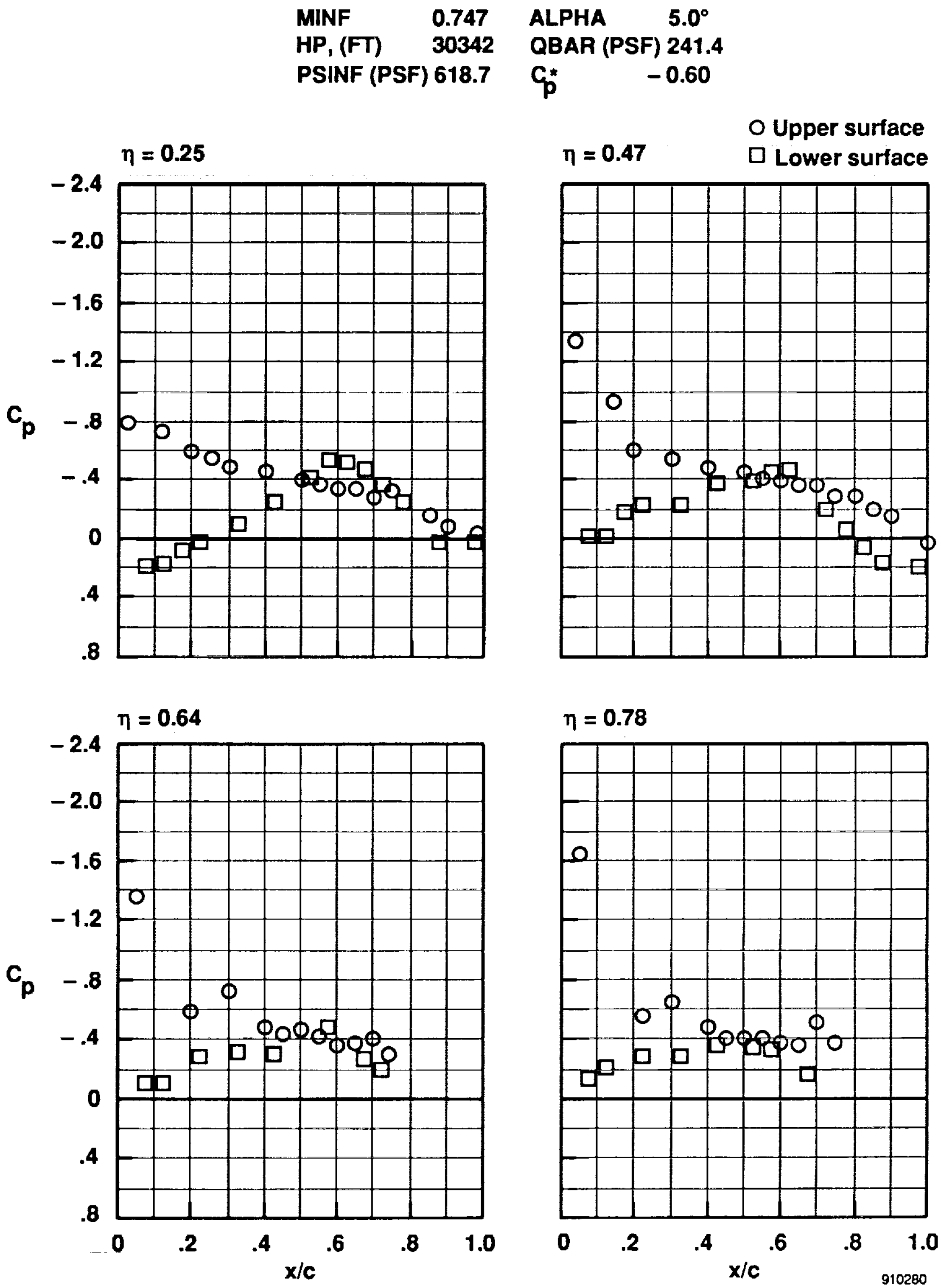

(b) Pylons off.

Figure 15. Concluded.

Near-Design Mach Number, $\alpha \approx 5.2°$ Figures 16 (a) and 16(b) show pressure distribution profile data near design conditions. In contrast to the results from the lower Mach numbers, the data of figure 16 (which are close to the design Mach number of 0.85) show some of the upper surface pressure profile features expected of a supercritical airfoil (see General Remarks section).

For both configurations, upper surface negative pressure coefficients of −0.7 or greater are maintained essentially to mid-chord for all four span stations; the gradients over these regions tend to be mild, though only for η = 0.25 and 0.64 could they be described as flattened. In addition, the upper surface pressure coefficients remain more negative than C_p^* to about x/c = 0.6, which also defines the extent of the supercritical pressure plateaus.

These pressure data, again referring to both configurations, indicate attached flow almost to the trailing edge at η = 0.25 for upper and lower surfaces. Corresponding data for η = 0.47 show attached flow throughout the entire chord length for the upper surface, however, flow cone data (figs. 17(a) and 17(b)), show evidence of velocity decay in the lower surface cusp region. In addition, incipient separation may exist in this region. For the longitudinal orifice rows at η = 0.64 and 0.78 which are outboard of the outrigger fairing, the flow cone patterns indicate lower surface flow separation in the aileron–cusp region. These observations apply to the pylons-on and the pylons-off configurations.

The model data from reference 12 for M = 0.85 and interpolated to $\alpha \approx 5.2°$ (fig. 18) show a significant amount of lower surface lift from the cusp region. The loading for the aft 30-percent chord for η = 0.64 and 0.78 tends to exceed, proportionately, that of η = 0.47. However, though the Mach number–angle-of-attack combination considered in figures 16(a) and 16(b), i.e., $M \approx 0.84$, $\alpha \approx 5.2°$, exhibits effective supercritical flow characteristics over the upper surface; the pressure data and flow cone data taken together reveal that the full-scale flight wing performance is compromised because the lower surface cusp region experiences flow separation and is not contributing lift as would be expected based on the model data seen in figure 18.

An orifice-by-orifice comparison of the pressure data for pylons on and pylons off (figs. 16(a) and 16(b)) would show that the differences caused by the pylons are limited to the lower surface, and are indicative of local shocks caused by the aforementioned convex fairings. Though there is evidence of this for all three outboard orifice rows, the data for η = 0.64 show the most graphic influence of the pylons. In figure 16(c), the pylons-on configuration has significantly higher negative pressure coefficient peaks (lower surface, square symbols) at x/c = 0.225 and 0.325 than for the pylons-off configuration. These peaks exceed the critical coefficient for sonic velocity. There is also a relatively strong local shock near x/c = 0.6 for both configurations. All these shocks, and local shocks at other locations throughout the span of the wing lower surface, go together to increase drag creep through shock losses, per se, and in some instances there is probable added drag from localized shock induced flow separation.

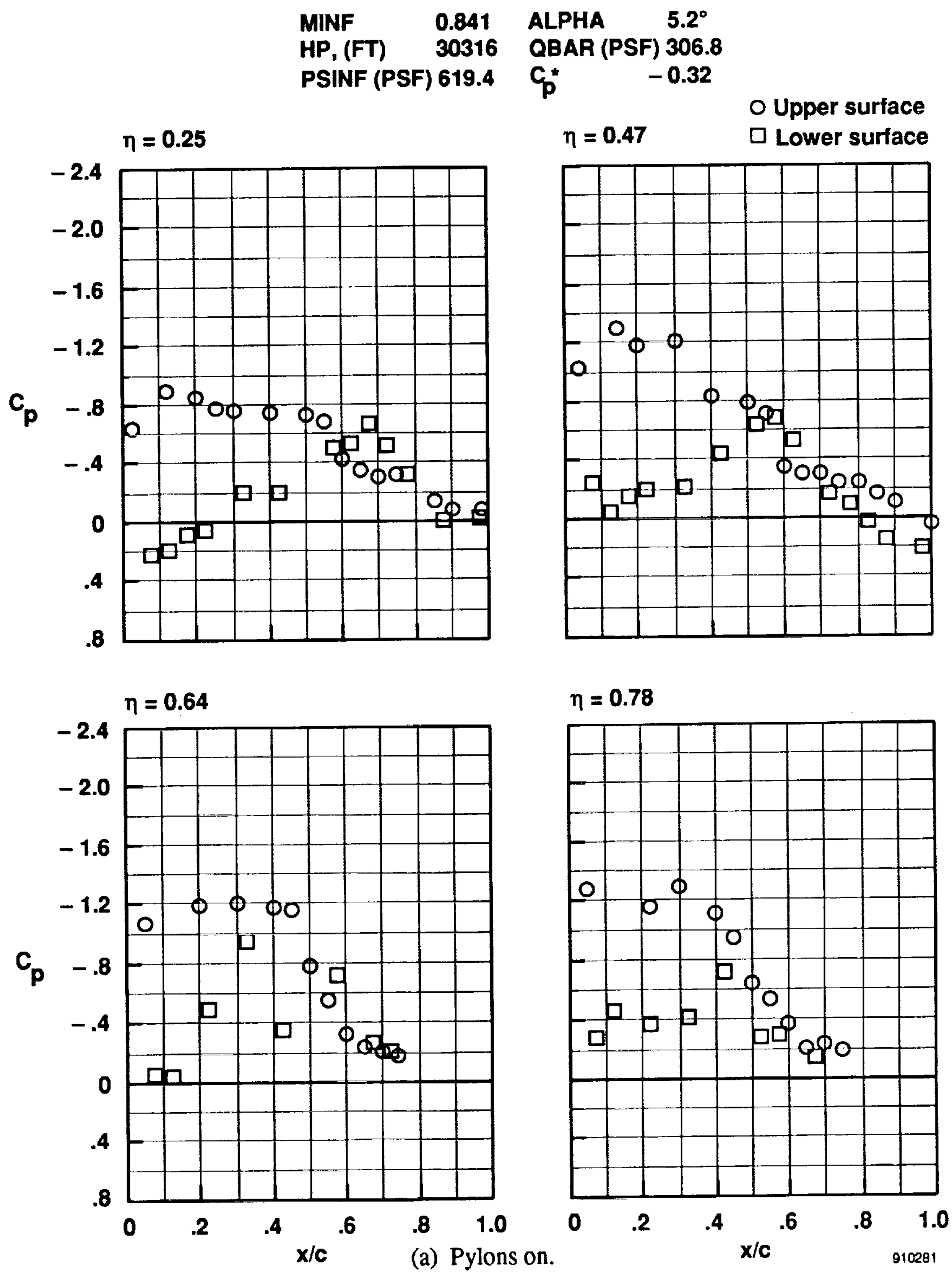

(a) Pylons on.

Figure 16. Chordwise distribution of pressure for $M \approx 0.84$, $\alpha \approx 5.2^\circ$.

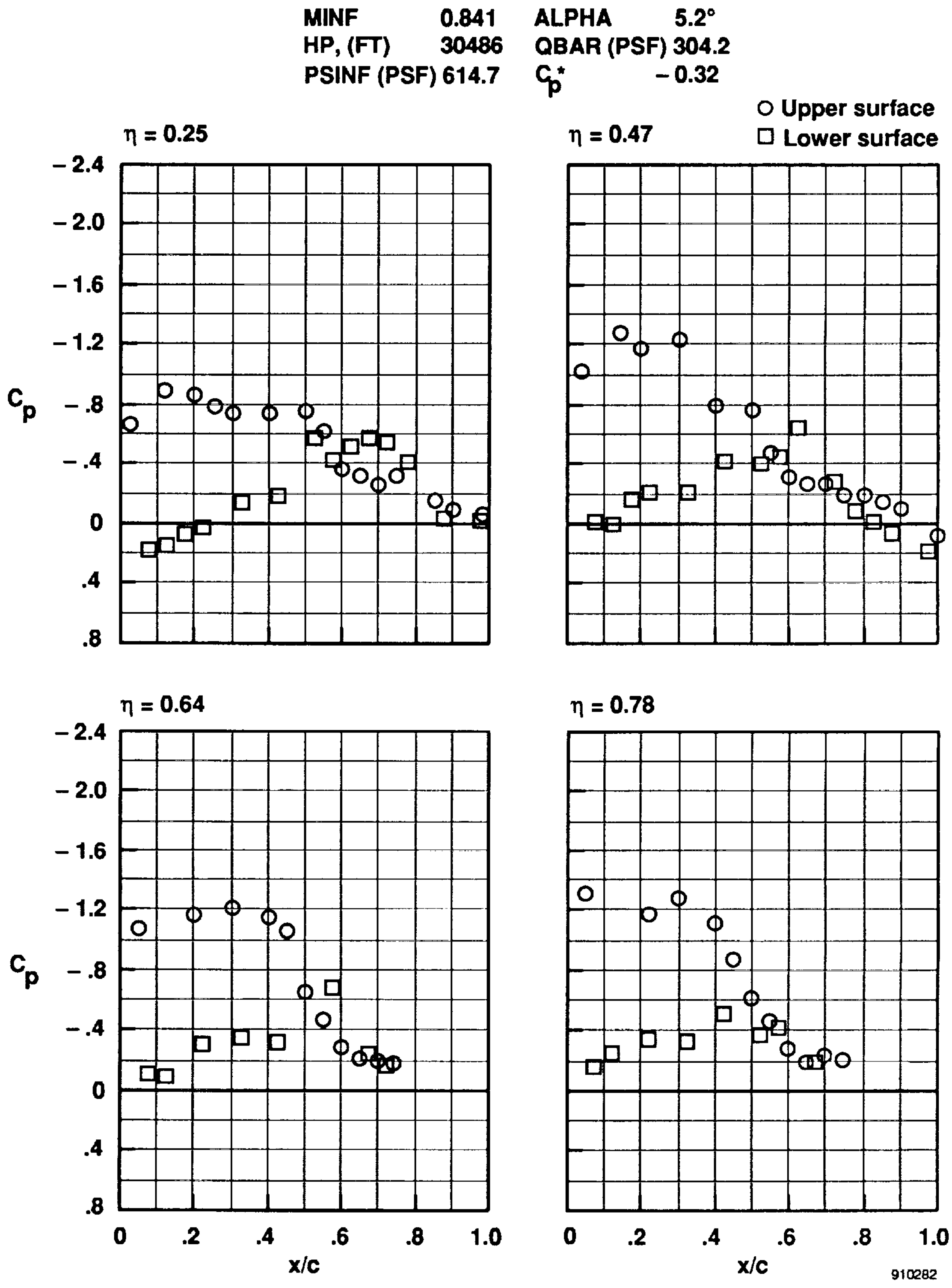

(b) Pylons off.

Figure 16. Continued.

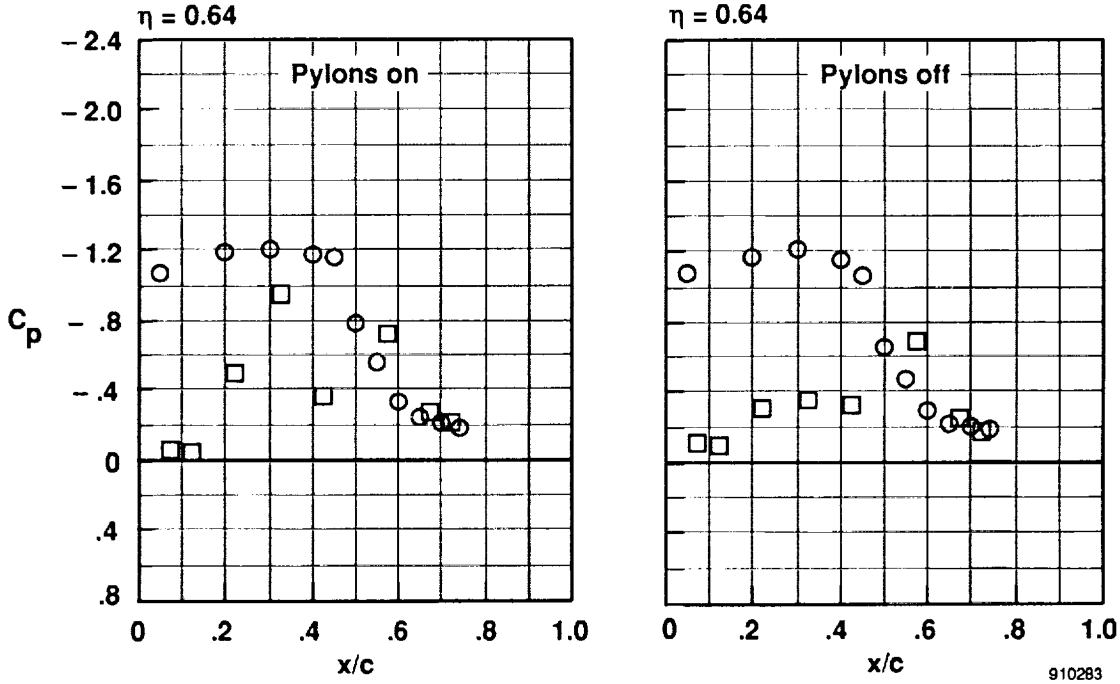

(c) Comparison for pylons on and pylons off at $\eta = 0.64$, $C_p^* = -0.32$.

Figure 16. Concluded.

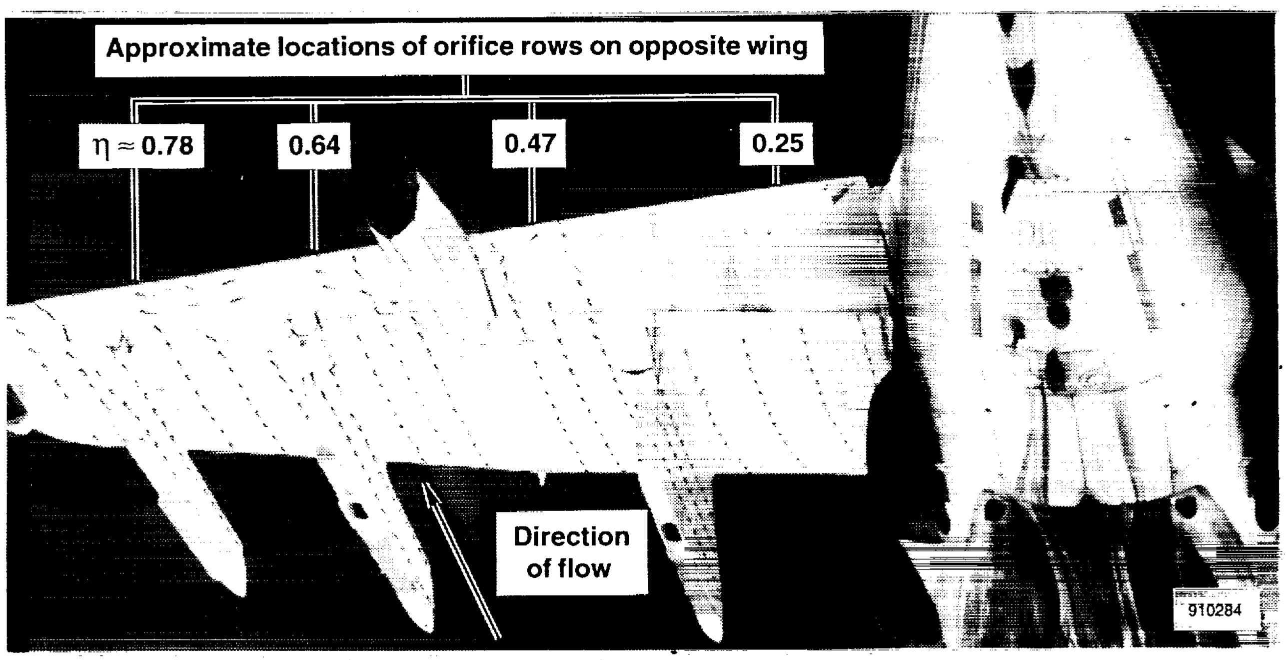

(a) Pylons on.

Figure 17. Flow cone patterns for the lower surface, $M \approx 0.84$, $\alpha \approx 5.2^\circ$.

ORIGINAL PAGE
BLACK AND WHITE PHOTOGRAPH

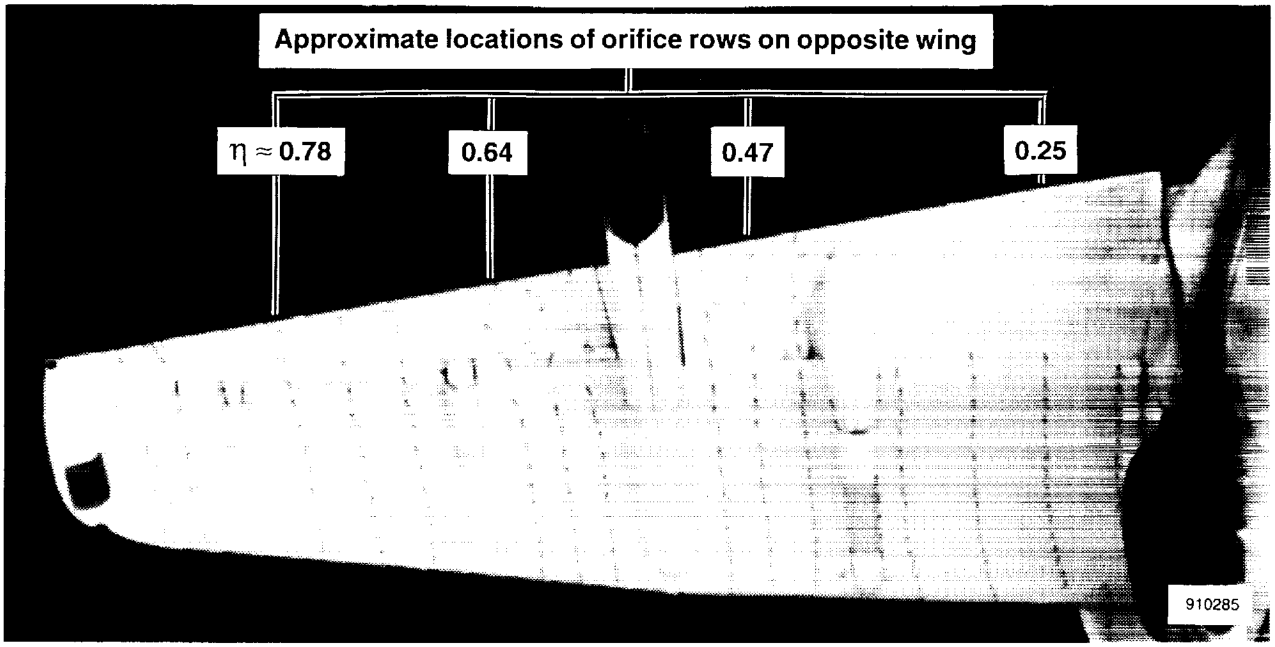

(b) Pylons off.

Figure 17. Concluded.

ORIGINAL PAGE
BLACK AND WHITE PHOTOGRAPH

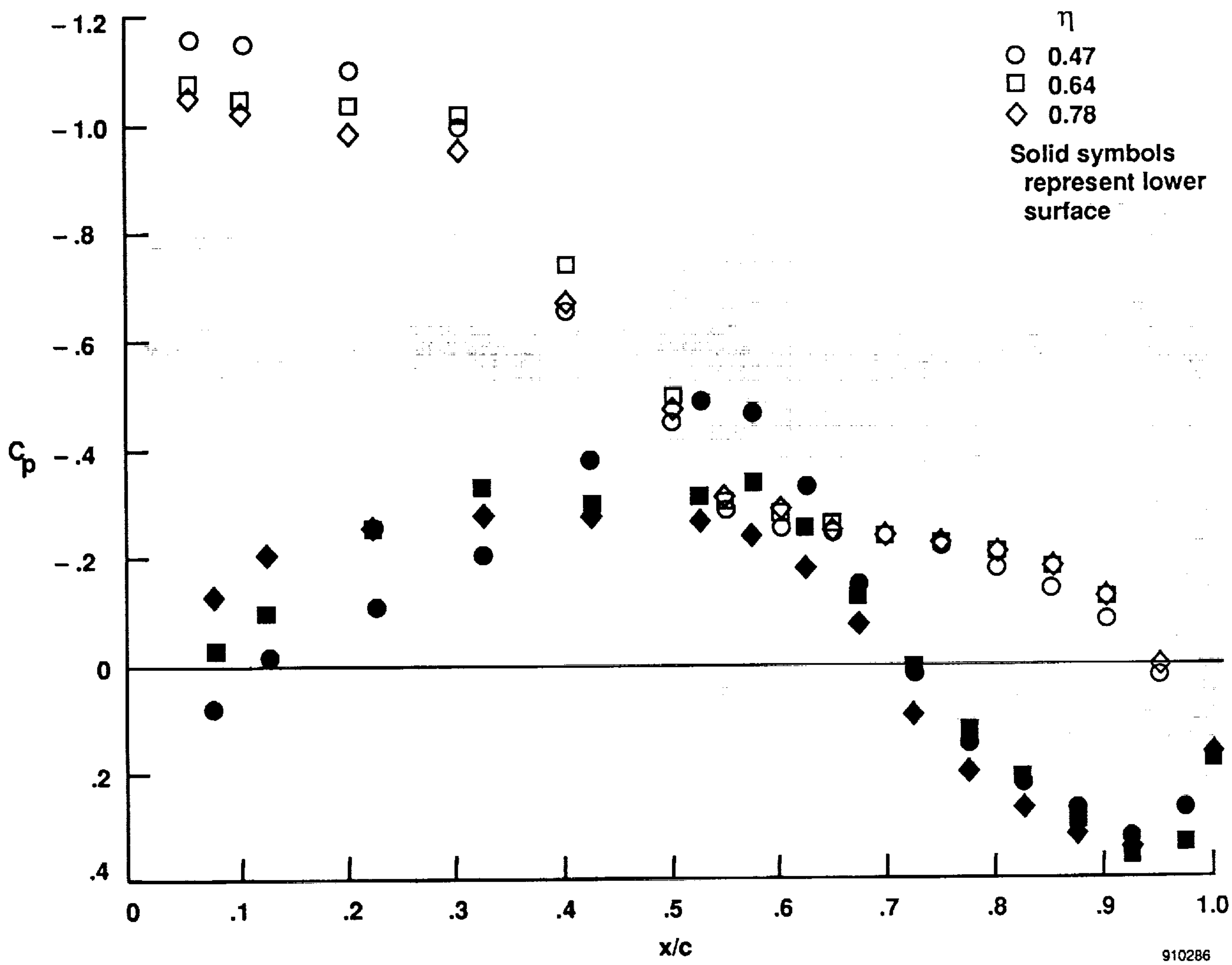

Figure 18. Relative aft loading from η = 0.47 to η = 0.78 for YAV-8B wing, 15-percent model data, M = 0.85, interpolated to $\alpha = 5.16^{\circ}$, reference 12.

Comparison at Near-Design Mach Number, $\alpha \approx 3.4°$

To achieve the characteristic supercritical chordwise pressure distribution, it is necessary to have the correct combination of Mach number and angle of attack (ref. 9). Figure 16 shows that some typical supercritical characteristics are evident for this wing at $M \approx 0.84$ and $\alpha \approx 5.2°$. There were no data for $M \approx 0.84$ at higher angles of attack, but there are data at lower angle of attack values, 3.3° to 3.4°. The data are shown in figures 19(a) and 19(b) where the upper surface pressure profiles are not well developed as compared to the levels for $\alpha \approx 5.2°$ (fig. 16). This would be expected based upon the well-known characteristic of supercritical airfoil performance to be sensitive to relatively small changes in Mach number and angle of attack. Thus, it is not surprising that the angle of attack for these data (fig. 19) is significantly below the Mach number–angle-of-attack envelope for high lift-drag ratio (L/D) shown in figure 13 whereas the conditions for figure 16 ($M \approx 0.84$, $\alpha \approx 5.2°$) are within the lower part of the envelope and closer to the design condition. Orifice-by-orifice examination of the data for figure 19 (pylons on to pylons off) reveals again the additional negative pressure coefficient peaks, for the lower surface associated with the convex fairings when pylons are installed. A noticeable example would be at x/c = 0.075 for η = 0.47 and x/c = 0.325 for η = 0.64.

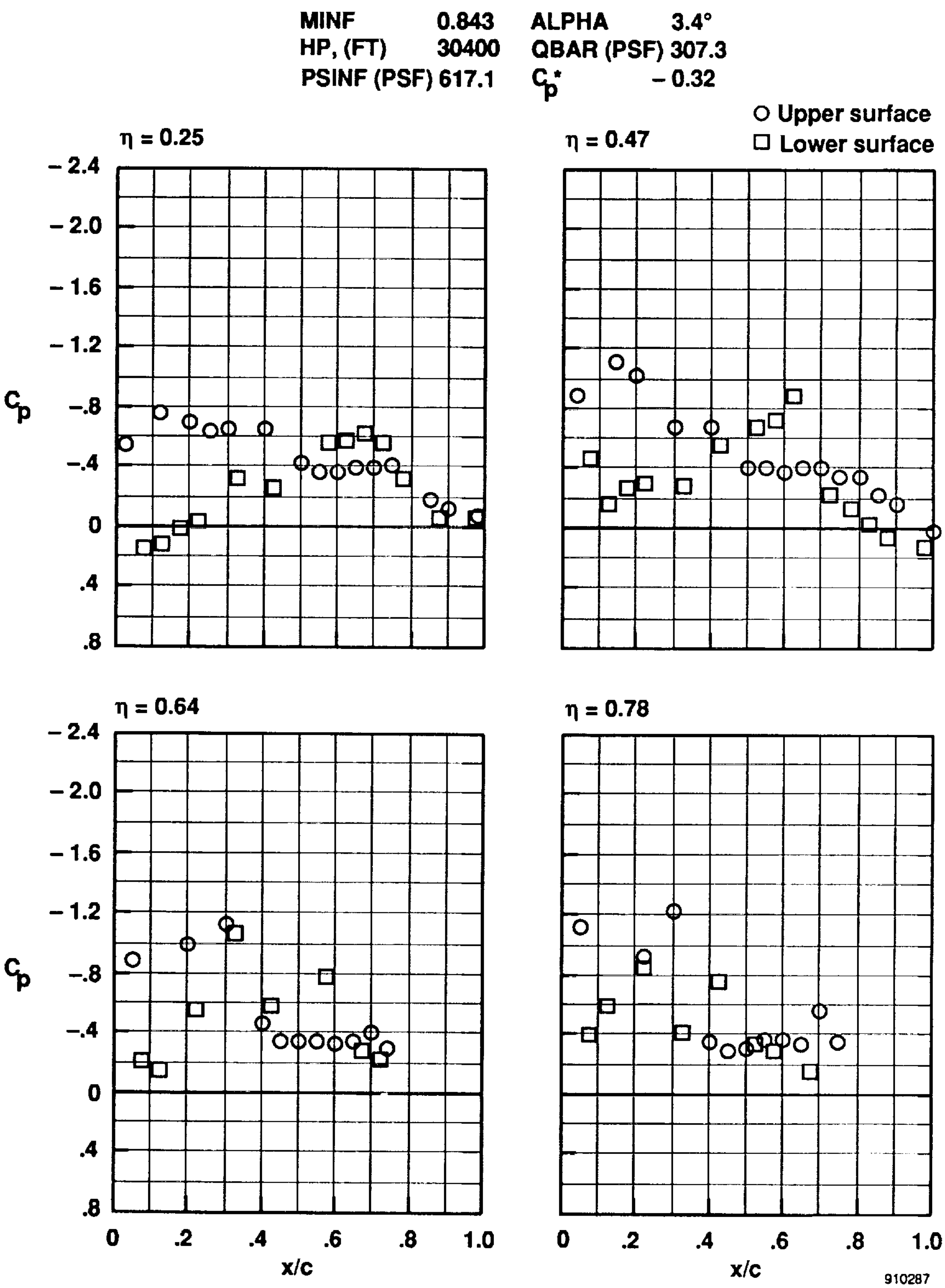

(a) Pylons on.

Figure 19. Chordwise distribution of pressure for $M \approx 0.84$, $\alpha \approx 3.3$ to 3.4°.

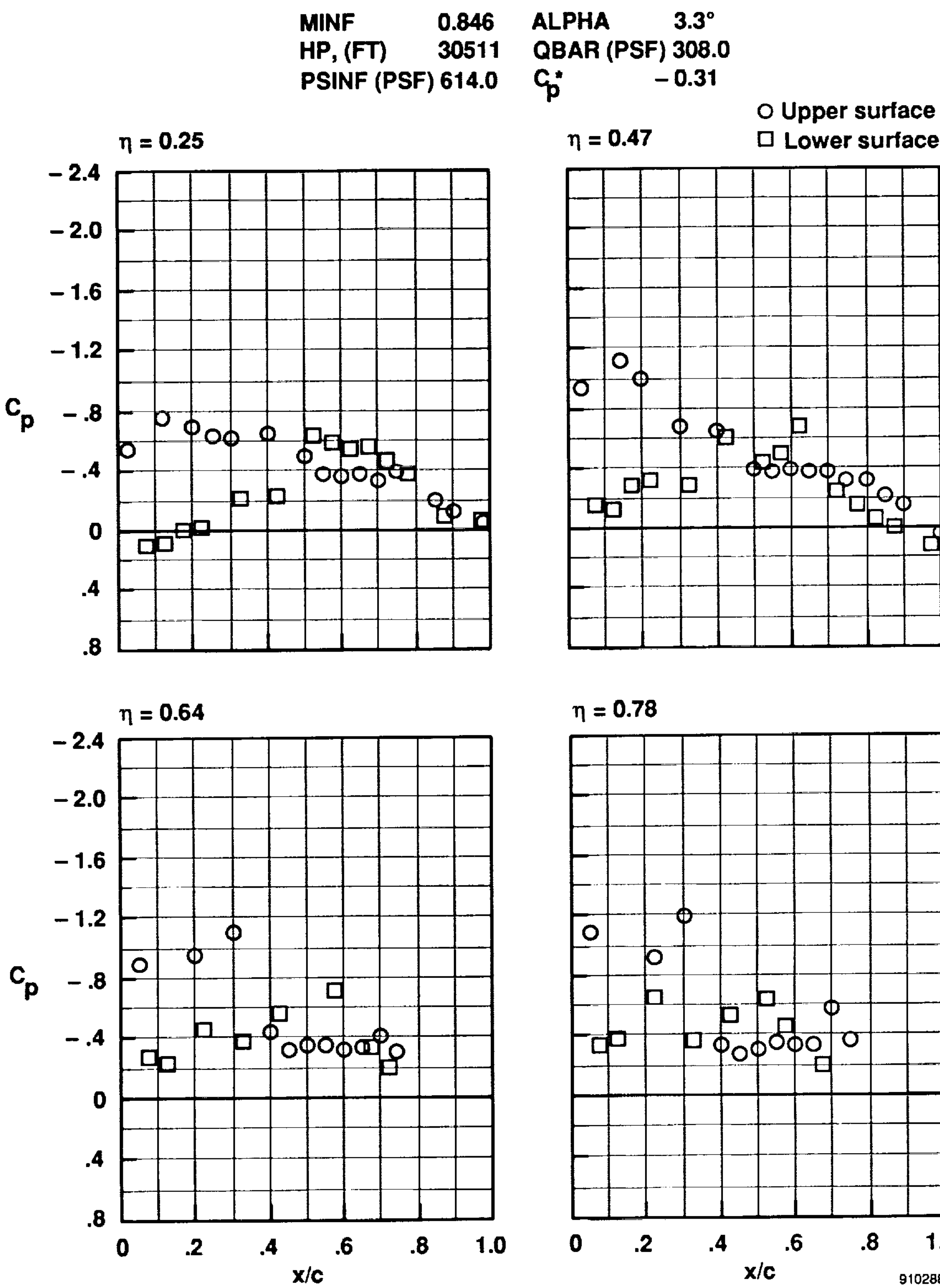

(b) Pylons off.

Figure 19. Concluded.

Comparison at Mach Numbers Near 0.87

The highest Mach number data obtained for an angle of attack reasonably close to the envelope for near-maximum L/D are shown in figures 20(a) and 20(b). Though the upper surface pressure coefficients for both configurations are less negative for this condition ($M \approx 0.87$, $\alpha \approx 4.0°$) than for some previously shown conditions which demonstrated supercritical pressure profiles; the recompression to sonic conditions, C_p^*, has been delayed to locations significantly farther aft on the wing, x/c $\geq$ 0.7. At η = 0.47, the flow over the upper surface appears to be attached over the entire instrumented portion of the section. For η = 0.25 attached flow is maintained to at least x/c = 0.9. There is no suggestion of separation for the two outboard rows where the pressure measurements end at the aileron hinge line. There are no corresponding flow cone data available to supplement the pressure data for this flight condition.

Though the upper surface pressure coefficients are unaffected by the pylons at these conditions; as noted earlier for $M \approx 0.84$, there are lower surface negative pressure coefficient peaks associated with the pylons. An example will be shown for η = 0.64 at three Mach numbers in figure 21, for $M \approx 0.87$ and two lower Mach numbers. These negative pressure coefficient peaks representing local shocks will be discussed in the next section.

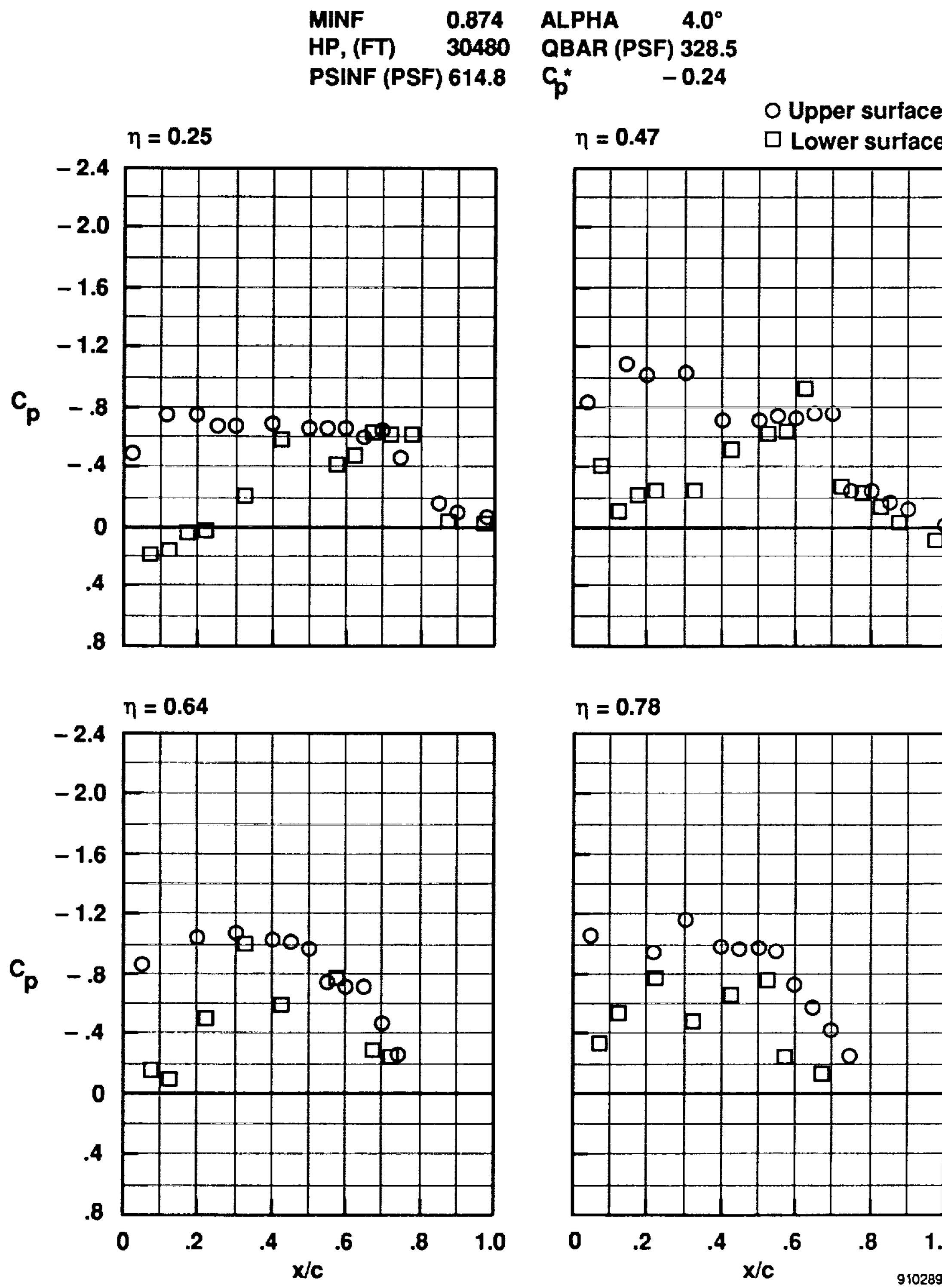

(a) Pylons on.

Figure 20. Chordwise distribution of pressure for $M \approx 0.875, \alpha \approx 4.0^\circ$.

MINF 0.875 ALPHA 4.0°
HP, (FT) 31192 QBAR (PSF) 318.6
PSINF (PSF) 595.1 C_p^* − 0.24

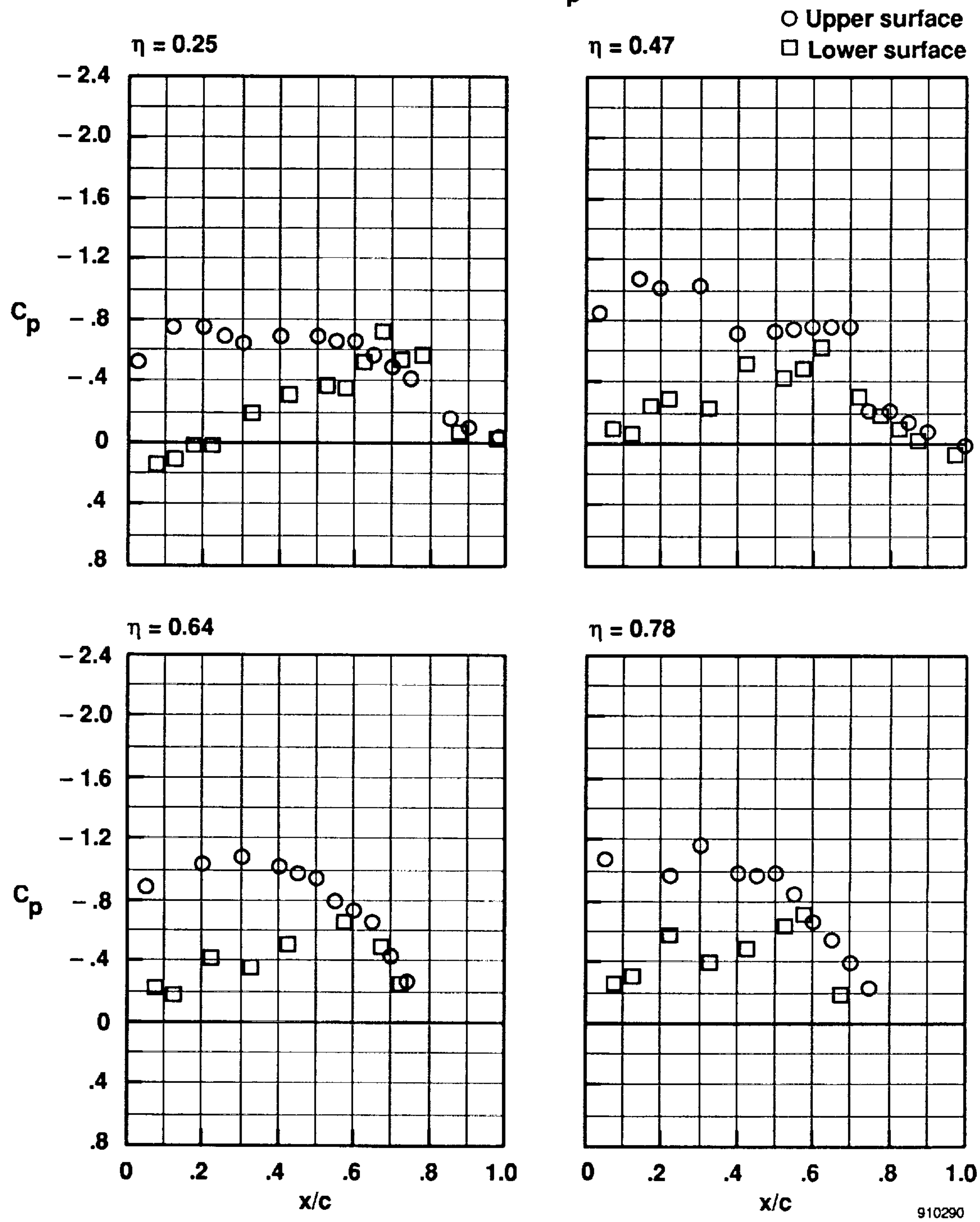

(b) Pylons off.

Figure 20. Concluded.

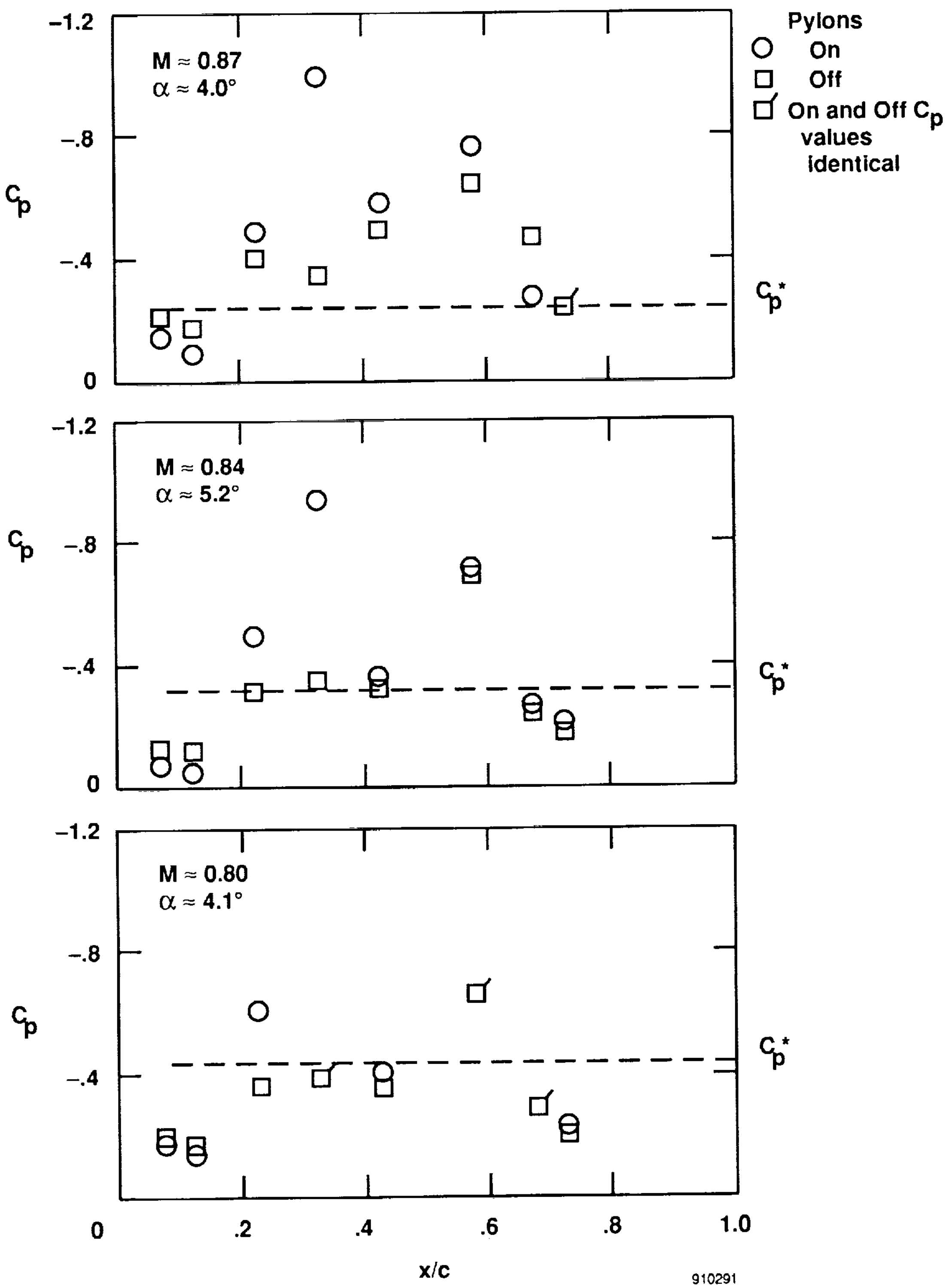

Figure 21. Effect of pylons on distribution of lower surface pressure at η = 0.64, for three Mach number–angle-of-attack combinations.

Comparison of Lower Surface Pressure Coefficients at Three Transonic Mach Numbers

In figure 21, pylons-on and pylons-off lower surface pressure profiles are compared for three transonic Mach numbers in which the Mach number and angle of attack for each configuration are closely matched. It has been previously established that the upper surface distribution of pressure is unaffected by the pylons for each Mach number. For the lower surface, however, there is a negative pressure coefficient peak associated with the pylons (see circular symbols, especially for x/c values from 0.22 to 0.32). As expected, the peak becomes more extreme as Mach number increases. Similar peaks, which represent local velocities that exceed the speed of sound, are also evident at the other semi-span stations having pressure orifices. The comparisons shown in figure 21 for $\eta = 0.64$ are the most graphic examples recorded, however.

For $M \approx 0.80$ and $M \approx 0.84$, critical pressure coefficient is exceeded (negatively) between x/c = 0.5 and 0.6 for the lower surface even without pylons, and a large portion of the lower surface section is supercritical at $M \approx 0.87$, without pylons. These local shocks are apparently caused by the flap–aileron actuator fairings and the large outrigger gear fairing. In summary, it is evident that at transonic speeds the wing lower surface experiences some shock losses without pylons and significantly greater shock losses when the pylons are installed. The accumulated effect of all the wing lower surface shocks results in wave drag and some related shock induced separation drag creeping upward as the transonic velocities increase.

Of the several orifice rows, the one at $\eta = 0.64$ shows the most prominent negative pressure coefficient peaks associated with the convex fairings. This is caused not only by the adjacent pylon and convex fairing located at $\eta = 0.70$ but it is probably compounded by the nearby outrigger fairing at $\eta = 0.56$ (fig. 7).

At Mach numbers significantly lower than those in figure 21, as compressibility effects diminish, the pressure peaks caused by the pylons are eliminated. Nevertheless, the general level of the lower surface pressure coefficients remains somewhat more negative for the outboard portions of the wing panel when the pylons are mounted. Thus, the wing lower surface contribution to overall lift is slightly reduced by the pylons throughout the Mach number range of these tests. The net effect of this will be evident through a different data format in following sections. The accumulated effects of the pylons will be presented through integrated pressure coefficients in the form of section and panel normal force coefficients.

Summary of Flight Conditions Providing Supercritical Upper Surface Pressure Plateaus

A typical supercritical upper surface pressure profile is described within the General Remarks portion of the Results and Discussion section. Figure 12 is a schematic of such a pressure profile, including the upper surface pressure plateau and the lower surface loading in the cusp region. Pressure profiles from flight exhibiting the upper surface pressure plateau characteristic have been shown in figures 16 and 20, and flight conditions which produce such profiles will be shown in subsequent figures.

Figure 22 shows the combinations of angle of attack and Mach number for all 59 data runs reported herein (39 runs for pylons off and 20 for pylons on). To qualify a data run as providing adequate upper surface supercritical pressure plateaus, as defined herein, the plateau must extend to x/c = 0.5 for all four orifice rows. The eight data runs in which the criterion was met are indicated by flagged symbols in figure 22. These eight data runs represent approximately one-fourth of the test conditions flown for $M \geq 0.8$. Note the symbols representing the approximate cruise and design conditions relative to these same eight flagged data run conditions. The performance enhancement in lift which occurs concurrently with meeting the preceding criterion will be evident in some of the panel normal force coefficient data to follow.

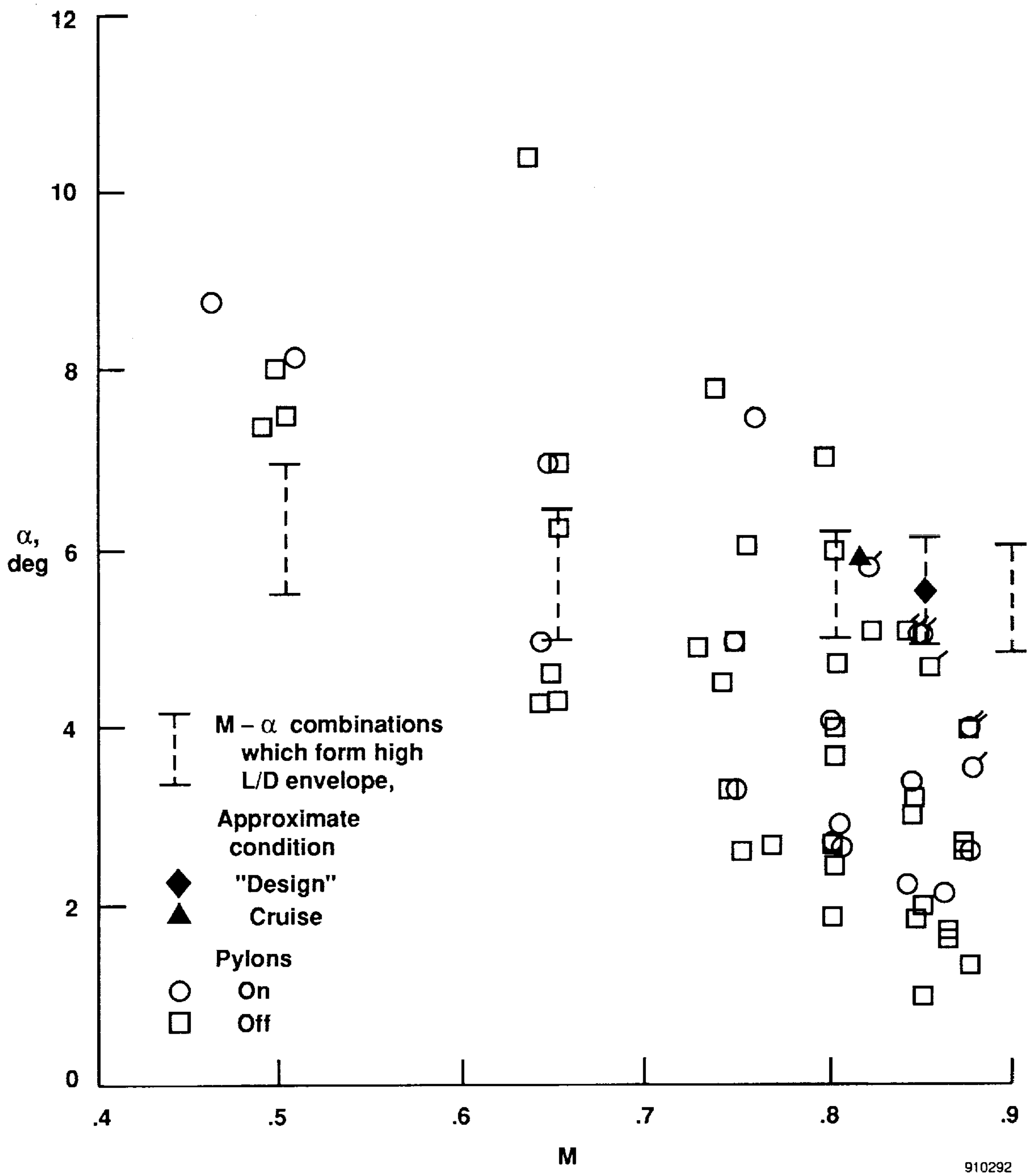

Figure 22. Mach number and angle-of-attack conditions for all flight data runs. Flagged symbols indicate supercritical upper surface pressure plateaus extend to $x/c \geq 0.5$.

Section and Panel Characteristics

General Remarks

To obtain section normal force coefficients from the pressure distribution data, it is necessary to integrate the pressures over the length of the local chord. Because pressure orifices were not included over the ailerons, there are no data available for the aft 30-percent chord for the two outboard rows of orifices, $\eta = 0.64$ and 0.78. Consequently, for these two sections the integrations to calculate c_n and c_m assumed linear pressure variations from the aft-most measured pressure to the trailing edge (assuming a trailing-edge pressure coefficient of zero). The pitching moment coefficients are considered, for this report, to be less important than the section and panel normal force coefficient data. However, because the moment coefficients are derived from the same pressure data as are the force coefficients, they have been computed and are tabulated in Appendixes G through L along with the c_n values.

Section Normal Force Coefficient

Section normal force coefficients presented as a function of angle of attack are presented for the four semi-span stations having pressure orifices, for pylons-on and pylons-off configurations, in figure 23. The abscissa origins are shifted to the right as consideration of each semi-span station changes from inboard to outboard.

Figure 23(a) is assembled from data for $M = 0.46$ to approximately 0.75 because for this range of Mach numbers it was assumed that compressibility effects, as a discriminator between the two configurations, would be a minor factor. For both configurations the slope, $dc_n/d\alpha$, is significantly greater for the three outboard stations than for the inboard station. Though the level of c_n for a given angle of attack is essentially the same for both configurations, at $\eta = 0.25$ and 0.47; the pylons tend to cause some reduction in loading, c_n, over the angle-of-attack range for the two outboard test sections. The average reduction is 0.03 to 0.04 in section normal force coefficient for the two outboard stations. For a Mach number of 0.8 (fig. 23 (b)), the data are limited; however, the trends in the data are similar to those for Mach numbers of 0.75 and below (fig. 23 (a)).

Figures 23(c) and 23(d) extend the comparison to Mach numbers of approximately 0.845 and 0.875 respectively. For these higher Mach numbers, the most inboard station again shows no significant effect of pylons on the level of c_n for a given angle of attack. On the other hand, the outboard station, $\eta = 0.78$, which showed some loss in loading (c_n per given angle of attack) with pylons at the lower Mach numbers now shows essentially the same loading for pylons on and off. In addition, the two middle stations experience reduced loading for the pylons-on configuration at $M \approx 0.845$ (fig. 23 (c)). Based on these observations and the detailed discussion of pressure distribution from earlier figures, this reduced loading results from changes in the lower surface pressure profiles because the upper surface pressure profiles are essentially identical for both configurations at these Mach numbers.

Though figure 23 provides identifiable differences in the level of c_n for a given angle of attack for the two configurations, differences in slope are minor and are not great enough to justify discrimination between the configurations. Therefore, slopes representative of both configurations have been combined for each semi-span station (row of orifices) and are shown in figure 24. The most significant features of the slopes are the higher values of the slopes for the three outboard stations, as compared to the inboard station, and the slopes all reach their maximum values near $M \approx 0.845$ and decrease somewhat at the higher Mach number, 0.875. The 15-percent scale model data (ref. 12) flagged symbols, also show lower slopes for the inboard row. At $M \approx 0.80$, the model slopes are significantly higher than the corresponding flight slopes for all four test chords.

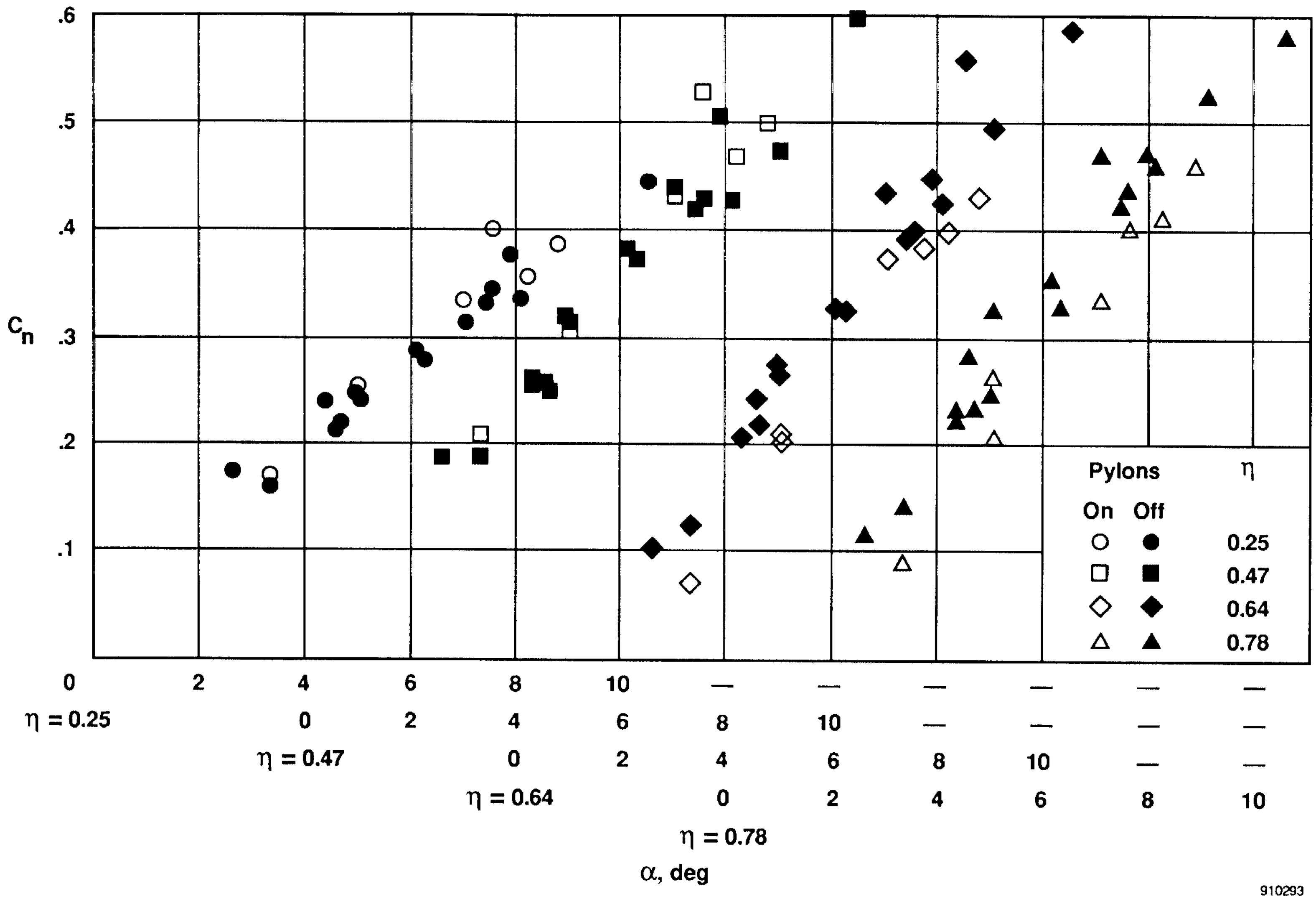

(a) $M \leq 0.75$.

Figure 23. The variation of section normal force coefficient with angle of attack, pylons on and pylons off.

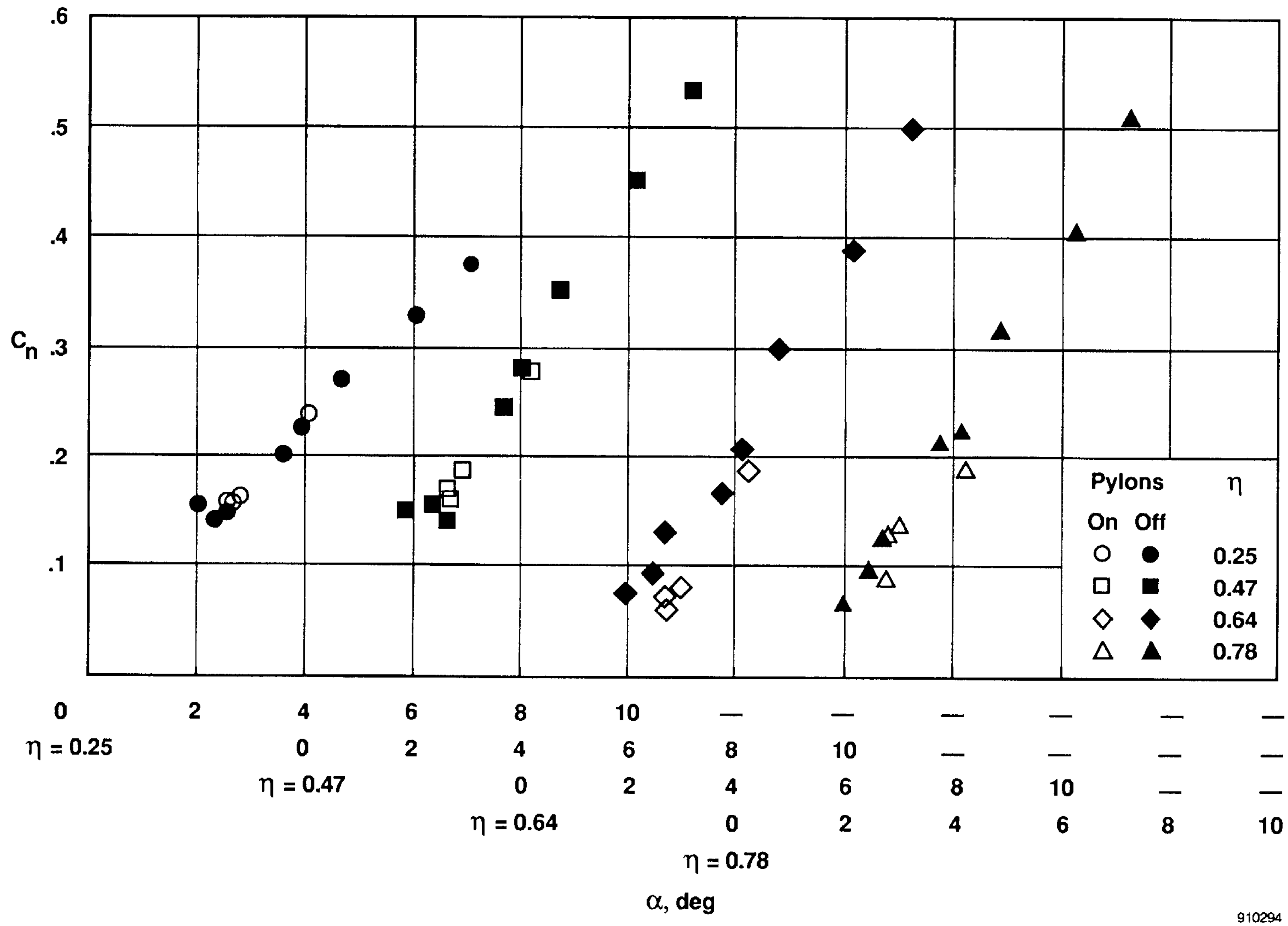

(b) $M \approx 0.80$.

Figure 23. Continued.

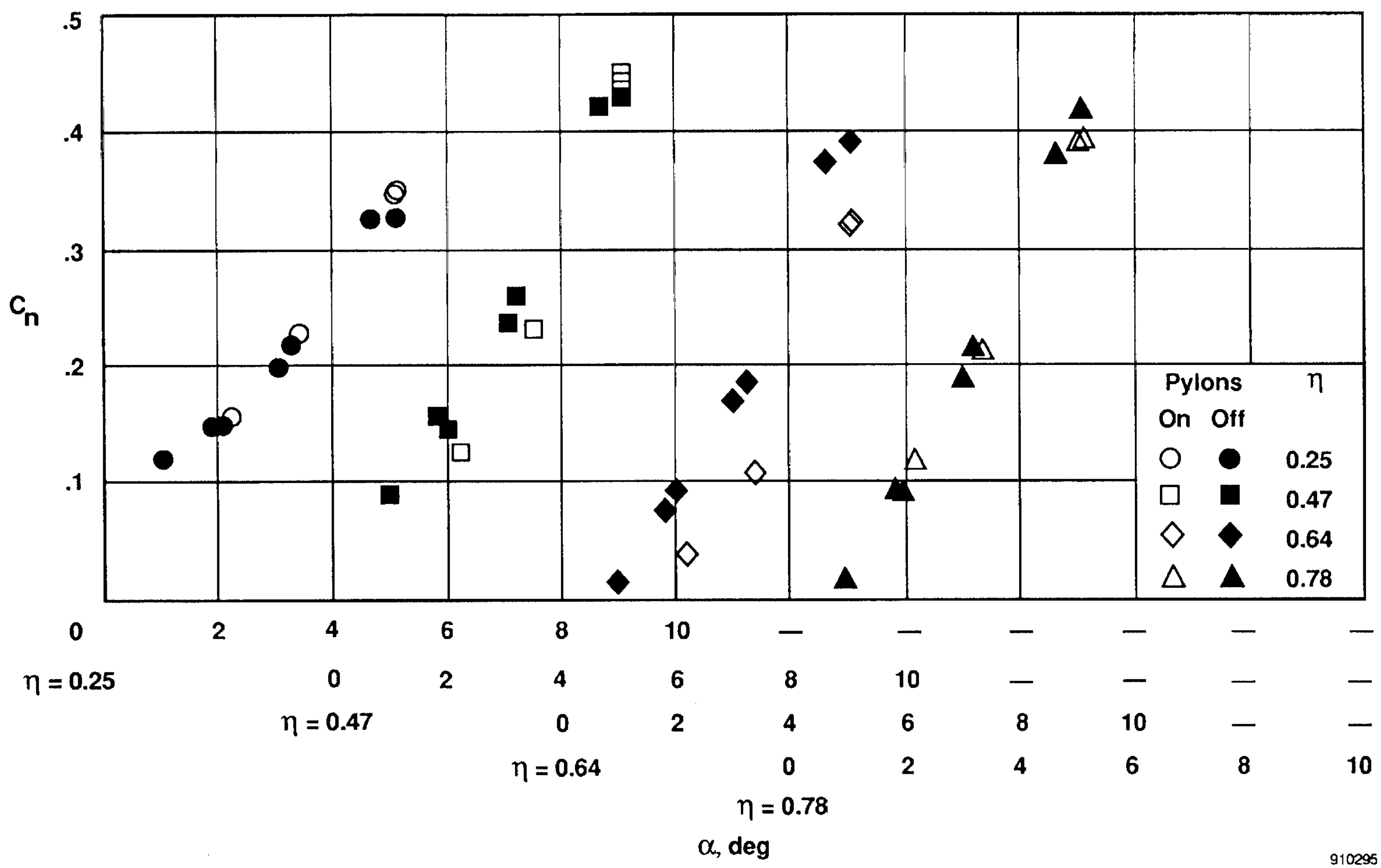

(c) $M \approx 0.845$.

Figure 23. Continued.

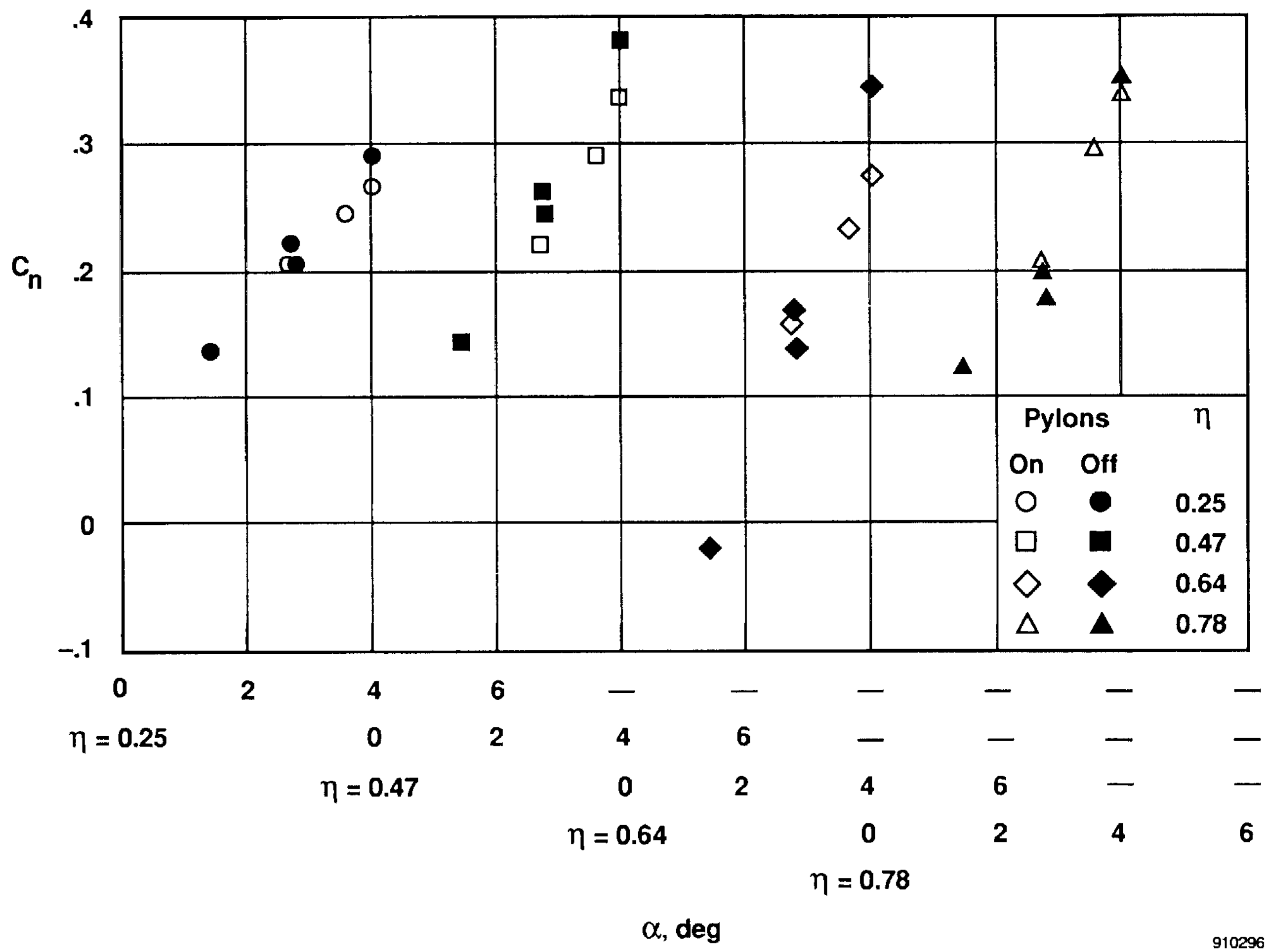

(d) $M \approx 0.875$.

Figure 23. Concluded.

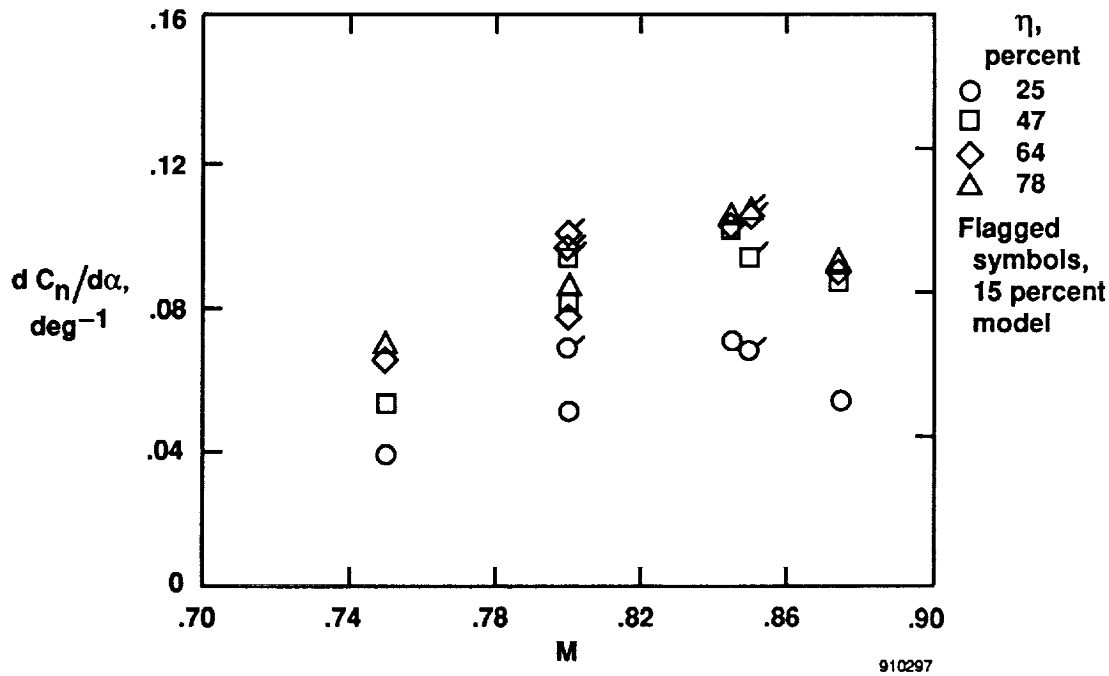

Figure 24. Slope of section normal force coefficients as a function of Mach number. Representative of pylons on and pylons off for flight and pylons off for 15-percent scale model.

Panel Normal Force Coefficient

Integration of chord-length weighted section normal force coefficients across the span has provided panel normal force coefficients for pylons-on and pylons-off configurations. Figure 25 is an example of the integrand for a flight condition where each of the four test stations displayed the characteristic flattened, supercritical, upper surface pressure plateau. The variation of the resulting panel normal force coefficients with angle of attack for both configurations is presented in figure 26 for the range of test Mach numbers. The level of $C_{N'}$ for a given angle of attack is close for the two configurations throughout the range of test Mach numbers; however, the values for pylons on tend to be slightly lower than for pylons off.

The data of figure 26 and corresponding data for $M \approx 0.82$ are assembled (all Mach numbers on the same plot) in figure 27 to make it easier to visualize Mach number and Mach number–angle-of-attack combination effects. As previously discussed, certain important combinations of Mach number and angle of attack are necessary to achieve the desired upper surface pressure coefficient plateau which is characteristic of supercritical flow. In figure 27, those data points in which all four test chords provided upper surface pressure plateaus extending at least to $x/c = 0.5$ have been flagged. The higher $C_{N'}$ values for each given angle of attack, for the flagged symbols, seem to demonstrate that panel normal force coefficient is enhanced when the supercritical plateau is extensive over the upper surface, which would be expected.

Figure 28 shows the variation of the slope of panel normal force coefficient with Mach number. The unflagged circular and square symbols show the mean flight slopes between $C_{N'} = 0$ and $C_{N'} = 0.3$ for the airplane with and without pylons, respectively. The effect of the addition of pylons on the panel normal force coefficient slopes is small and the differences shown are within the accuracy for these slopes. The diamond symbol at $M = 0.845$ represents the mean slope from the flight data for both configurations when considering only the data between $C_{N'} \approx 0.15$ and $C_{N'} \approx 0.30$ (or angles of attack above 3°). This greater slope for $M = 0.845$ and $\alpha > 3°$ relates to the earlier discussion about figure 27 in which it was observed that the presence of extended upper surface chordwise pressure plateaus was providing higher levels of $C_{N'}$ for a given angle of attack, as would be expected.

The flagged symbols in figure 28 represent the 15-percent scale model pressure data derived from reference 12. The flight panel $C_{N'}$ slope value at $M = 0.80$ is significantly lower, approximately 23 percent, than the model derived slope. The individual section normal force coefficient slopes for flight were also significantly lower than the model slopes for $M = 0.8$ as shown in figure 24.

The lower panel normal force coefficient slope for the full-scale YAV-8B (as compared to the model), especially at $M = 0.80$, is also evident in the format of figure 29. Here a panel normal force coefficient slope parameter, N, is plotted as a function of a planform or aspect ratio parameter F. This format was proposed by Diederich in 1951 (ref. 13) and later applied by Hoerner and Borst (ref. 14) as an aid in correlating lift curve slope data for configurations having different wing sweeps and aspect ratios for subsonic and low transonic compressible flow Mach numbers. This format has been used in figure 29[1] so that panel normal force coefficient slope data from the YAV-8B can be compared with slopes from other current aircraft with some accounting for differences in planform and Mach number.

The slopes for the other aircraft are from unpublished flight data for the AFTI/F-111, represented by a square symbol and flight data from the variable sweep F-14, various diamond symbols (ref. 15). Because this analysis procedure is restricted to "subsonic Mach numbers preferably not too near 1," as stated in reference 13, the comparisons of results from the three aircraft should be regarded as qualitative, and this is acknowledged through the format used in figure 30.

On this basis, the ratio of the N parameter for the three aircraft to the corresponding theoretical N parameter is plotted at the respective F parameter values in figure 30. The low value of this ratio at $M = 0.80$ for the YAV-8B, may be related to the fact that the panel normal force coefficient slope for flight is significantly lower than for the model as seen in figures 28 and 29. However, the YAV-8B panel efficiency ranks with the panel efficiency of the other aircraft as defined by this parameter for the Mach numbers equal to 0.845 or above, solid symbols. This format for portraying panel lifting efficiency is oblivious to the respective drag levels for the three wing panels considered in figures 29 and 30.

[1] The ordinate for the theoretical curve for figure 29, refs. 13 and 14, would be: $10 \frac{dC_L}{d\alpha} \frac{\sqrt{1-(M\cos\Lambda')^2}}{\cos\Lambda'}$

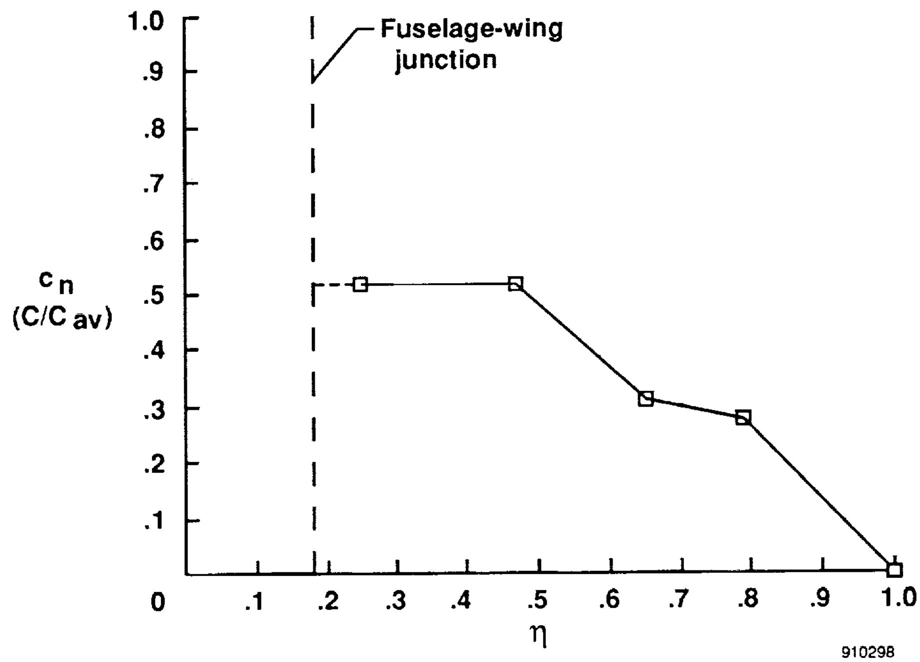

Figure 25. Example of integrand for obtaining panel normal force coefficient. $M \approx 0.82$, $\alpha \approx 5.9^\circ$, pylons on.

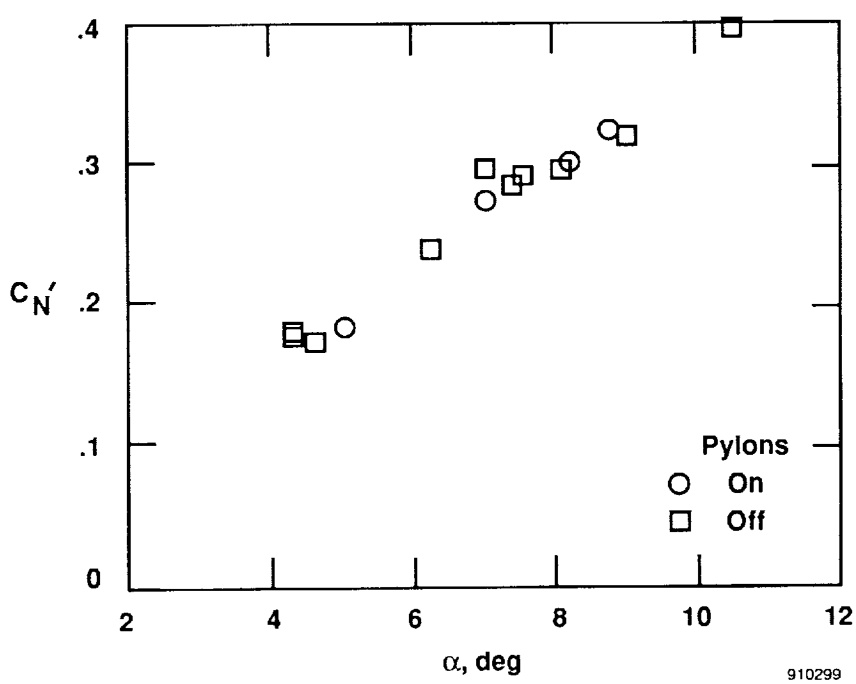

(a) $M \leq 0.65$.

Figure 26. The variation of panel normal force coefficient with angle of attack; pylons on and pylons off.

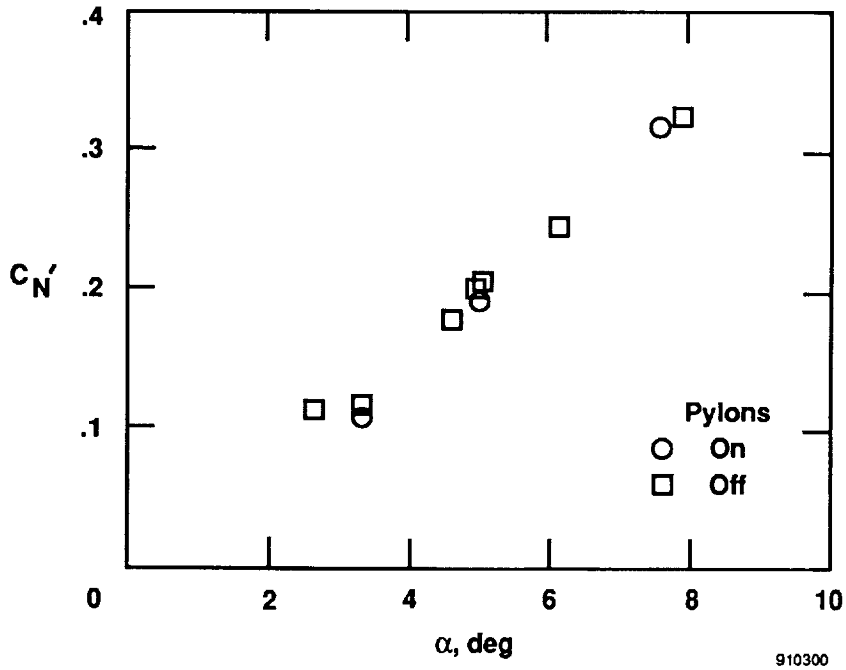

(b) $M \approx 0.75$.

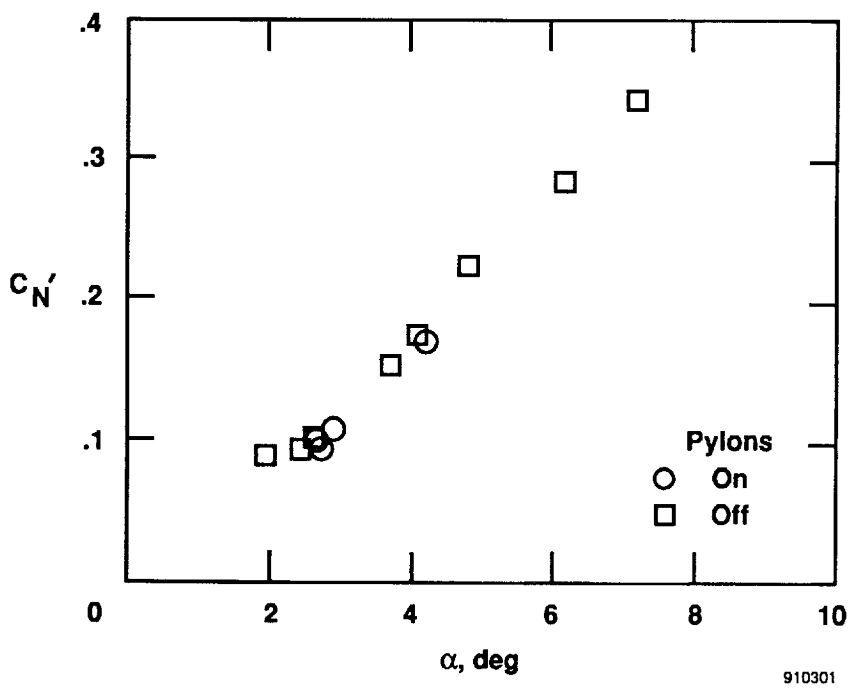

(c) $M \approx 0.80$.

Figure 26. Continued.

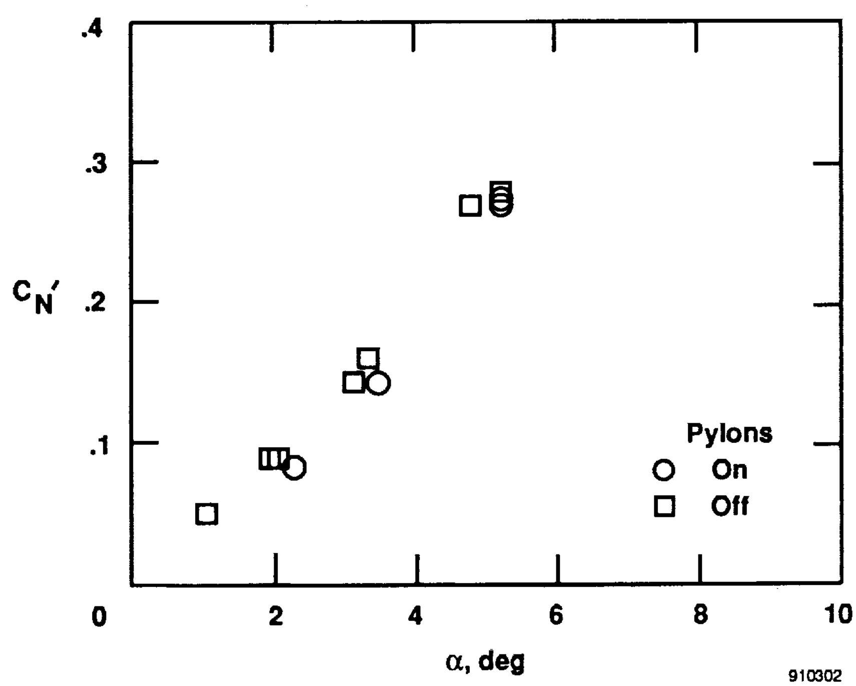

(d) $M \approx 0.845$.

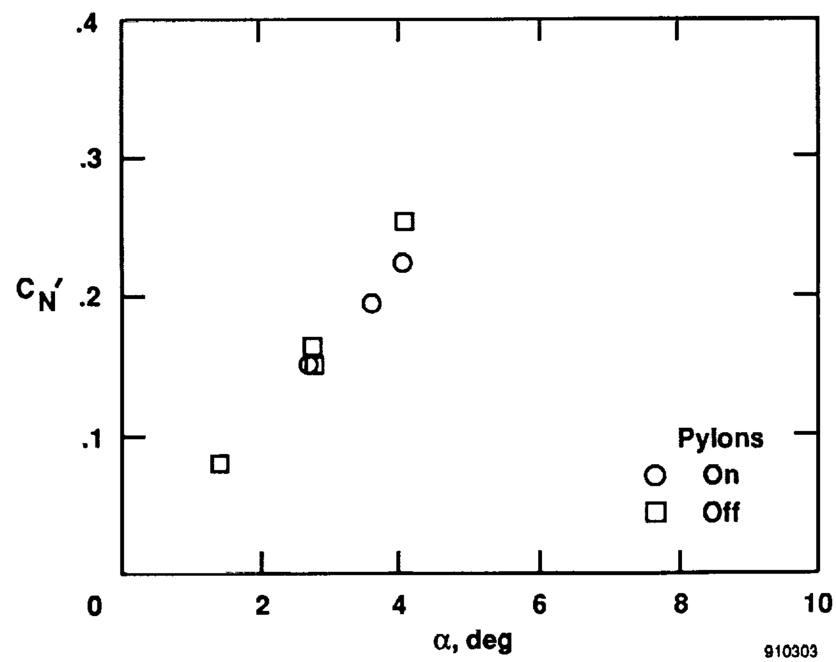

(e) $M \approx 0.875$.

Figure 26. Concluded.

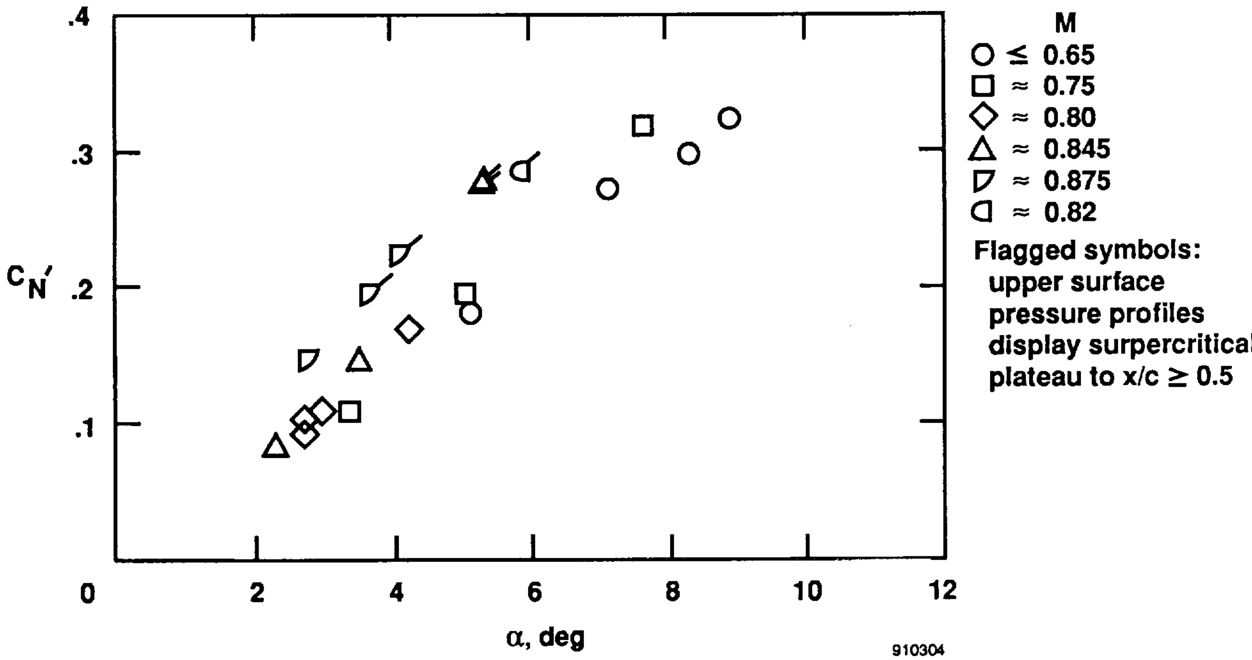

(a) Pylons on.

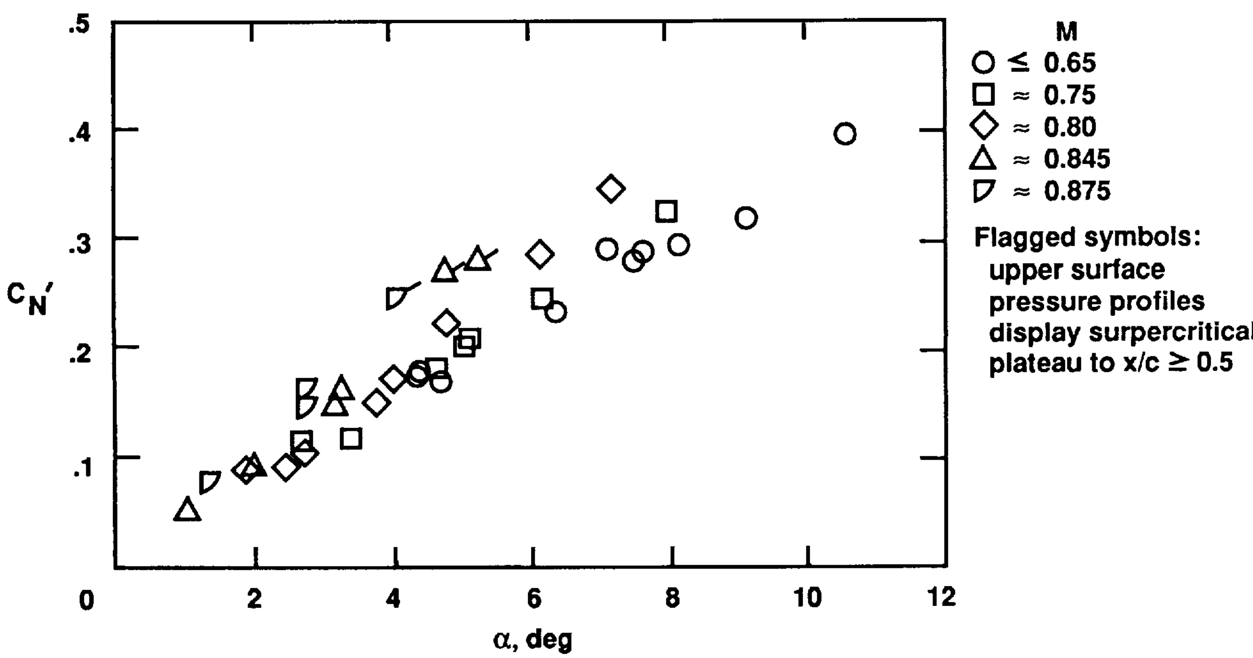

(b) Pylons off.

Figure 27. Panel normal force coefficient as a function of angle of attack for a range of Mach numbers.

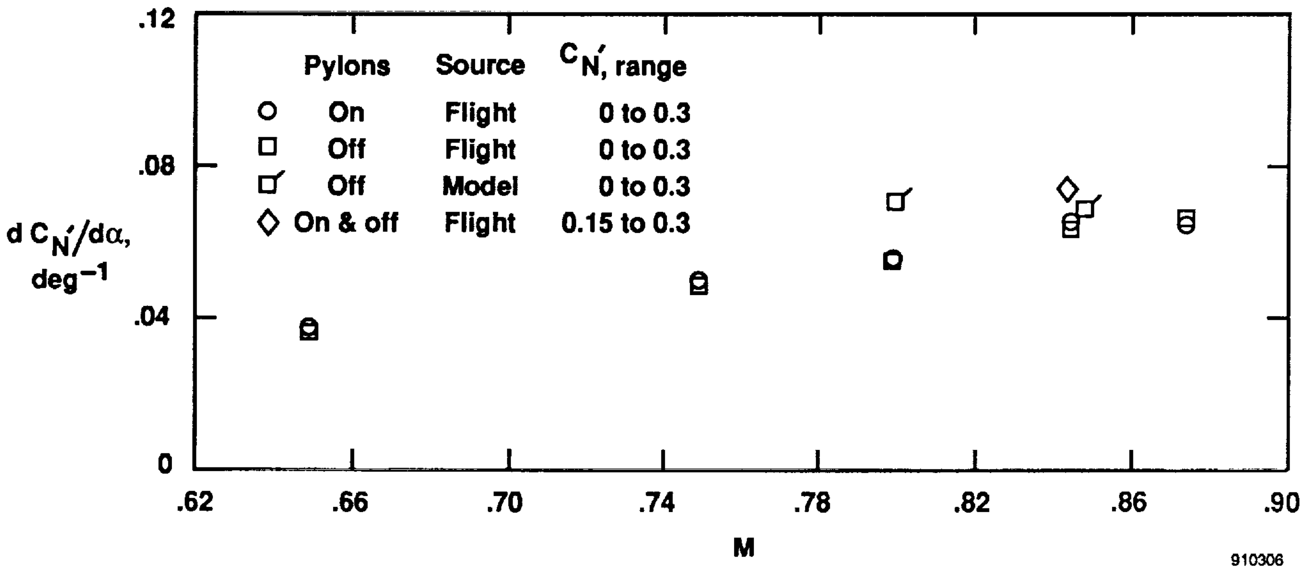

Figure 28. Slope of panel normal force coefficient as a function of Mach number.

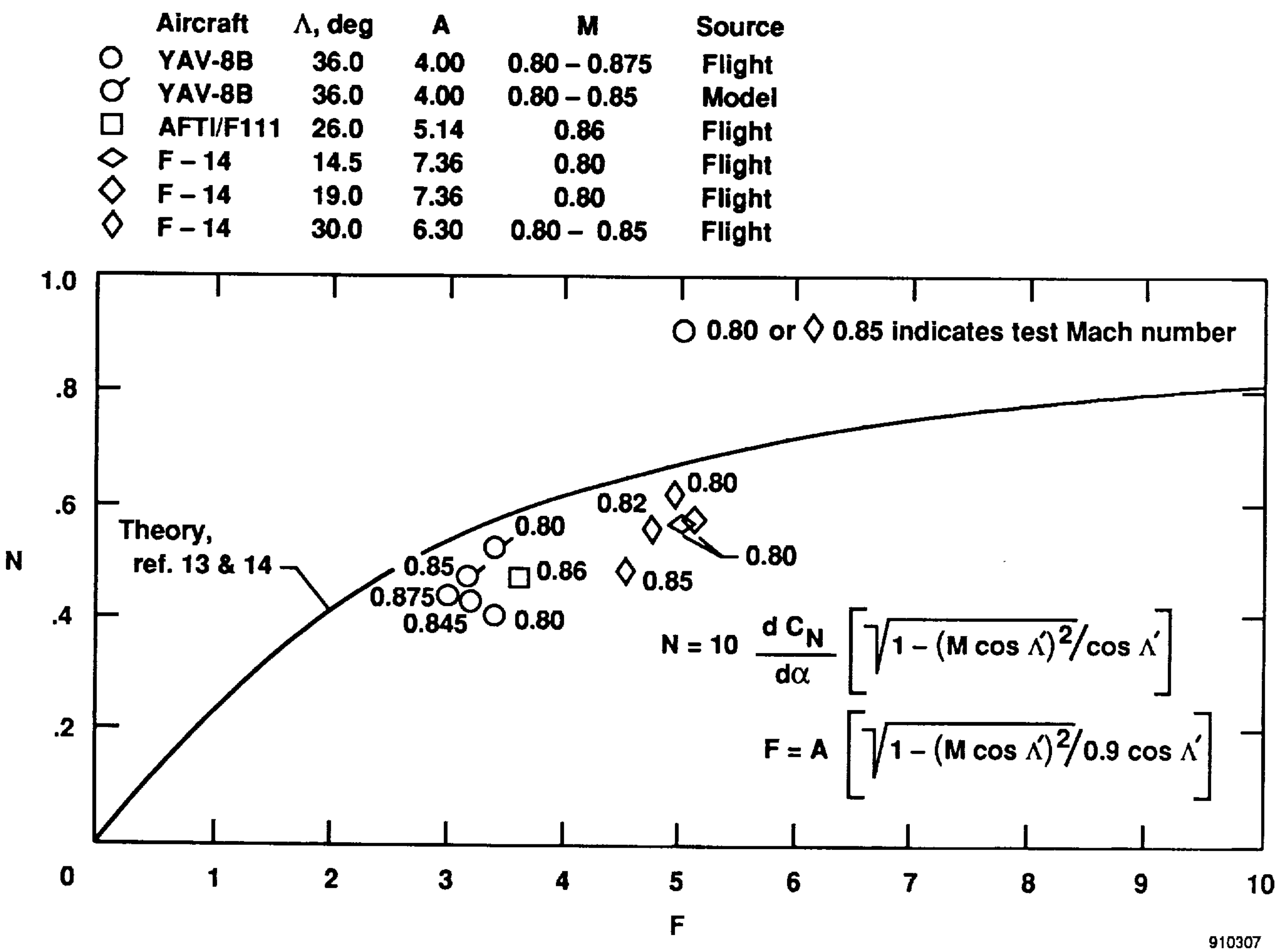

Figure 29. Panel normal force coefficient slope parameter, N, as a function of planform parameter, F, for swept wings at high subsonic Mach numbers.

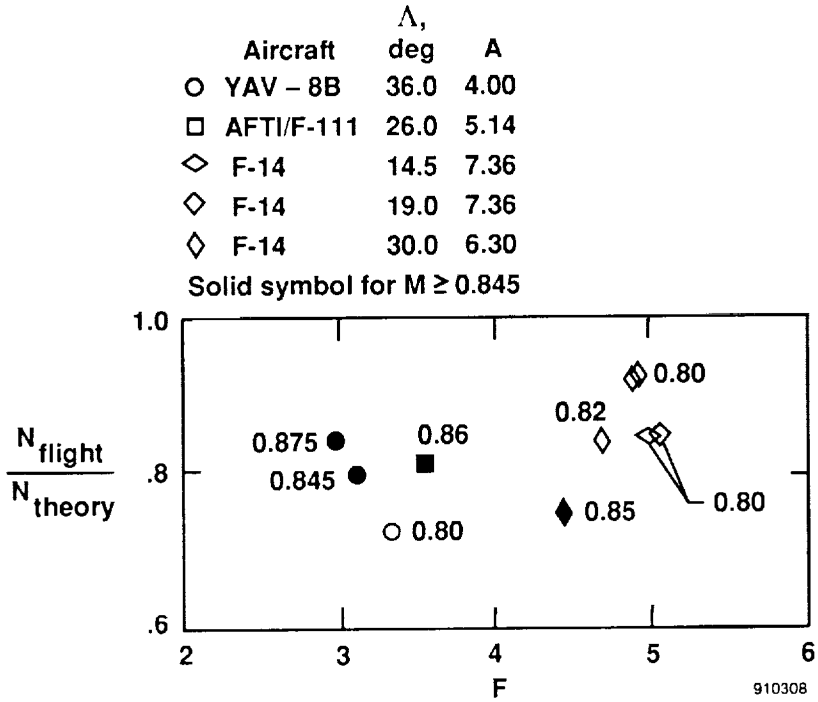

Figure 30. Ratio of panel normal force coefficient slope parameter for flight and theory (relative panel lifting efficiency) for three aircraft.

CONCLUDING REMARKS

Pressure distribution data have been obtained in flight at four span stations on the wing panel of the YAV-8B airplane having a supercritical airfoil. Data have been obtained for the wing panel with and without pylons installed over a Mach number range from 0.46 to approximately 0.88. The altitude ranged from approximately 20,000 to 40,000 ft and the resultant Reynolds numbers varied from approximately 7.2 million to 28.7 million based on the mean aerodynamic chord. Analysis of these flight data resulted in the following observations:

1. The chordwise pressure distribution data and flow visualization results show that the full-scale flight wing performance is compromised because the lower surface cusp region experiences flow separation for some important transonic flight conditions. This occurs while the upper surface flow is producing extensive supercritical pressure plateaus as well as at angles of attack and Mach numbers that are too low to provide the characteristic upper surface supercritical chordwise pressure profiles.

2. Local shocks occur on the lower surface of the wing (mostly between 20-and 35-percent chord) when the pylons are installed for Mach numbers of approximately 0.8 and above. It is believed that convex fairings which cover the pylon attachment flanges cause these local shocks. Pressure coefficients significantly more negative than that for sonic flow also occur farther aft on the lower surface (near 60-percent chord) irrespective of whether the pylons are installed for $M \geq 0.8$. It is probable that these negative pressure coefficient peaks cause drag creep from the shock losses, per se, and in some instances, from local shock induced separation.

3. The more negative pressure coefficients associated with the local shocks and the convex fairings on the wing lower surface, with pylons, cause the level of C_N for a given angle of attack to be somewhat lower than for

the wing without pylons, for $M \geq 0.8$. However, the effect of pylons on the slope of C_N with angle of attack was not significant.

4. The slope of the panel normal force coefficient with angle of attack for the full-scale wing was significantly lower (approximately 23 percent) than for the 15-percent scale model at Mach 0.8.

5. Upper surface chordwise pressure distributions demonstrate a characteristic supercritical pressure plateau for Mach numbers from 0.82 to about 0.87 for angles of attack near 5.9° and 4.0°, respectively. These flight conditions provide similar upper surface pressure profiles for the wing with and without pylons.

6. Flow visualization data show attached flow over the entire wing panel upper surface throughout the Mach number and angle-of-attack range and of these tests irrespective of whether the pylons were installed.

Table 1. Physical dimensions of the YAV-8B. Information extracted from ref. 5.

	Wing (theo)	Stabilator	V-tail
S (projected), ft^2	230.0	47.54	25.83
Aspect ratio	4.0	4.08	1.23
λ, taper ratio	0.300	.201	.268
b (projected), ft	30.33	13.92	--
b/2 (projected), in.	181.99	83.54	(h) 67.50
C, root (projected), in.	139.99	67.39	86.93
C, tip (projected), in.	42.00	17.83	23.30
$\bar{c}$ (projected), in.	99.79	46.44	61.24
Λ L.E. (projected)	36°	39.80°	47.36°
Λ C/4 (projected)	30.62°	33.91°	40.37°
t/c, root, percent	11.5	7.0	8.2
t/c, tip, percent	7.5	7.0	5.2
Incidence	3°	--	--
Dihedral	−11°	−15.84°	--
Twist	−8°	--	--
Displacement	--	+12.75°, −11.75°*	--
Airfoil	Modified Supercritical	HSA**	HSA

*Includes ±1°30' autostab

**Hawker Siddeley Aviation

Control surface	Area (projected)	Span (projected)	Deflection
Flap	15.49 ft^2/side	64.54 in./side	+7°, +25°, +61.7°
Aileron	6.19 ft^2/side	58.90 in./side	±27°**
Rudder	5.27 ft^2	60.75 in.	±15°
Speedbrake	4.5 ft^2	36.5 in.	66°

**Includes 15° aileron droop and ±2° autostab

Wetted areas, ft^2	
Fuselage	541
Wing	379
H-tail	84
V-tail	52
Outrigger pod	45
Ventral	11
Total	1112

Table 2(a). Coordinates for the four test sections, z′.

	Harrier YAV-88 wing ordinates, in.							
	η = 0.25		η = 0.47		η = 0.64		η = 0.79*	
Station, percent	Upper surface	Lower surface	Upper surface	Lower surface	Upper surface	Lower surface	Upper surface	Lower surface
0.00	−0.994	– –	−3.266	– –	−3.762	– –	−3.149	– –
0.25	0.037	−1.909	−2.355	−4.197	−3.080	−4.560	−2.673	−3.014
0.50	0.513	−2.789	−2.031	−4.509	−2.814	−4.710	−2.440	−3.847
0.75	0.827	−3.132	−1.789	−4.736	−2.634	−4.871	−2.272	−3.997
1.00	1.064	−3.383	−1.585	−4.922	−2.470	−5.015	−2.153	−4.096
1.25	1.300	−3.635	−1.387	−5.102	−2.325	−5.137	−2.034	−4.195
1.50	1.468	−3.812	−1.261	−5.206	−2.221	−5.212	−1.955	−4.246
1.75	1.613	−3.965	−1.134	−5.310	−2.117	−5.288	−1.875	−4.297
2.00	1.759	−4.118	−1.008	−5.414	−2.013	−5.364	−1.796	−4.349
3.00	2.260	−4.657	−0.573	−5.709	−1.670	−5.583	−1.522	−4.502
4.00	2.626	−5.070	−0.233	−5.994	−1.395	−5.722	−1.304	−4.605
5.00	2.895	−5.408	0.045	−6.170	−1.156	−5.816	−1.114	−4.705
6.00	3.119	−5.702	0.287	−6.305	−0.944	−5.888	−0.946	−4.728
8.00	3.489	−6.204	0.717	−6.509	−0.573	−5.983	−0.647	−4.743
10.00	3.785	−6.617	1.090	−6.648	−0.236	−6.028	−0.369	−4.751
15.00	4.348	−7.396	1.872	−6.841	0.489	−6.016	0.231	−4.677
20.00	4.753	−7.930	2.501	−6.883	1.093	−5.892	0.738	−4.517
25.00	5.000	−8.306	3.005	−6.800	1.620	−5.682	1.192	−4.293
30.00	5.174	−8.474	3.437	−6.639	2.088	−5.406	1.600	−4.021
35.00	5.282	−8.569	3.812	−6.407	2.508	−5.068	1.971	−3.651
40.00	5.322	−8.557	4.133	−6.090	2.891	−4.597	2.312	−3.349
45.00	5.296	−8.433	4.404	−5.597	3.243	−4.220	2.622	−2.956
50.00	5.202	−8.121	4.629	−5.199	3.563	−3.705	2.901	−2.525
55.00	5.069	−7.788	4.814	−4.620	3.854	−3.119	3.158	−2.033
60.00	4.920	−7.189	4.974	−3.909	4.111	−2.433	3.390	−1.394
65.00	4.748	−6.269	5.103	−2.985	4.350	−1.499	3.595	−0.846
70.00	4.506	−5.058	5.167	−1.718	4.552	−0.620	3.772	−0.785
72.00	4.300	−4.509	5.177	−1.346	4.617	−0.191	3.822	0.248
74.00	4.216	−3.752	5.176	−0.828	4.669	0.251	3.863	0.586
76.00	4.057	−3.402	5.164	−0.298	4.714	0.707	3.899	0.931
78.00	3.888	−2.811	5.142	0.243	4.750	1.166	3.931	1.274
80.00	3.710	−2.198	5.109	0.784	4.779	1.621	3.957	1.610
82.00	3.524	−1.598	5.064	1.304	4.799	2.054	3.979	2.061
84.00	3.328	−1.037	5.005	1.796	4.808	2.459	3.991	2.250
86.00	3.123	−0.549	4.934	2.233	4.803	2.970	3.992	2.486
88.00	2.904	−0.145	4.844	2.597	4.780	3.190	3.977	2.713
90.00	2.672	0.196	4.726	2.930	4.740	3.387	3.943	2.895
92.00	2.429	0.468	4.577	3.148	4.671	3.576	3.888	3.033
94.00	2.179	0.665	4.401	3.246	4.573	3.707	3.809	3.128

Table 2(a). Concluded.

	Harrier YAV-88 wing ordinates, in.							
	$\eta = 0.25$		$\eta = 0.47$		$\eta = 0.64$		$\eta = 0.79$*	
Station percent	Upper surface	Lower surface	Upper surface	Lower surface	Upper surface	Lower surface	Upper surface	Lower surface
96.00	1.922	0.785	4.196	3.309	4.445	3.774	3.707	3.172
98.00	1.662	0.779	3.971	3.285	4.298	3.773	3.586	3.164
100.00	1.401	0.680	3.729	3.155	4.137	3.688	3.451	3.081

*Note: the manufacturer provided dimensions for $\eta = 0.79$ but the orifice row was as $\eta = 0.78$ because of access hatch location.

Table 2(b). Location of orifices, percent chord.

Orifice	η = 0.25		η = 0.47		η = 0.64		η = 0.78	
order	Upper	Lower	Upper	Lower	Upper	Lower	Upper	Lower
1	2.5	7.5	4	7.5	5	7.5	5	7.5
2	12	12.5	14	12.5	20	12.5	22	12.5
3	20	17.5	20	17.5	30	22.5	30	22.5
4	25	22.5	30	22.5	40	32.5	40	32.5
5	30	32.5	40	32.5	45	42.5	45	42.5
6	40	42.5	50	42.5	50	~~52.5~~	50	52.5
7	50	(52.5)	55	52.5	55	57.5	55	57.5
8	55	57.5	60	57.5	60	67.5	60	67.5
9	60	62.5	65	62.5	65	72.5	65	
10	65	67.5	70	~~67.5~~	70		70	
11	70	72.5	75	72.5	74		75	
12	75	77.5	80	77.5				
13	85	~~82.5~~	85	82.5				
14	90	87.5	90	87.5				
15	98.4	97.5	100	97.5				
C,in.	126.0		96.5		75.4		61.6	

Note: a location "slashed-out," as ~~52.5~~ , means orifice was inoperative for all flights.
A location indicated as (52.5) means orifice was inoperative for some flights.

APPENDIX A
SURFACE PRESSURE COEFFICIENTS, PYLONS ON, HP $\approx$ 20,000 FT

	M	α, deg
1	.456	8.8
2	.504	8.2
3	.640	5.1
4	.747	3.3
5	.800	2.7
6	.803	2.9
7	.805	2.7
8	.842	2.3
9	.859	2.2

Table A-1

MINF = .456
HP = 20229
PSINF = 963.2
PRI = 951.3
QBAR = 140.1
ALPHA = 8.8

Upper surface

X/C	CP	X/C	CP	X/C	CP	X/C	CP
η = 0.25		η = 0.47		η = 0.64		η = 0.78	
.025	−1.257	.040	−1.525	.050	−1.432	.050	−1.492
.120	−.824	.140	−.848	.200	−.756	.220	−.672
.200	−.704	.200	−.775	.300	−.743	.300	−.707
.250	−.601	.300	−.649	.400	−.543	.400	−.556
.300	−.647	.400	−.568	.450	−.514	.450	−.487
.400	−.503	.500	−.474	.500	−.479	.500	−.451
.500	−.404	.550	−.448	.550	−.425	.550	−.448
.550	−.357	.600	−.374	.600	−.371	.600	−.438
.600	−.405	.650	−.393	.650	−.384	.650	−.398
.650	−.318	.700	−.393	.700	−.391	.700	−.494
.700	−.282	.750	−.283	.740	−.317	.750	−.388
.750	−.242	.800	−.283				
.850	−.119	.850	−.214				
.900	−.057	.900	−.169				
.984	−.040	1.000	−.018				

Lower surface

X/C	CP	X/C	CP	X/C	CP	X/C	CP
η = 0.25		η = 0.47		η = 0.64		η = 0.78	
.075	.280	.075	.147	.075	.241	.075	.126
.125	.297	.125	.160	.125	.175	.125	.035
.175	.166	.175	.050	.225	−.085	.225	−.088
.225	.136	.225	−.005	.325	−.141	.325	−.152
.325	.040	.325	−.021	.425	−.194	.425	−.215
.425	−.188	.425	−.160	.525	−.248	.525	−.226
.525	−.294	.525	−.218	.575	−.303	.575	−.196
.575	−.401	.575	−.224	.675	−.149	.675	−.080
.625	−.442	.625	−.259	.725	−.119		
.675	−.343	.725	−.086				
.725	−.342	.775	.001				
.775	−.085	.825	.093				
.825	.011	.875	.211				
.875	.109	.975	.177				
.975	.033						

Table A-2

MINF = .504
HP = 20423
PSINF = 955.4
PRI = 939.8
QBAR = 169.8
ALPHA = 8.2

Upper surface

X/C	CP	X/C	CP	X/C	CP	X/C	CP
η = 0.25		η = 0.47		η = 0.64		η = 0.78	
.025	−1.261	.040	−1.464	.050	−1.357	.050	−1.378
.120	−.784	.140	−.817	.200	−.725	.220	−.640
.200	−.665	.200	−.749	.300	−.723	.300	−.689
.250	−.557	.300	−.632	.400	−.520	.400	−.532
.300	−.566	.400	−.553	.450	−.496	.450	−.453
.400	−.470	.500	−.463	.500	−.469	.500	−.435
.500	−.387	.550	−.440	.550	−.417	.550	−.431
.550	−.342	.600	−.375	.600	−.369	.600	−.417
.600	−.386	.650	−.389	.650	−.383	.650	−.383
.650	−.321	.700	−.389	.700	−.381	.700	−.487
.700	−.281	.750	−.283	.740	−.311	.750	−.367
.750	−.251	.800	−.283				
.850	−.123	.850	−.218				
.900	−.056	.900	−.170				
.984	−.039	1.000	−.013				

Lower surface

X/C	CP	X/C	CP	X/C	CP	X/C	CP
η = 0.25		η = 0.47		η = 0.64		η = 0.78	
.075	.276	.075	.098	.075	.191	.075	.088
.125	.274	.125	.121	.125	.134	.125	−.107
.175	.153	.175	.019	.225	−.126	.225	−.120
.225	.120	.225	−.040	.325	−.172	.325	−.167
.325	.008	.325	−.051	.425	−.206	.425	−.242
.425	−.202	.425	−.190	.525	−.262	.525	−.239
.525	−.304	.525	−.237	.575	−.318	.575	−.211
.575	−.405	.575	−.250	.675	−.158	.675	−.088
.625	−.450	.625	−.277	.725	−.119		
.675	−.356	.725	−.095				
.725	−.333	.775	−.006				
.775	−.108	.825	.094				
.825	−.001	.875	.212				
.875	.105	.975	.181				
.975	.044						

Table A-3

MINF = .640
HP= 20352
PSINF = 958.2
PRI = 925.1
QBAR = 274.4
ALPHA = 5.1

Upper surface

X/C	CP	X/C	CP	X/C	CP	X/C	CP
η = 0.25		η = 0.47		η = 0.64		η = 0.78	
.025	−1.002	.040	−1.229	.050	−.939	.050	−.909
.120	−.652	.140	−.646	.200	−.585	.220	−.502
.200	−.568	.200	−.641	.300	−.654	.300	−.604
.250	−.512	.300	−.546	.400	−.454	.400	−.444
.300	−.485	.400	−.495	.450	−.424	.450	−.386
.400	−.433	.500	−.428	.500	−.434	.500	−.380
.500	−.375	.550	−.408	.550	−.384	.550	−.380
.550	−.351	.600	−.355	.600	−.352	.600	−.361
.600	−.355	.650	−.368	.650	−.361	.650	−.336
.650	−.333	.700	−.368	.700	−.368	.700	−.456
.700	−.298	.750	−.292	.740	−.295	.750	−.343
.750	−.295	.800	−.292				
.850	−.153	.850	−.214				
.900	−.087	.900	−.175				
.984	−.073	1.000	.013				

Lower surface

X/C	CP	X/C	CP	X/C	CP	X/C	CP
η = 0.25		η = 0.47		η = 0.64		η = 0.78	
.075	.172	.075	−.168	.075	−.100	.075	−.212
.125	.157	.125	−.063	.125	−.098	.125	−.250
.175	.046	.175	−.171	.225	−.378	.225	−.321
.225	−.012	.225	−.210	.325	−.338	.325	−.344
.325	−.133	.325	−.216	.425	−.331	.425	−.393
.425	−.303	.425	−.350	.525	−.387	.525	−.340
.525	−.380	.525	−.358	.575	−.444	.575	−.312
.575	−.457	.575	−.370	.675	−.226	.675	−.145
.625	−.501	.625	−.382	.725	−.166		
.675	−.419	.725	−.151				
.725	−.353	.775	−.047				
.775	−.203	.825	.073				
.825	−.079	.875	.192				
.875	.044	.975	.190				
.975	.041						

Table A-4

MINF =	.747
HP=	20350
PSINF =	958.3
PRI =	905.3
QBAR =	373.9
ALPHA =	3.3

Upper surface

X/C	CP	X/C	CP	X/C	CP	X/C	CP
η = 0.25		η = 0.47		η = 0.64		η = 0.78	
.025	−.753	.040	−1.161	.050	−.672	.050	−.662
.120	−.589	.140	−.544	.200	−.532	.220	−.461
.200	−.532	.200	−.611	.300	−.662	.300	−.595
.250	−.493	.300	−.520	.400	−.435	.400	−.433
.300	−.464	.400	−.487	.450	−.405	.450	−.376
.400	−.429	.500	−.427	.500	−.436	.500	−.375
.500	−.380	.550	−.410	.550	−.387	.550	−.374
.550	−.353	.600	−.368	.600	−.353	.600	−.350
.600	−.353	.650	−.380	.650	−.356	.650	−.327
.650	−.350	.700	−.380	.700	−.384	.700	−.472
.700	−.323	.750	−.314	.740	−.288	.750	−.346
.750	−.330	.800	−.314				
.850	−.166	.850	−.215				
.900	−.101	.900	−.172				
.984	−.089	1.000	.028				

Lower surface

X/C	CP	X/C	CP	X/C	CP	X/C	CP
η = 0.25		η = 0.47		η = 0.64		η = 0.78	
.075	.106	.075	−.384	.075	−.270	.075	−.459
.125	.089	.125	−.184	.125	−.235	.125	−.477
.175	−.017	.175	−.286	.225	−.697	.225	−.484
.225	−.095	.225	−.323	.325	−.450	.325	−.515
.325	−.226	.325	−.326	.425	−.419	.425	−.524
.425	−.357	.425	−.512	.525	−.497	.525	−.409
.525	−.423	.525	−.475	.575	−.574	.575	−.357
.575	−.490	.575	−.472	.675	−.280	.675	−.164
.625	−.545	.625	−.472	.725	−.211		
.675	−.446	.725	−.173				
.725	−.384	.775	−.034				
.775	−.264	.825	.030				
.825	−.147	.875	.133				
.875	−.030	.975	.196				
.975	.001						

Table A-5

MINF = .800
HP= 20454
PSINF = 954.1
PRI = 887.0
QBAR = 427.1
ALPHA = 2.7

Upper surface

X/C	CP	X/C	CP	X/C	CP	X/C	CP
η = 0.25		η = 0.47		η = 0.64		η = 0.78	
.025	−.598	.040	−.970	.050	−.887	.050	−.853
.120	−.585	.140	−.641	.200	−.572	.220	−.517
.200	−.582	.200	−.548	.300	−.902	.300	−.619
.250	−.505	.300	−.523	.400	−.453	.400	−.458
.300	−.470	.400	−.501	.450	−.418	.450	−.389
.400	−.451	.500	−.452	.500	−.464	.500	−.394
.500	−.401	.550	−.429	.550	−.412	.550	−.398
.550	−.370	.600	−.392	.600	−.373	.600	−.364
.600	−.374	.650	−.401	.650	−.378	.650	−.341
.650	−.375	.700	−.401	.700	−.421	.700	−.524
.700	−.358	.750	−.335	.740	−.307	.750	−.365
.750	−.372	.800	−.335				
.850	−.189	.850	−.229				
.900	−.121	.900	−.173				
.984	−.091	1.000	.037				

Lower surface

X/C	CP	X/C	CP	X/C	CP	X/C	CP
η = 0.25		η = 0.47		η = 0.64		η = 0.78	
.075	.105	.075	−.514	.075	−.286	.075	−.478
.125	.088	.125	−.205	.125	−.232	.125	−.700
.175	−.018	.175	−.309	.225	−.665	.225	−.477
.225	−.095	.225	−.336	.325	−1.111	.325	−.528
.325	−.253	.325	−.335	.425	−.404	.425	−.839
.425	−.356	.425	−.568	.525	−.547	.525	−.383
.525	−.444	.525	−.738	.575	−.690	.575	−.341
.575	−.532	.575	−.671	.675	−.288	.675	−.153
.625	−.636	.625	−.470	.725	−.216		
.675	−.504	.725	−.173				
.725	−.397	.775	−.080				
.775	−.284	.825	−.002				
.825	−.191	.875	.119				
.875	−.097	.975	.185				
.975	−.076						

Table A-6

MINF = .803
HP= 20489
PSINF = 952.7
PRI = 885.8
QBAR = 429.6
ALPHA = 2.9

Upper surface

X/C	CP	X/C	CP	X/C	CP	X/C	CP
η = 0.25		η = 0.47		η = 0.64		η = 0.78	
.025	−.590	.040	−.944	.050	−.930	.050	−1.052
.120	−.611	.140	−.937	.200	−.608	.220	−.563
.200	−.601	.200	−.514	.300	−.938	.300	−.649
.250	−.530	.300	−.516	.400	−.460	.400	−.463
.300	−.477	.400	−.502	.450	−.424	.450	−.389
.400	−.457	.500	−.457	.500	−.469	.500	−.397
.500	−.406	.550	−.430	.550	−.416	.550	−.400
.550	−.368	.600	−.389	.600	−.375	.600	−.368
.600	−.380	.650	−.398	.650	−.382	.650	−.344
.650	−.370	.700	−.398	.700	−.425	.700	−.551
.700	−.348	.750	−.334	.740	−.320	.750	−.379
.750	−.364	.800	−.334				
.850	−.187	.850	−.229				
.900	−.116	.900	−.175				
.984	−.085	1.000	.038				

Lower surface

X/C	CP	X/C	CP	X/C	CP	X/C	CP
η = 0.25		η = 0.47		η = 0.64		η = 0.78	
.075	.119	.075	−.491	.075	−.271	.075	−.453
.125	.108	.125	−.190	.125	−.214	.125	−.672
.175	−.002	.175	−.294	.225	−.651	.225	−.466
.225	−.074	.225	−.320	.325	−1.142	.325	−.511
.325	−.245	.325	−.324	.425	−.398	.425	−.823
.425	−.338	.425	−.555	.525	−.552	.525	−.365
.525	−.447	.525	−.727	.575	−.706	.575	−.327
.575	−.555	.575	−.757	.675	−.282	.675	−.141
.625	−.623	.625	−.460	.725	−.205		
.675	−.521	.725	−.175				
.725	−.422	.775	−.085				
.775	−.282	.825	−.003				
.825	−.191	.875	.118				
.875	−.101	.975	.187				
.975	−.079						

Table A-7

MINF = .805
HP= 20569
PSINF = 949.5
PRI = 882.3
QBAR = 431.2
ALPHA = 2.7

Upper surface

X/C	CP	X/C	CP	X/C	CP	X/C	CP
$\eta = 0.25$		$\eta = 0.47$		$\eta = 0.64$		$\eta = 0.78$	
.025	−.577	.040	−.924	.050	−.882	.050	−.926
.120	−.664	.140	−.836	.200	−.602	.220	−.552
.200	−.578	.200	−.512	.300	−.926	.300	−.639
.250	−.510	.300	−.514	.400	−.452	.400	−.461
.300	−.472	.400	−.495	.450	−.415	.450	−.387
.400	−.451	.500	−.451	.500	−.465	.500	−.397
.500	−.404	.550	−.428	.550	−.413	.550	−.401
.550	−.360	.600	−.389	.600	−.373	.600	−.374
.600	−.385	.650	−.394	.650	−.382	.650	−.349
.650	−.366	.700	−.394	.700	−.433	.700	−.573
.700	−.346	.750	−.337	.740	−.335	.750	−.410
.750	−.356	.800	−.337				
.850	−.185	.850	−.227				
.900	−.112	.900	−.177				
.984	−.088	1.000	.036				

Lower surface

X/C	CP	X/C	CP	X/C	CP	X/C	CP
$\eta = 0.25$		$\eta = 0.47$		$\eta = 0.64$		$\eta = 0.78$	
.075	.113	.075	−.514	.075	−.284	.075	−.463
.125	.115	.125	−.200	.125	−.226	.125	−.683
.175	−.004	.175	−.304	.225	−.651	.225	−.439
.225	−.071	.225	−.329	.325	−1.160	.325	−.512
.325	−.244	.325	−.330	.425	−.395	.425	−.819
.425	−.332	.425	−.559	.525	−.549	.525	−.354
.525	−.465	.525	−.721	.575	−.702	.575	−.318
.575	−.598	.575	−.777	.675	−.272	.675	−.132
.625	−.613	.625	−.444	.725	−.200		
.675	−.517	.725	−.174				
.725	−.442	.775	−.091				
.775	−.273	.825	−.006				
.825	−.194	.875	.115				
.875	−.116	.975	.183				
.975	−.094						

Table A-8

MINF =	.842
HP=	20547
PSINF =	950.4
PRI =	873.8
QBAR =	472.1
ALPHA =	2.3

Upper surface

X/C	CP	X/C	CP	X/C	CP	X/C	CP
η = 0.25		η = 0.47		η = 0.64		η = 0.78	
.025	−.463	.040	−.818	.050	−.782	.050	−.978
.120	−.727	.140	−1.068	.200	−.804	.220	−.407
.200	−.594	.200	−.593	.300	−.721	.300	−.944
.250	−.569	.300	−.427	.400	−.485	.400	−.494
.300	−.589	.400	−.523	.450	−.417	.450	−.447
.400	−.444	.500	−.466	.500	−.511	.500	−.393
.500	−.420	.550	−.439	.550	−.456	.550	−.417
.550	−.389	.600	−.414	.600	−.383	.600	−.368
.600	−.394	.650	−.405	.650	−.381	.650	−.338
.650	−.391	.700	−.405	.700	−.458	.700	−.606
.700	−.377	.750	−.337	.740	−.330	.750	−.381
.750	−.403	.800	−.337				
.850	−.187	.850	−.217				
.900	−.116	.900	−.152				
.984	−.088	1.000	.054				

Lower surface

X/C	CP	X/C	CP	X/C	CP	X/C	CP
η = 0.25		η = 0.47		η = 0.64		η = 0.78	
.075	.117	.075	−.558	.075	−.285	.075	−.436
.125	.105	.125	−.209	.125	−.210	.125	−.631
.175	−.021	.175	−.314	.225	−.592	.225	−.884
.225	−.042	.225	−.331	.325	−1.128	.325	−.655
.325	−.352	.325	−.313	.425	−.635	.425	−.680
.425	−.390	.425	−.595	.525	−.735	.525	−.342
.525	−.436	.525	−.690	.575	−.834	.575	−.275
.575	−.481	.575	−.712	.675	−.277	.675	−.129
.625	−.603	.625	−.954	.725	−.211		
.675	−.687	.725	−.230				
.725	−.597	.775	−.141				
.775	−.320	.825	−.067				
.825	−.204	.875	.029				
.875	−.090	.975	.113				
.975	−.070						

Table A-9

MINF = .859
HP= 20659
PSINF = 945.9
PRI = 861.8
QBAR = 488.8
ALPHA = 2.2

Upper surface

X/C	CP	X/C	CP	X/C	CP	X/C	CP
η = 0.25		η = 0.47		η = 0.64		η = 0.78	
.025	−.405	.040	−.766	.050	−.726	.050	−.930
.120	−.635	.140	−1.026	.200	−.810	.220	−.832
.200	−.585	.200	−.651	.300	−.830	.300	−.893
.250	−.535	.300	−.571	.400	−.529	.400	−.360
.300	−.591	.400	−.560	.450	−.456	.450	−.342
.400	−.587	.500	−.578	.500	−.392	.500	−.400
.500	−.486	.550	−.382	.550	−.383	.550	−.453
.550	−.347	.600	−.355	.600	−.399	.600	−.389
.600	−.396	.650	−.378	.650	−.394	.650	−.326
.650	−.386	.700	−.378	.700	−.486	.700	−.580
.700	−.398	.750	−.338	.740	−.398	.750	−.554
.750	−.443	.800	−.338				
.850	−.175	.850	−.208				
.900	−.100	.900	−.127				
.984	−.084	1.000	.049				

Lower surface

X/C	CP	X/C	CP	X/C	CP	X/C	CP
η = 0.25		η = 0.47		η = 0.64		η = 0.78	
.075	.129	.075	−.537	.075	−.289	.075	−.414
.125	.121	.125	−.199	.125	−.207	.125	−.613
.175	−.019	.175	−.312	.225	−.571	.225	−.855
.225	−.028	.225	−.326	.325	−1.102	.325	−.783
.325	−.290	.325	−.306	.425	−.627	.425	−.687
.425	−.657	.425	−.609	.525	−.734	.525	−.430
.525	−.582	.525	−.665	.575	−.840	.575	−.224
.575	−.508	.575	−.673	.675	−.302	.675	−.133
.625	−.516	.625	−.844	.725	−.259		
.675	−.664	.725	−.263				
.725	−.629	.775	−.227				
.775	−.394	.825	−.162				
.825	−.237	.875	−.080				
.875	−.081	.975	.061				
.975	−.057						

APPENDIX B
SURFACE PRESSURE COEFFICIENTS, PYLONS ON, HP ≈ 30,000 FT

	M	α, deg
1	.642	7.0
2	.747	5.0
3	.796	4.2
4	.841	5.2
5	.843	3.4
6	.874	4.0
7	.876	3.5
8	.877	2.7

Table B-1

MINF = .642
HP= 30100
PSINF = 625.6
PRI = 608.4
QBAR = 180.7
ALPHA = 7.0

Upper surface

X/C	CP	X/C	CP	X/C	CP	X/C	CP
η = 0.25		η = 0.47		η = 0.64		η = 0.78	
.025	−1.108	.040	−1.757	.050	−1.895	.050	−1.403
.120	−.777	.140	−.912	.200	−.719	.220	−.634
.200	−.668	.200	−.750	.300	−.750	.300	−.694
.250	−.624	.300	−.634	.400	−.528	.400	−.530
.300	−.556	.400	−.558	.450	−.497	.450	−.463
.400	−.505	.500	−.479	.500	−.480	.500	−.431
.500	−.423	.550	−.446	.550	−.432	.550	−.426
.550	−.421	.600	−.386	.600	−.378	.600	−.408
.600	−.384	.650	−.403	.650	−.382	.650	−.370
.650	−.369	.700	−.403	.700	−.377	.700	−.468
.700	−.326	.750	−.276	.740	−.289	.750	−.341
.750	−.333	.800	−.276				
.850	−.167	.850	−.211				
.900	−.111	.900	−.153				
.984	−.074	1.000	−.025				

Lower surface

X/C	CP	X/C	CP	X/C	CP	X/C	CP
η = 0.25		η = 0.47		η = 0.64		η = 0.78	
.075	.227	.075	−.025	.075	.078	.075	−.044
.125	.181	.125	.035	.125	.041	.125	−.127
.175	.092	.175	−.074	.225	−.257	.225	−.221
.225	.029	.225	−.121	.325	−.269	.325	−.279
.325	−.104	.325	−.137	.425	−.293	.425	−.353
.425	−.256	.425	−.287	.525	−.365	.525	−.337
.525	−.325	.525	−.320	.575	−.436	.575	−.310
.575	−.394	.575	−.332	.675	−.237	.675	−.158
.625	−.470	.625	−.359	.725	−.201		
.675	−.413	.725	−.139				
.725	−.286	.775	−.051				
.775	−.207	.825	.063				
.825	−.069	.875	.184				
.875	.070	.975	.166				
.975	.042						

Table B-2

MINF =	.747
HP=	30346
PSINF =	618.6
PRI =	589.1
QBAR =	241.8
ALPHA =	5.0

Upper surface

X/C	CP	X/C	CP	X/C	CP	X/C	CP
η = 0.25		η = 0.47		η = 0.64		η = 0.78	
.025	−.787	.040	−1.314	.050	−1.364	.050	−1.592
.120	−.757	.140	−.956	.200	−.590	.220	−.561
.200	−.622	.200	−.611	.300	−.732	.300	−.665
.250	−.572	.300	−.563	.400	−.495	.400	−.505
.300	−.519	.400	−.533	.450	−.463	.450	−.431
.400	−.478	.500	−.468	.500	−.474	.500	−.419
.500	−.407	.550	−.445	.550	−.424	.550	−.415
.550	−.397	.600	−.388	.600	−.377	.600	−.389
.600	−.372	.650	−.407	.650	−.377	.650	−.357
.650	−.371	.700	−.407	.700	−.387	.700	−.482
.700	−.345	.750	−.305	.740	−.285	.750	−.334
.750	−.354	.800	−.305				
.850	−.176	.850	−.224				
.900	−.113	.900	−.163				
.984	−.086	1.000	.017				

Lower surface

X/C	CP	X/C	CP	X/C	CP	X/C	CP
η = 0.25		η = 0.47		η = 0.64		η = 0.78	
.075	.177	.075	−.218	.075	−.104	.075	−.262
.125	.143	.125	−.083	.125	−.104	.125	−.298
.175	.047	.175	−.188	.225	−.530	.225	−.369
.225	−.029	.225	−.232	.325	−.392	.325	−.427
.325	−.160	.325	−.248	.425	−.383	.425	−.480
.425	−.315	.425	−.431	.525	−.471	.525	−.405
.525	−.378	.525	−.435	.575	−.559	.575	−.367
.575	−.440	.575	−.440	.675	−.282	.675	−.180
.625	−.536	.625	−.453	.725	−.225		
.675	−.460	.725	−.162				
.725	−.353	.775	−.055				
.775	−.261	.825	.044				
.825	−.122	.875	.153				
.875	.014	.975	.191				
.975	.019						

Table B-3

MINF =	.796
HP=	30309
PSINF =	619.6
PRI =	581.1
QBAR =	274.8
ALPHA =	4.2

Upper surface

X/C	CP	X/C	CP	X/C	CP	X/C	CP
η = 0.25		η = 0.47		η = 0.64		η = 0.78	
.025	−.651	.040	−1.078	.050	−1.115	.050	−1.341
.120	−.849	.140	−1.308	.200	−.922	.220	−.467
.200	−.712	.200	−.733	.300	−.610	.300	−.629
.250	−.648	.300	−.480	.400	−.461	.400	−.501
.300	−.522	.400	−.510	.450	−.445	.450	−.426
.400	−.475	.500	−.464	.500	−.474	.500	−.419
.500	−.411	.550	−.446	.550	−.429	.550	−.422
.550	−.395	.600	−.399	.600	−.380	.600	−.389
.600	−.375	.650	−.414	.650	−.385	.650	−.358
.650	−.381	.700	−.414	.700	−.405	.700	−.520
.700	−.357	.750	−.322	.740	−.295	.750	−.346
.750	−.368	.800	−.322				
.850	−.175	.850	−.229				
.900	−.114	.900	−.164				
.984	−.087	1.000	.030				

Lower surface

X/C	CP	X/C	CP	X/C	CP	X/C	CP
η = 0.25		η = 0.47		η = 0.64		η = 0.78	
.075	.163	.075	−.319	.075	−.170	.075	−.375
.125	.134	.125	−.125	.125	−.136	.125	−.428
.175	.034	.175	−.231	.225	−.615	.225	−.438
.225	−.046	.225	−.266	.325	−.383	.325	−.494
.325	−.175	.325	−.278	.425	−.411	.425	−.629
.425	−.365	.425	−.507	.525	−.541	.525	−.414
.525	−.413	.525	−.680	.575	−.671	.575	−.368
.575	−.461	.575	−.490	.675	−.294	.675	−.173
.625	−.675	.625	−.490	.725	−.230		
.675	−.487	.725	−.168				
.725	−.361	.775	−.072				
.775	−.277	.825	.002				
.825	−.154	.875	.121				
.875	−.032	.975	.197				
.975	−.001						

Table B-4

MINF = .841
HP= 30316
PSINF = 619.4
PRI = 583.0
QBAR = 306.8
ALPHA = 5.2

Upper surface

X/C	CP	X/C	CP	X/C	CP	X/C	CP
η = 0.25		η = 0.47		η = 0.64		η = 0.78	
.025	−.636	.040	−1.026	.050	−1.068	.050	−1.282
.120	−.891	.140	−1.295	.200	−1.193	.220	−1.155
.200	−.852	.200	−1.178	.300	−1.211	.300	−1.291
.250	−.768	.300	−1.215	.400	−1.184	.400	−1.116
.300	−.751	.400	−.825	.450	−1.158	.450	−.957
.400	−.737	.500	−.778	.500	−.783	.500	−.650
.500	−.719	.550	−.710	.550	−.558	.550	−.543
.550	−.685	.600	−.343	.600	−.334	.600	−.371
.600	−.426	.650	−.304	.650	−.234	.650	−.205
.650	−.340	.700	−.304	.700	−.210	.700	−.236
.700	−.308	.750	−.247	.740	−.175	.750	−.201
.750	−.316	.800	−.247				
.850	−.136	.850	−.170				
.900	−.078	.900	−.113				
.984	−.068	1.000	.042				

Lower surface

X/C	CP	X/C	CP	X/C	CP	X/C	CP
η = 0.25		η = 0.47		η = 0.64		η = 0.78	
.075	.233	.075	−.246	.075	−.067	.075	−.289
.125	.199	.125	−.050	.125	−.042	.125	−.468
.175	.090	.175	−.157	.225	−.500	.225	−.373
.225	.055	.225	−.197	.325	−.951	.325	−.422
.325	−.203	.325	−.206	.425	−.366	.425	−.731
.425	−.196	.425	−.444	.525	−.546	.525	−.294
.525	−.344	.525	−.632	.575	−.726	.575	−.296
.575	−.491	.575	−.683	.675	−.274	.675	−.148
.625	−.526	.625	−.524	.725	−.214		
.675	−.662	.725	−.173				
.725	−.520	.775	−.084				
.775	−.322	.825	.030				
.825	−.161	.875	.146				
.875	.001	.975	.212				
.975	−.016						

Table B-5

MINF = .843
HP= 30400
PSINF = 617.1
PR1 = 574.9
QBAR = 307.3
ALPHA = 3.4

Upper surface

X/C	CP	X/C	CP	X/C	CP	X/C	CP
η = 0.25		η = 0.47		η = 0.64		η = 0.78	
.025	−.536	.040	−.870	.050	−.897	.050	−1.117
.120	−.748	.140	−1.109	.200	−.989	.220	−.926
.200	−.697	.200	−1.014	.300	−1.126	.300	−1.219
.250	−.636	.300	−.671	.400	−.465	.400	−.341
.300	−.655	.400	−.668	.450	−.350	.450	−.283
.400	−.648	.500	−.396	.500	−.343	.500	−.309
.500	−.423	.550	−.388	.550	−.346	.550	−.360
.550	−.367	.600	−.369	.600	−.335	.600	−.355
.600	−.367	.650	−.395	.650	−.352	.650	−.335
.650	−.389	.700	−.395	.700	−.403	.700	−.566
.700	−.393	.750	−.325	.740	−.305	.750	−.353
.750	−.408	.800	−.325				
.850	−.181	.850	−.216				
.900	−.116	.900	−.144				
.984	−.075	1.000	.033				

Lower surface

X/C	CP	X/C	CP	X/C	CP	X/C	CP
η = 0.25		η = 0.47		η = 0.64		η = 0.78	
.075	.155	.075	−.457	.075	−.205	.075	−.389
.125	.128	.125	−.154	.125	−.145	.125	−.594
.175	.015	.175	−.257	.225	−.563	.225	−.846
.225	−.023	.225	−.282	.325	−1.068	.325	−.415
.325	−.323	.325	−.276	.425	−.584	.425	−.748
.425	−.255	.425	−.538	.525	−.687	.525	−.325
.525	−.404	.525	−.668	.575	−.790	.575	−.280
.575	−.553	.575	−.706	.675	−.293	.675	−.146
.625	−.568	.625	−.875	.725	−.233		
.675	−.620	.725	−.208				
.725	−.555	.775	−.125				
.775	−.312	.825	−.021				
.825	−.188	.875	.075				
.875	−.065	.975	.141				
.975	−.061						

Table B-6

MINF = .874
HP= 30480
PSINF = 614.8
PRI = 566.8
QBAR = 328.5
ALPHA = 4.0

Upper surface

X/C	CP	X/C	CP	X/C	CP	X/C	CP
η = 0.25		η = 0.47		η = 0.64		η = 0.78	
.025	−.484	.040	−.836	.050	−.865	.050	−1.074
.120	−.742	.140	−1.094	.200	−1.042	.220	−.963
.200	−.734	.200	−1.007	.300	−1.075	.300	−1.173
.250	−.662	.300	−1.029	.400	−1.024	.400	−.997
.300	−.666	.400	−.712	.450	−1.004	.450	−.979
.400	−.680	.500	−.714	.500	−.971	.500	−.984
.500	−.654	.550	−.744	.550	−.736	.550	−.964
.550	−.645	.600	−.718	.600	−.716	.600	−.737
.600	−.650	.650	−.762	.650	−.706	.650	−.581
.650	−.594	.700	−.762	.700	−.474	.700	−.415
.700	−.631	.750	−.238	.740	−.263	.750	−.255
.750	−.458	.800	−.238				
.850	−.147	.850	−.173				
.900	−.086	.900	−.115				
.984	−.065	1.000	−.010				

Lower surface

X/C	CP	X/C	CP	X/C	CP	X/C	CP
η = 0.25		η = 0.47		η = 0.64		η = 0.78	
.075	.196	.075	−.406	.075	−.148	.075	−.326
.125	.168	.125	−.113	.125	−.087	.125	−.523
.175	.044	.175	−.218	.225	−.498	.225	−.774
.225	.024	.225	−.243	.325	−1.003	.325	−.496
.325	−.200	.325	−.236	.425	−.591	.425	−.663
.425	−.575	.425	−.513	.525	−.684	.525	−.765
.525	−.493	.525	−.612	.575	−.776	.575	−.232
.575	−.412	.575	−.632	.675	−.282	.675	−.147
.625	−.461	.625	−.926	.725	−.246		
.675	−.626	.725	−.272				
.725	−.603	.775	−.222				
.775	−.600	.825	−.135				
.825	−.313	.875	−.028				
.875	−.025	.975	.096				
.975	−.013						

Table B-7

MINF = .876
HP= 30453
PSINF = 615.6
PRI = 564.8
QBAR = 330.4
ALPHA = 3.5

Upper surface

X/C	CP	X/C	CP	X/C	CP	X/C	CP
η = 0.25		η = 0.47		η = 0.64		η = 0.78	
.025	−.471	.040	−.799	.050	−.826	.050	−1.034
.120	−.718	.140	−1.049	.200	−.963	.220	−.897
.200	−.693	.200	−.961	.300	−1.059	.300	−1.168
.250	−.634	.300	−.884	.400	−.952	.400	−.957
.300	−.646	.400	−.670	.450	−.841	.450	−.904
.400	−.647	.500	−.694	.500	−.799	.500	−.920
.500	−.639	.550	−.716	.550	−.707	.550	−.856
.550	−.623	.600	−.702	.600	−.711	.600	−.660
.600	−.620	.650	−.732	.650	−.700	.650	−.498
.650	−.577	.700	−.732	.700	−.538	.700	−.405
.700	−.621	.750	−.251	.740	−.281	.750	−.270
.750	−.511	.800	−.251				
.850	−.146	.850	−.177				
.900	−.085	.900	−.115				
.984	−.071	1.000	−.009				

Lower surface

X/C	CP	X/C	CP	X/C	CP	X/C	CP
η = 0.25		η = 0.47		η = 0.64		η = 0.78	
.075	.179	.075	−.437	.075	−.183	.075	−.351
.125	.153	.125	−.137	.125	−.115	.125	−.541
.175	.024	.175	−.242	.225	−.509	.225	−.787
.225	.009	.225	−.263	.325	−1.025	.325	−.557
.325	−.210	.325	−.251	.425	−.603	.425	−.666
.425	−.591	.425	−.545	.525	−.685	.525	−.767
.525	−.519	.525	−.624	.575	−.767	.575	−.247
.575	−.448	.575	−.641	.675	−.284	.675	−.160
.625	−.458	.625	−.923	.725	−.259		
.675	−.624	.725	−.280				
.725	−.597	.775	−.228				
.775	−.597	.825	−.157				
.825	−.313	.875	−.063				
.875	−.037	.975	.070				
.975	−.017						

Table B-8

MINF =	.877
HP=	30671
PSINF =	609.5
PRI =	553.7
QBAR =	328.0
ALPHA =	2.7

Upper surface

X/C	CP	X/C	CP	X/C	CP	X/C	CP
$\eta = 0.25$		$\eta = 0.47$		$\eta = 0.64$		$\eta = 0.78$	
.025	−.440	.040	−.737	.050	−.746	.050	−.963
.120	−.658	.140	−1.006	.200	−.844	.220	−.849
.200	−.638	.200	−.887	.300	−1.034	.300	−1.156
.250	−.594	.300	−.658	.400	−.742	.400	−.837
.300	−.601	.400	−.626	.450	−.582	.450	−.839
.400	−.618	.500	−.664	.500	−.647	.500	−.791
.500	−.600	.550	−.688	.550	−.607	.550	−.653
.550	−.603	.600	−.655	.600	−.661	.600	−.555
.600	−.557	.650	−.684	.650	−.667	.650	−.381
.650	−.537	.700	−.684	.700	−.645	.700	−.420
.700	−.594	.750	−.276	.740	−.331	.750	−.300
.750	−.566	.800	−.276				
.850	−.149	.850	−.190				
.900	−.089	.900	−.115				
.984	−.078	1.000	−.002				

Lower surface

X/C	CP	X/C	CP	X/C	CP	X/C	CP
$\eta = 0.25$		$\eta = 0.47$		$\eta = 0.64$		$\eta = 0.78$	
.075	.152	.075	−.492	.075	−.249	.075	−.388
.125	.123	.125	−.174	.125	−.165	.125	−.577
.175	−.017	.175	−.280	.225	−.534	.225	−.816
.225	−.031	.225	−.298	.325	−1.058	.325	−.743
.325	−.218	.325	−.283	.425	−.628	.425	−.674
.425	−.620	.425	−.586	.525	−.686	.525	−.801
.525	−.557	.525	−.645	.575	−.743	.575	−.290
.575	−.495	.575	−.673	.675	−.299	.675	−.181
.625	−.466	.625	−.840	.725	−.285		
.675	−.601	.725	−.287				
.725	−.597	.775	−.247				
.775	−.600	.825	−.188				
.825	−.325	.875	−.110				
.875	−.052	.975	.035				
.975	−.025						

APPENDIX C
SURFACE PRESSURE COEFFICIENTS, PYLONS ON, HP ≈ 40,000 FT

	M	α, deg
1	.754	7.6
2	.818	5.9
3	.843	5.2

Table C-1

MINF = .754
HP= 40334
PSINF = 385.5
PRI = 370.4
QBAR = 153.2
ALPHA = 7.6

Upper surface

X/C	CP	X/C	CP	X/C	CP	X/C	CP
η = 0.25		η = 0.47		η = 0.64		η = 0.78	
.025	−1.110	.040	−1.549	.050	−1.576	.050	−1.838
.120	−1.243	.140	−1.789	.200	−1.307	.220	−1.099
.200	−.927	.200	−1.034	.300	−.859	.300	−.748
.250	−.717	.300	−.850	.400	−.520	.400	−.429
.300	−.588	.400	−.635	.450	−.474	.450	−.390
.400	−.521	.500	−.479	.500	−.409	.500	−.378
.500	−.439	.550	−.441	.550	−.382	.550	−.392
.550	−.427	.600	−.379	.600	−.330	.600	−.383
.600	−.405	.650	−.396	.650	−.339	.650	−.351
.650	−.381	.700	−.396	.700	−.334	.700	−.419
.700	−.352	.750	−.269	.740	−.261	.750	−.304
.750	−.344	.800	−.269				
.850	−.154	.850	−.204				
.900	−.091	.900	−.159				
.984	−.072	1.000	−.038				

Lower surface

X/C	CP	X/C	CP	X/C	CP	X/C	CP
η = 0.25		η = 0.47		η = 0.64		η = 0.78	
.075	.267	.075	−.017	.075	.091	.075	−.053
.125	.242	.125	.054	.125	.054	.125	−.131
.175	.146	.175	−.048	.225	−.320	.225	−.232
.225	.084	.225	−.106	.325	−.294	.325	−.313
.325	−.038	.325	−.127	.425	−.323	.425	−.412
.425	−.249	.425	−.324	.525	−.418	.525	−.389
.525	−.320	.525	−.370	.575	−.514	.575	−.356
.575	−.392	.575	−.389	.675	−.259	.675	−.177
.625	−.542	.625	−.419	.725	−.208		
.675	−.506	.725	−.156				
.725	−.406	.775	−.043				
.775	−.252	.825	.044				
.825	−.103	.875	.157				
.875	.046	.975	.183				
.975	.033						

Table C-2

MINF = .818
HP= 40385
PSINF = 384.5
PRI = 363.0
QBAR = 180.0
ALPHA = 5.9

Upper surface

X/C	CP	X/C	CP	X/C	CP	X/C	CP
η = 0.25		η = 0.47		η = 0.64		η = 0.78	
.025	−.771	.040	−1.139	.050	−1.181	.050	−1.406
.120	−1.009	.140	−1.440	.200	−1.285	.220	−1.274
.200	−.930	.200	−1.284	.300	−1.321	.300	−1.354
.250	−.841	.300	−1.334	.400	−.965	.400	−.837
.300	−.789	.400	−.804	.450	−.709	.450	−.571
.400	−.773	.500	−.411	.500	−.493	.500	−.391
.500	−.407	.550	−.350	.550	−.340	.550	−.286
.550	−.373	.600	−.299	.600	−.249	.600	−.261
.600	−.360	.650	−.337	.650	−.247	.650	−.248
.650	−.355	.700	−.337	.700	−.263	.700	−.341
.700	−.334	.750	−.267	.740	−.206	.750	−.257
.750	−.329	.800	−.267				
.850	−.139	.850	−.190				
.900	−.080	.900	−.144				
.984	−.063	1.000	.016				

Lower surface

X/C	CP	X/C	CP	X/C	CP	X/C	CP
η = 0.25		η = 0.47		η = 0.64		η = 0.78	
.075	.247	.075	−.167	.075	−.032	.075	−.246
.125	.214	.125	−.028	.125	−.034	.125	−.287
.175	.112	.175	−.129	.225	−.505	.225	−.344
.225	.059	.225	−.182	.325	−.329	.325	−.422
.325	−.122	.325	−.194	.425	−.384	.425	−.734
.425	−.220	.425	−.426	.525	−.552	.525	−.391
.525	−.356	.525	−.658	.575	−.720	.575	−.351
.575	−.492	.575	−.469	.675	−.286	.675	−.173
.625	−.572	.625	−.501	.725	−.236		
.675	−.550	.725	−.167				
.725	−.489	.775	−.061				
.775	−.278	.825	.002				
.825	−.140	.875	.113				
.875	−.000	.975	.211				
.975	.038						

Table C-3

MINF = .843
HP= 40431
PSINF = 383.7
PRI = 362.7
QBAR = 191.0
ALPHA = 5.2

Upper surface

X/C	CP	X/C	CP	X/C	CP	X/C	CP
η = 0.25		η = 0.47		η = 0.64		η = 0.78	
.025	−.653	.040	−1.007	.050	−1.062	.050	−1.277
.120	−.887	.140	−1.300	.200	−1.189	.220	−1.158
.200	−.841	.200	−1.173	.300	−1.211	.300	−1.284
.250	−.773	.300	−1.220	.400	−1.180	.400	−1.131
.300	−.751	.400	−.829	.450	−1.167	.450	−.983
.400	−.741	.500	−.788	.500	−.775	.500	−.645
.500	−.720	.550	−.757	.550	−.566	.550	−.562
.550	−.699	.600	−.384	.600	−.362	.600	−.390
.600	−.461	.650	−.320	.650	−.256	.650	−.218
.650	−.354	.700	−.320	.700	−.217	.700	−.237
.700	−.313	.750	−.236	.740	−.175	.750	−.195
.750	−.313	.800	−.236				
.850	−.134	.850	−.164				
.900	−.078	.900	−.108				
.984	−.063	1.000	.035				

Lower surface

X/C	CP	X/C	CP	X/C	CP	X/C	CP
η = 0.25		η = 0.47		η = 0.64		η = 0.78	
.075	.226	.075	−.253	.075	−.063	.075	−.303
.125	.184	.125	−.063	.125	−.038	.125	−.477
.175	.072	.175	−.162	.225	−.494	.225	−.376
.225	.045	.225	−.204	.325	−.922	.325	−.422
.325	−.219	.325	−.206	.425	−.380	.425	−.731
.425	−.256	.425	−.434	.525	−.553	.525	−.313
.525	−.313	.525	−.642	.575	−.726	.575	−.296
.575	−.370	.575	−.687	.675	−.286	.675	−.160
.625	−.551	.625	−.554	.725	−.237		
.675	−.680	.725	−.183				
.725	−.498	.775	−.090				
.775	−.376	.825	−.008				
.825	−.190	.875	.106				
.875	−.003	.975	.197				
.975	−.008						

APPENDIX D
SURFACE PRESSURE COEFFICIENTS, PYLONS OFF, HP ≈ 20,000 FT

	M	α, deg
1	.486	7.4
2	.495	8.1
3	.500	7.6
4	.642	4.3
5	.647	4.7
6	.651	4.3
7	.725	5.0
8	.742	3.3
9	.750	2.6
10	.767	2.7
11	.799	2.4
12	.799	2.7
13	.800	1.9
14	.801	4.8
15	.820	5.2
16	.845	1.9
17	.848	2.0
18	.851	1.0
19	.866	1.6
20	.866	1.7
21	.876	1.4

Table D-1

MINF = .485
HP= 18919
PSINF = 1017.3
PRI = 1003.3
QBAR = 167.8
ALPHA = 7.4

Upper surface

X/C	CP	X/C	CP	X/C	CP	X/C	CP
η = 0.25		η = 0.47		η = 0.64		η = 0.78	
.025	−1.285	.040	−1.277	.050	−1.215	.050	−1.266
.120	−.724	.140	−.771	.200	−.679	.220	−.597
.200	−.624	.200	−.722	.300	−.695	.300	−.636
.250	−.545	.300	−.584	.400	−.472	.400	−.490
.300	−.526	.400	−.506	.450	−.427	.450	−.433
.400	−.428	.500	−.454	.500	−.434	.500	−.393
.500	−.371	.550	−.412	.550	−.422	.550	−.410
.550	−.356	.600	−.387	.600	−.357	.600	−.400
.600	−.322	.650	−.363	.650	−.360	.650	−.370
.650	−.210	.700	−.363	.700	−.401	.700	−.494
.700	−.098	.750	−.269	.740	−.327	.750	−.381
.750	−.098	.800	−.269				
.850	−.131	.850	−.215				
.900	−.079	.900	−.098				
.984	−.042	1.000	.014				

Lower surface

X/C	CP	X/C	CP	X/C	CP	X/C	CP
η = 0.25		η = 0.47		η = 0.64		η = 0.78	
.075	.239	.075	.167	.075	.155	.075	.140
.125	.221	.125	.143	.125	.098	.125	.011
.175	.140	.175	−.016	.225	−.068	.225	−.084
.225	.082	.225	−.081	.325	−.125	.325	−.111
.325	−.007	.325	−.068	.425	−.150	.425	−.185
.425	−.165	.425	−.192	.525	−.207	.525	−.186
.525	−.326	.525	−.221	.575	−.263	.575	−.168
.575	−.325	.575	−.270	.675	−.142	.675	−.053
.625	−.392	.625	−.274	.725	−.101		
.675	−.098	.725	−.098				
.725	−.241	.775	−.020				
.775	−.096	.825	.111				
.825	.001	.875	.205				
.875	.110	.975	.147				
.975	.029						

Table D-2

MINF = .495
HP= 20132
PSINF = 967.1
PRI = 952.3
QBAR = 166.1
ALPHA = 8.1

Upper surface

X/C	CP	X/C	CP	X/C	CP	X/C	CP
η = 0.25		η = 0.47		η = 0.64		η = 0.78	
.025	−1.321	.040	−1.404	.050	−1.334	.050	−1.409
.120	−.769	.140	−.806	.200	−.721	.220	−.638
.200	−.655	.200	−.746	.300	−.734	.300	−.680
.250	−.587	.300	−.617	.400	−.506	.400	−.510
.300	−.543	.400	−.521	.450	−.454	.450	−.440
.400	−.459	.500	−.444	.500	−.471	.500	−.423
.500	−.388	.550	−.413	.550	−.427	.550	−.419
.550	−.327	.600	−.391	.600	−.366	.600	−.408
.600	−.331	.650	−.350	.650	−.375	.650	−.386
.650	−.268	.700	−.350	.700	−.404	.700	−.506
.700	−.205	.750	−.245	.740	−.328	.750	−.400
.750	−.239	.800	−.245				
.850	−.125	.850	−.186				
.900	−.062	.900	−.158				
.984	−.032	1.000	.004				

Lower surface

X/C	CP	X/C	CP	X/C	CP	X/C	CP
η = 0.25		η = 0.47		η = 0.64		η = 0.78	
.075	.259	.075	.215	.075	.175	.075	.167
.125	.251	.125	.169	.125	.112	.125	.064
.175	.149	.175	.008	.225	−.057	.225	−.072
.225	.108	.225	−.036	.325	−.123	.325	−.083
.325	.005	.325	−.066	.425	−.134	.425	−.175
.425	−.184	.425	−.198	.525	−.200	.525	−.172
.525	−.383	.525	−.229	.575	−.267	.575	−.167
.575	−.385	.575	−.281	.675	−.141	.675	−.067
.625	−.452	.625	−.294	.725	−.099		
.675	−.299	.725	−.306				
.725	−.332	.775	−.034				
.775	−.144	.825	.104				
.825	−.038	.875	.208				
.875	.066	.975	.169				
.975	.038						

Table D-3

MINF = .500
HP= 19970
PSINF = 973.7
PRI = 958.9
QBAR = 170.6
ALPHA = 7.6

Upper surface

X/C	CP	X/C	CP	X/C	CP	X/C	CP
η = 0.25		η = 0.47		η = 0.64		η = 0.78	
.025	−1.312	.040	−1.315	.050	−1.257	.050	−1.320
.120	−.741	.140	−.778	.200	−.687	.220	−.610
.200	−.648	.200	−.736	.300	−.727	.300	−.654
.250	−.572	.300	−.599	.400	−.496	.400	−.515
.300	−.530	.400	−.529	.450	−.438	.450	−.429
.400	−.458	.500	−.467	.500	−.449	.500	−.408
.500	−.383	.550	−.426	.550	−.408	.550	−.434
.550	−.337	.600	−.394	.600	−.364	.600	−.371
.600	−.336	.650	−.351	.650	−.394	.650	−.394
.650	−.219	.700	−.351	.700	−.391	.700	−.510
.700	−.102	.750	−.283	.740	−.330	.750	−.392
.750	−.102	.800	−.283				
.850	−.150	.850	−.217				
.900	−.080	.900	−.102				
.984	−.035	1.000	.000				

Lower surface

X/C	CP	X/C	CP	X/C	CP	X/C	CP
η = 0.25		η = 0.47		η = 0.64		η = 0.78	
.075	.239	.075	.175	.075	.151	.075	.124
.125	.220	.125	.151	.125	.089	.125	.033
.175	.133	.175	−.005	.225	−.088	.225	−.067
.225	.087	.225	−.035	.325	−.137	.325	−.085
.325	−.004	.325	−.088	.425	−.142	.425	−.187
.425	−.163	.425	−.186	.525	−.213	.525	−.193
.525	−.337	.525	−.253	.575	−.285	.575	−.187
.575	−.318	.575	−.281	.675	−.154	.675	−.067
.625	−.385	.625	−.277	.725	−.092		
.675	−.102	.725	−.102				
.725	−.247	.775	−.024				
.775	−.098	.825	.082				
.825	.001	.875	.197				
.875	.100	.975	.127				
.975	.031						

Table D-4

MINF = .642
HP= 20024
PSINF = 971.5
PRI = 945.5
QBAR = 280.4
ALPHA = 4.3

Upper surface

X/C	CP	X/C	CP	X/C	CP	X/C	CP
η = 0.25		η = 0.47		η = 0.64		η = 0.78	
.025	−1.013	.040	−.881	.050	−.816	.050	−.811
.120	−.593	.140	−.593	.200	−.530	.220	−.462
.200	−.523	.200	−.597	.300	−.617	.300	−.557
.250	−.471	.300	−.504	.400	−.401	.400	−.408
.300	−.436	.400	−.446	.450	−.374	.450	−.358
.400	−.401	.500	−.406	.500	−.403	.500	−.351
.500	−.346	.550	−.374	.550	−.364	.550	−.359
.550	−.307	.600	−.356	.600	−.333	.600	−.327
.600	−.310	.650	−.327	.650	−.338	.650	−.315
.650	−.215	.700	−.327	.700	−.365	.700	−.457
.700	−.120	.750	−.268	.740	−.295	.750	−.356
.750	−.120	.800	−.268				
.850	−.151	.850	−.193				
.900	−.086	.900	−.120				
.984	−.035	1.000	.036				

Lower surface

X/C	CP	X/C	CP	X/C	CP	X/C	CP
η = 0.25		η = 0.47		η = 0.64		η = 0.78	
.075	.151	.075	−.029	.075	−.105	.075	−.146
.125	.147	.125	−.019	.125	−.096	.125	−.194
.175	.046	.175	−.171	.225	−.249	.225	−.252
.225	−.002	.225	−.197	.325	−.268	.325	−.239
.325	−.094	.325	−.204	.425	−.261	.425	−.306
.425	−.226	.425	−.321	.525	−.319	.525	−.284
.525	−.355	.525	−.330	.575	−.376	.575	−.267
.575	−.359	.575	−.376	.675	−.213	.675	−.125
.625	−.413	.625	−.381	.725	−.150		
.675	−.120	.725	−.120				
.725	−.260	.775	−.054				
.775	−.138	.825	.085				
.825	−.034	.875	.188				
.875	.069	.975	.169				
.975	.032						

Table D-5

MINF = .647
HP= 20225
PSINF = 963.4
PRI = 930.3
QBAR = 282.3
ALPHA = 4.7

Upper surface

X/C	CP	X/C	CP	X/C	CP	X/C	CP
$\eta = 0.25$		$\eta = 0.47$		$\eta = 0.64$		$\eta = 0.78$	
.025	−1.020	.040	−1.069	.050	−.884	.050	−.882
.120	−.626	.140	−.623	.200	−.564	.220	−.487
.200	−.545	.200	−.621	.300	−.646	.300	−.589
.250	−.501	.300	−.532	.400	−.432	.400	−.430
.300	−.461	.400	−.458	.450	−.391	.450	−.372
.400	−.414	.500	−.412	.500	−.425	.500	−.373
.500	−.368	.550	−.380	.550	−.382	.550	−.370
.550	−.322	.600	−.368	.600	−.336	.600	−.346
.600	−.324	.650	−.333	.650	−.349	.650	−.338
.650	−.277	.700	−.333	.700	−.377	.700	−.469
.700	−.231	.750	−.249	.740	−.304	.750	−.364
.750	−.277	.800	−.249				
.850	−.149	.850	−.187				
.900	−.085	.900	−.164				
.984	−.045	1.000	.020				

Lower surface

X/C	CP	X/C	CP	X/C	CP	X/C	CP
$\eta = 0.25$		$\eta = 0.47$		$\eta = 0.64$		$\eta = 0.78$	
.075	.150	.075	−.023	.075	−.115	.075	−.143
.125	.139	.125	−.024	.125	−.107	.125	−.197
.175	.047	.175	−.181	.225	−.261	.225	−.265
.225	−.009	.225	−.225	.325	−.289	.325	−.258
.325	−.114	.325	−.219	.425	−.275	.425	−.322
.425	−.278	.425	−.342	.525	−.341	.525	−.298
.525	−.442	.525	−.362	.575	−.407	.575	−.287
.575	−.455	.575	−.404	.675	−.231	.675	−.139
.625	−.500	.625	−.418	.725	−.167		
.675	−.326	.725	−.367				
.725	−.360	.775	−.077				
.775	−.222	.825	.065				
.825	−.104	.875	.170				
.875	.014	.975	.179				
.975	.030						

Table D-6

MINF = .651
HP= 20134
PSINF = 967.0
PRI = 936.1
QBAR = 286.7
ALPHA = 4.3

Upper surface

X/C	CP	X/C	CP	X/C	CP	X/C	CP
η = 0.25		η = 0.47		η = 0.64		η = 0.78	
.025	−1.014	.040	−.982	.050	−.835	.050	−.846
.120	−.610	.140	−.615	.200	−.541	.220	−.477
.200	−.536	.200	−.626	.300	−.634	.300	−.582
.250	−.506	.300	−.526	.400	−.405	.400	−.437
.300	−.452	.400	−.450	.450	−.390	.450	−.373
.400	−.418	.500	−.404	.500	−.426	.500	−.362
.500	−.360	.550	−.401	.550	−.376	.550	−.387
.550	−.321	.600	−.353	.600	−.335	.600	−.352
.600	−.322	.650	−.350	.650	−.357	.650	−.327
.650	−.229	.700	−.350	.700	−.388	.700	−.483
.700	−.136	.750	−.277	.740	−.308	.750	−.406
.750	−.136	.800	−.277				
.850	−.176	.850	−.215				
.900	−.107	.900	−.136				
.984	−.060	1.000	.009				

Lower surface

X/C	CP	X/C	CP	X/C	CP	X/C	CP
η = 0.25		η = 0.47		η = 0.64		η = 0.78	
.075	.137	.075	−.044	.075	−.116	.075	−.159
.125	.126	.125	−.046	.125	−.117	.125	−.212
.175	.033	.175	−.193	.225	−.256	.225	−.264
.225	−.024	.225	−.224	.325	−.279	.325	−.244
.325	−.109	.325	−.219	.425	−.275	.425	−.316
.425	−.247	.425	−.343	.525	−.339	.525	−.284
.525	−.375	.525	−.351	.575	−.404	.575	−.288
.575	−.377	.575	−.395	.675	−.224	.675	−.145
.625	−.415	.625	−.395	.725	−.164		
.675	−.136	.725	−.136				
.725	−.263	.775	−.070				
.775	−.155	.825	.072				
.825	−.050	.875	.162				
.875	.055	.975	.146				
.975	.017						

Table D-7

MINF = .725
HP= 19748
PSINF = 982.8
PRI = 944.2
QBAR = 361.7
ALPHA = 5.0

Upper surface

X/C	CP	X/C	CP	X/C	CP	X/C	CP
$\eta = 0.25$		$\eta = 0.47$		$\eta = 0.64$		$\eta = 0.78$	
.025	−.858	.040	−1.387	.050	−1.252	.050	−.841
.120	−.674	.140	−.781	.200	−.601	.220	−.533
.200	−.574	.200	−.637	.300	−.710	.300	−.632
.250	−.539	.300	−.557	.400	−.460	.400	−.487
.300	−.484	.400	−.501	.450	−.420	.450	−.409
.400	−.453	.500	−.448	.500	−.461	.500	−.402
.500	−.382	.550	−.412	.550	−.405	.550	−.392
.550	−.351	.600	−.386	.600	−.363	.600	−.362
.600	−.342	.650	−.354	.650	−.365	.650	−.354
.650	−.242	.700	−.354	.700	−.392	.700	−.514
.700	−.141	.750	−.282	.740	−.327	.750	−.391
.750	−.141	.800	−.282				
.850	−.167	.850	−.204				
.900	−.097	.900	−.141				
.984	−.052	1.000	.026				

Lower surface

X/C	CP	X/C	CP	X/C	CP	X/C	CP
$\eta = 0.25$		$\eta = 0.47$		$\eta = 0.64$		$\eta = 0.78$	
.075	.175	.075	−.015	.075	−.092	.075	−.126
.125	.157	.125	−.013	.125	−.089	.125	−.211
.175	.075	.175	−.183	.225	−.254	.225	−.265
.225	.023	.225	−.215	.325	−.295	.325	−.270
.325	−.086	.325	−.212	.425	−.276	.425	−.334
.425	−.247	.425	−.343	.525	−.357	.525	−.317
.525	−.399	.525	−.364	.575	−.438	.575	−.314
.575	−.411	.575	−.420	.675	−.244	.675	−.149
.625	−.470	.625	−.439	.725	−.167		
.675	−.141	.725	−.141				
.725	−.313	.775	−.069				
.775	−.187	.825	.063				
.825	−.074	.875	.159				
.875	.040	.975	.157				
.975	.015						

Table D-8

MINF = .742
HP= 20379
PSINF = 957.1
PRI = 906.9
QBAR = 369.1
ALPHA = 3.3

Upper surface

X/C	CP	X/C	CP	X/C	CP	X/C	CP
η = 0.25		η = 0.47		η = 0.64		η = 0.78	
.025	−.792	.040	−1.128	.050	−.661	.050	−.683
.120	−.588	.140	−.561	.200	−.532	.220	−.458
.200	−.527	.200	−.607	.300	−.659	.300	−.582
.250	−.492	.300	−.516	.400	−.421	.400	−.423
.300	−.456	.400	−.452	.450	−.384	.450	−.365
.400	−.421	.500	−.418	.500	−.427	.500	−.371
.500	−.375	.550	−.389	.550	−.383	.550	−.372
.550	−.328	.600	−.367	.600	−.340	.600	−.345
.600	−.328	.650	−.344	.650	−.351	.650	−.331
.650	−.286	.700	−.344	.700	−.391	.700	−.490
.700	−.244	.750	−.259	.740	−.300	.750	−.370
.750	−.299	.800	−.259				
.850	−.161	.850	−.199				
.900	−.096	.900	−.170				
.984	−.048	1.000	.040				

Lower surface

X/C	CP	X/C	CP	X/C	CP	X/C	CP
η = 0.25		η = 0.47		η = 0.64		η = 0.78	
.075	.100	.075	−.135	.075	−.253	.075	−.298
.125	.092	.125	−.107	.125	−.213	.125	−.340
.175	.004	.175	−.272	.225	−.371	.225	−.378
.225	−.054	.225	−.311	.325	−.392	.325	−.353
.325	−.168	.325	−.294	.425	−.355	.425	−.415
.425	−.321	.425	−.439	.525	−.438	.525	−.376
.525	−.472	.525	−.441	.575	−.520	.575	−.370
.575	−.557	.575	−.497	.675	−.280	.675	−.185
.625	−.521	.625	−.507	.725	−.194		
.675	−.347	.725	−.377				
.725	−.468	.775	−.096				
.775	−.264	.825	.029				
.825	−.158	.875	.130				
.875	−.053	.975	.169				
.975	−.012						

Table D-9

MINF = .750
HP= 20339
PSINF = 958.7
PRI = 914.0
QBAR = 378.0
ALPHA = 2.6

Upper surface

X/C	CP	X/C	CP	X/C	CP	X/C	CP
$\eta = 0.25$		$\eta = 0.47$		$\eta = 0.64$		$\eta = 0.78$	
.025	−.759	.040	−.995	.050	−.596	.050	−.577
.120	−.533	.140	−.535	.200	−.487	.220	−.428
.200	−.508	.200	−.583	.300	−.639	.300	−.562
.250	−.472	.300	−.506	.400	−.411	.400	−.408
.300	−.458	.400	−.442	.450	−.373	.450	−.349
.400	−.431	.500	−.429	.500	−.414	.500	−.355
.500	−.370	.550	−.398	.550	−.389	.550	−.372
.550	−.338	.600	−.362	.600	−.344	.600	−.345
.600	−.328	.650	−.348	.650	−.360	.650	−.335
.650	−.241	.700	−.348	.700	−.409	.700	−.511
.700	−.155	.750	−.322	.740	−.320	.750	−.411
.750	−.155	.800	−.322				
.850	−.196	.850	−.235				
.900	−.132	.900	−.155				
.984	−.053	1.000	.027				

Lower surface

X/C	CP	X/C	CP	X/C	CP	X/C	CP
$\eta = 0.25$		$\eta = 0.47$		$\eta = 0.64$		$\eta = 0.78$	
.075	.046	.075	−.183	.075	−.305	.075	−.376
.125	.063	.125	−.139	.125	−.250	.125	−.395
.175	−.036	.175	−.308	.225	−.412	.225	−.432
.225	−.089	.225	−.328	.325	−.407	.325	−.384
.325	−.177	.325	−.317	.425	−.370	.425	−.431
.425	−.312	.425	−.437	.525	−.450	.525	−.387
.525	−.406	.525	−.431	.575	−.529	.575	−.379
.575	−.407	.575	−.475	.675	−.275	.675	−.171
.625	−.445	.625	−.479	.725	−.181		
.675	−.155	.725	−.155				
.725	−.302	.775	−.098				
.775	−.194	.825	.006				
.825	−.113	.875	.081				
.875	−.036	.975	.145				
.975	−.037						

Table D-10

MINF = .766
HP= 20409
PSINF = 956.0
PRI = 903.2
QBAR = 390.4
ALPHA = 2.7

Upper surface

X/C	CP	X/C	CP	X/C	CP	X/C	CP
η = 0.25		η = 0.47		η = 0.64		η = 0.78	
.025	−.657	.040	−.909	.050	−.637	.050	−.732
.120	−.595	.140	−.694	.200	−.566	.220	−.498
.200	−.554	.200	−.607	.300	−.773	.300	−.737
.250	−.517	.300	−.520	.400	−.467	.400	−.469
.300	−.488	.400	−.502	.450	−.428	.450	−.419
.400	−.472	.500	−.486	.500	−.490	.500	−.423
.500	−.430	.550	−.457	.550	−.444	.550	−.432
.550	−.391	.600	−.442	.600	−.428	.600	−.407
.600	−.382	.650	−.418	.650	−.419	.650	−.378
.650	.310	.700	−.418	.700	−.469	.700	.578
.700	1.002	.750	−.367	.740	−.388	.750	−.449
.750	−.177	.800	−.367				
.850	−.212	.850	−.246				
.900	−.153	.900	−.177				
.984	−.065	1.000	.022				

Lower surface

X/C	CP	X/C	CP	X/C	CP	X/C	CP
η = 0.25		η = 0.47		η = 0.64		η = 0.78	
.075	.057	.075	−.189	.075	−.310	.075	−.396
.125	.061	.125	−.142	.125	−.251	.125	−.442
.175	−.048	.175	−.322	.225	−.441	.225	−.498
.225	−.081	.225	−.350	.325	−.501	.325	−.467
.325	−.178	.325	−.320	.425	−.440	.425	−.495
.425	−.353	.425	−.488	.525	−.524	.525	−.470
.525	−.460	.525	−.512	.575	−.609	.575	−.494
.575	−.449	.575	−.518	.675	−.308	.675	−.190
.625	−.487	.625	−.547	.725	−.207		
.675	−.177	.725	−.177				
.725	−.346	.775	−.126				
.775	−.275	.825	−.031				
.825	−.163	.875	.049				
.875	−.052	.975	.102				
.975	−.066						

Table D-11

MINF = .799
HP= 20403
PSINF = 956.2
PRI = 892.6
QBAR = 427.6
ALPHA = 2.4

Upper surface

X/C	CP	X/C	CP	X/C	CP	X/C	CP
$\eta = 0.25$		$\eta = 0.47$		$\eta = 0.64$		$\eta = 0.78$	
.025	−.606	.040	−1.011	.050	−.725	.050	−.803
.120	−.566	.140	−.499	.200	−.504	.220	−.453
.200	−.536	.200	−.574	.300	−.889	.300	−.588
.250	−.507	.300	−.515	.400	−.432	.400	−.438
.300	−.467	.400	−.456	.450	−.393	.450	−.373
.400	−.444	.500	−.439	.500	−.451	.500	−.381
.500	−.397	.550	−.412	.550	−.406	.550	−.381
.550	−.362	.600	−.392	.600	−.362	.600	−.348
.600	−.346	.650	−.373	.650	−.366	.650	−.330
.650	−.359	.700	−.373	.700	−.418	.700	−.518
.700	−.310	.750	−.318	.740	−.300	.750	−.357
.750	−.366	.800	−.318				
.850	−.198	.850	−.219				
.900	−.131	.900	−.173				
.984	−.058	1.000	.048				

Lower surface

X/C	CP	X/C	CP	X/C	CP	X/C	CP
$\eta = 0.25$		$\eta = 0.47$		$\eta = 0.64$		$\eta = 0.78$	
.075	.067	.075	−.204	.075	−.341	.075	−.411
.125	.051	.125	−.159	.125	−.287	.125	−.468
.175	−.030	.175	−.329	.225	−.472	.225	−.496
.225	−.094	.225	−.367	.325	−.475	.325	−.426
.325	−.184	.325	−.336	.425	−.411	.425	−.552
.425	−.409	.425	−.531	.525	−.593	.525	−.441
.525	−.451	.525	−.509	.575	−.775	.575	−.455
.575	−.524	.575	−.547	.675	−.309	.675	−.213
.625	−.647	.625	−.657	.725	−.218		
.675	−.442	.725	−.224				
.725	−.383	.775	−.101				
.775	−.314	.825	−.002				
.825	−.209	.875	.082				
.875	−.103	.975	.181				
.975	−.073						

Table D-12

MINF = .799
HP= 20477
PSINF = 953.2
PRI = 890.4
QBAR = 425.8
ALPHA = 2.7

Upper surface

X/C	CP	X/C	CP	X/C	CP	X/C	CP
η = 0.25		η = 0.47		η = 0.64		η = 0.78	
.025	−.629	.040	−.929	.050	−.905	.050	−.873
.120	−.605	.140	−.637	.200	−.557	.220	−.483
.200	−.551	.200	−.553	.300	−.893	.300	−.610
.250	−.500	.300	−.515	.400	−.435	.400	−.445
.300	−.471	.400	−.461	.450	−.391	.450	−.375
.400	−.441	.500	−.438	.500	−.446	.500	−.385
.500	−.394	.550	−.409	.550	−.403	.550	−.388
.550	−.351	.600	−.388	.600	−.356	.600	−.355
.600	−.345	.650	−.361	.650	−.368	.650	−.338
.650	−.311	.700	−.361	.700	−.417	.700	−.541
.700	−.277	.750	−.284	.740	−.306	.750	−.381
.750	−.337	.800	−.284				
.850	−.187	.850	−.205				
.900	−.121	.900	−.168				
.984	−.045	1.000	.047				

Lower surface

X/C	CP	X/C	CP	X/C	CP	X/C	CP
η = 0.25		η = 0.47		η = 0.64		η = 0.78	
.075	.085	.075	−.189	.075	−.318	.075	−.390
.125	.078	.125	−.147	.125	−.266	.125	−.449
.175	−.011	.175	−.316	.225	−.459	.225	−.482
.225	−.073	.225	−.356	.325	−.470	.325	−.418
.325	−.162	.325	−.328	.425	−.402	.425	−.542
.425	−.394	.425	−.520	.525	−.579	.525	−.431
.525	−.464	.525	−.504	.575	−.756	.575	−.441
.575	−.520	.575	−.548	.675	−.301	.675	−.198
.625	−.646	.625	−.672	.725	−.206		
.675	−.335	.725	−.349				
.725	−.476	.775	−.112				
.775	−.291	.825	−.013				
.825	−.202	.875	.070				
.875	−.113	.975	.163				
.975	−.083						

Table D-13

MINF = .801
HP= 20433
PSINF = 955.0
PRI = 902.2
QBAR = 428.3
ALPHA = 1.9

Upper surface

X/C	CP	X/C	CP	X/C	CP	X/C	CP
η = 0.25		η = 0.47		η = 0.64		η = 0.78	
.025	−.593	.040	−.828	.050	−.483	.050	−.462
.120	−.538	.140	−.445	.200	−.517	.220	−.425
.200	−.514	.200	−.601	.300	−.846	.300	−.567
.250	−.475	.300	−.509	.400	−.423	.400	−.430
.300	−.454	.400	−.466	.450	−.389	.450	−.369
.400	−.439	.500	−.444	.500	−.445	.500	−.395
.500	−.391	.550	−.416	.550	−.403	.550	−.383
.550	−.345	.600	−.371	.600	−.350	.600	−.352
.600	−.349	.650	−.364	.650	−.372	.650	−.339
.650	−.256	.700	−.364	.700	−.441	.700	−.569
.700	−.163	.750	−.334	.740	−.340	.750	−.419
.750	−.163	.800	−.334				
.850	−.222	.850	−.246				
.900	−.162	.900	−.163				
.984	−.052	1.000	.039				

Lower surface

X/C	CP	X/C	CP	X/C	CP	X/C	CP
η = 0.25		η = 0.47		η = 0.64		η = 0.78	
.075	.036	.075	−.236	.075	−.366	.075	−.448
.125	.044	.125	−.173	.125	−.305	.125	−.497
.175	−.058	.175	−.337	.225	−.498	.225	−.522
.225	−.096	.225	−.370	.325	−.473	.325	−.438
.325	−.190	.325	−.338	.425	−.406	.425	−.546
.425	−.333	.425	−.506	.525	−.580	.525	−.431
.525	−.415	.525	−.475	.575	−.755	.575	−.428
.575	−.429	.575	−.536	.675	−.301	.675	−.198
.625	−.455	.625	−.516	.725	−.187		
.675	−.163	.725	−.163				
.725	−.304	.775	−.112				
.775	−.222	.825	−.022				
.825	−.159	.875	.044				
.875	−.097	.975	.101				
.975	−.077						

Table D-14

MINF = .801
HP= 21039
PSINF = 930.9
PRI = 885.5
QBAR = 418.3
ALPHA = 4.8

Upper surface

X/C	CP	X/C	CP	X/C	CP	X/C	CP
η = 0.25		η = 0.47		η = 0.64		η = 0.78	
.025	−.673	.040	−1.115	.050	−1.186	.050	−1.315
.120	−.890	.140	−1.314	.200	−1.221	.220	−1.011
.200	−.735	.200	−1.176	.300	−.676	.300	−.508
.250	−.662	.300	−.522	.400	−.351	.400	−.374
.300	−.580	.400	−.422	.450	−.357	.450	−.361
.400	−.462	.500	−.418	.500	−.410	.500	−.381
.500	−.398	.550	−.394	.550	−.385	.550	−.388
.550	−.354	.600	−.374	.600	−.346	.600	−.351
.600	−.340	.650	−.357	.650	−.348	.650	−.341
.650	−.244	.700	−.357	.700	−.392	.700	−.541
.700	−.148	.750	−.283	.740	−.311	.750	−.389
.750	−.148	.800	−.283				
.850	−.163	.850	−.199				
.900	−.087	.900	−.148				
.984	−.042	1.000	.058				

Lower surface

X/C	CP	X/C	CP	X/C	CP	X/C	CP
η = 0.25		η = 0.47		η = 0.64		η = 0.78	
.075	.187	.075	−.021	.075	−.102	.075	−.146
.125	.181	.125	−.007	.125	−.112	.125	−.233
.175	.093	.175	−.176	.225	−.287	.225	−.299
.225	.045	.225	−.225	.325	−.331	.325	−.298
.325	−.077	.325	−.225	.425	−.309	.425	−.401
.425	−.255	.425	−.387	.525	−.436	.525	−.352
.525	−.408	.525	−.406	.575	−.563	.575	−.364
.575	−.495	.575	−.477	.675	−.255	.675	−.147
.625	−.489	.625	−.506	.725	−.166		
.675	−.148	.725	−.148				
.725	−.361	.775	−.071				
.775	−.226	.825	.043				
.825	−.115	.875	.132				
.875	−.005	.975	.179				
.975	−.013						

Table D-15

MINF =	.820
HP=	19372
PSINF =	998.4
PRI =	948.4
QBAR =	470.2
ALPHA =	5.2

Upper surface

X/C	CP	X/C	CP	X/C	CP	X/C	CP
η = 0.25		η = 0.47		η = 0.64		η = 0.78	
.025	−.685	.040	−1.080	.050	−1.151	.050	−.148
.120	−.892	.140	−1.163	.200	−1.156	.220	−1.113
.200	−.824	.200	−1.139	.300	−.768	.300	−.148
.250	−.742	.300	−.148	.400	−.638	.400	−.679
.300	−.704	.400	−.612	.450	−.481	.450	−.421
.400	−.148	.500	−.388	.500	−.401	.500	−.351
.500	−.433	.550	−.343	.550	−.311	.550	−.316
.550	−.342	.600	−.323	.600	−.273	.600	−.261
.600	−.332	.650	−.316	.650	−.277	.650	−.280
.650	−.240	.700	−.316	.700	−.324	.700	−.428
.700	−.148	.750	−.267	.740	−.276	.750	−.329
.750	−.148	.800	−.267				
.850	−.161	.850	−.196				
.900	−.095	.900	−.148				
.984	−.050	1.000	.052				

Lower surface

X/C	CP	X/C	CP	X/C	CP	X/C	CP
η = 0.25		η = 0.47		η = 0.64		η = 0.78	
.075	.185	.075	.003	.075	−.085	.075	−.130
.125	.186	.125	.012	.125	−.096	.125	−.219
.175	.101	.175	−.160	.225	−.272	.225	−.307
.225	.058	.225	−.211	.325	−.327	.325	−.301
.325	−.062	.325	−.207	.425	−.308	.425	−.449
.425	−.245	.425	−.388	.525	−.493	.525	−.370
.525	−.395	.525	−.397	.575	−.678	.575	−.396
.575	−.435	.575	−.468	.675	−.260	.675	−.166
.625	−.487	.625	−.595	.725	−.175		
.675	−.148	.725	−.148				
.725	−.342	.775	−.079				
.775	−.205	.825	.019				
.825	−.092	.875	.112				
.875	.015	.975	.168				
.975	−.002						

Table D-16

MINF = .845
HP= 20625
PSINF = 947.3
PRI = 876.8
QBAR = 473.4
ALPHA = 1.9

Upper surface

X/C	CP	X/C	CP	X/C	CP	X/C	CP
η = 0.25		η = 0.47		η = 0.64		η = 0.78	
.025	−.456	.040	−.790	.050	−.732	.050	−.841
.120	−.647	.140	−1.019	.200	−.464	.220	−.496
.200	−.569	.200	−.552	.300	−.885	.300	−.971
.250	−.548	.300	−.476	.400	−.528	.400	−.433
.300	−.526	.400	−.484	.450	−.443	.450	−.361
.400	−.507	.500	−.512	.500	−.531	.500	−.392
.500	−.417	.550	−.434	.550	−.426	.550	−.409
.550	−.387	.600	−.424	.600	−.378	.600	−.357
.600	−.377	.650	−.392	.650	−.379	.650	−.332
.650	−.386	.700	−.392	.700	−.461	.700	−.611
.700	−.352	.750	−.338	.740	−.325	.750	−.378
.750	−.419	.800	−.338				
.850	−.211	.850	−.222				
.900	−.142	.900	−.162				
.984	−.052	1.000	.050				

Lower surface

X/C	CP	X/C	CP	X/C	CP	X/C	CP
η = 0.25		η = 0.47		η = 0.64		η = 0.78	
.075	.067	.075	−.238	.075	−.368	.075	−.435
.125	.048	.125	−.185	.125	−.305	.125	−.567
.175	−.050	.175	−.357	.225	−.512	.225	−.674
.225	−.054	.225	−.377	.325	−.617	.325	−.637
.325	−.304	.325	−.314	.425	−.628	.425	−.541
.425	−.259	.425	−.640	.525	−.670	.525	−.628
.525	−.598	.525	−.624	.575	−.711	.575	−.527
.575	−.570	.575	−.572	.675	−.296	.675	−.206
.625	−.552	.625	−.636	.725	−.194		
.675	−.548	.725	−.238				
.725	−.452	.775	−.143				
.775	−.370	.825	−.065				
.825	−.249	.875	.010				
.875	−.127	.975	.133				
.975	−.107						

Table D-17

MINF =	.848
HP=	20641
PSINF =	946.7
PRI =	875.8
QBAR =	476.3
ALPHA =	2.0

Upper surface

X/C	CP	X/C	CP	X/C	CP	X/C	CP
η = 0.25		η = 0.47		η = 0.64		η = 0.78	
.025	−.466	.040	−.756	.050	−.752	.050	−.892
.120	−.658	.140	−1.028	.200	−.725	.220	−.367
.200	−.573	.200	−.574	.300	−.697	.300	−1.000
.250	−.544	.300	−.542	.400	−.499	.400	−.463
.300	−.533	.400	−.434	.450	−.414	.450	−.422
.400	−.518	.500	−.486	.500	−.524	.500	−.383
.500	−.395	.550	−.432	.550	−.447	.550	−.410
.550	−.363	.600	−.421	.600	−.382	.600	−.357
.600	−.352	.650	−.386	.650	−.376	.650	−.329
.650	−.366	.700	−.386	.700	−.462	.700	−.608
.700	−.381	.750	−.307	.740	−.330	.750	−.388
.750	−.386	.800	−.307				
.850	−.207	.850	−.212				
.900	−.139	.900	−.162				
.984	−.044	1.000	.050				

Lower surface

X/C	CP	X/C	CP	X/C	CP	X/C	CP
η = 0.25		η = 0.47		η = 0.64		η = 0.78	
.075	.084	.075	−.230	.075	−.355	.075	−.426
.125	.068	.125	−.179	.125	−.290	.125	−.547
.175	−.040	.175	−.357	.225	−.505	.225	−.667
.225	−.030	.225	−.374	.325	−.610	.325	−.621
.325	−.293	.325	−.307	.425	−.614	.425	−.543
.425	−.279	.425	−.624	.525	−.673	.525	−.623
.525	−.567	.525	−.611	.575	−.732	.575	−.602
.575	−.550	.575	−.564	.675	−.307	.675	−.196
.625	−.574	.625	−.655	.725	−.195		
.675	−.454	.725	−.302				
.725	−.546	.775	−.165				
.775	−.372	.825	−.088				
.825	−.254	.875	−.010				
.875	−.135	.975	.098				
.975	−.109						

Table D-18

MINF = .851
HP= 20621
PSINF = 947.5
PRI = 882.6
QBAR = 480.1
ALPHA = 1.0

Upper surface

X/C	CP	X/C	CP	X/C	CP	X/C	CP
η = 0.25		η = 0.47		η = 0.64		η = 0.78	
.025	−.378	.040	−.586	.050	−.368	.050	−.181
.120	−.525	.140	−.525	.200	−.496	.220	−.489
.200	−.528	.200	−.510	.300	−.920	.300	−.868
.250	−.481	.300	−.467	.400	−.441	.400	−.449
.300	−.450	.400	−.541	.450	−.396	.450	−.360
.400	−.465	.500	−.450	.500	−.454	.500	−.371
.500	−.449	.550	−.411	.550	−.422	.550	−.409
.550	−.383	.600	−.428	.600	−.373	.600	−.351
.600	−.366	.650	−.381	.650	−.378	.650	−.339
.650	−.274	.700	−.381	.700	−.479	.700	−.593
.700	−.181	.750	−.363	.740	−.375	.750	−.496
.750	−.181	.800	−.363				
.850	−.232	.850	−.245				
.900	−.164	.900	−.181				
.984	−.065	1.000	.036				

Lower surface

X/C	CP	X/C	CP	X/C	CP	X/C	CP
η = 0.25		η = 0.47		η = 0.64		η = 0.78	
.075	−.011	.075	−.309	.075	−.432	.075	−.563
.125	.020	.125	−.238	.125	−.358	.125	−.620
.175	−.076	.175	−.404	.225	−.553	.225	−.665
.225	−.118	.225	−.405	.325	−.710	.325	−.774
.325	−.234	.325	−.332	.425	−.701	.425	−.595
.425	−.385	.425	−.637	.525	−.713	.525	−.567
.525	−.493	.525	−.629	.575	−.724	.575	−.378
.575	−.476	.575	−.555	.675	−.281	.675	−.194
.625	−.504	.625	−.631	.725	−.181		
.675	−.181	.725	−.181				
.725	−.338	.775	−.152				
.775	−.277	.825	−.080				
.825	−.203	.875	−.011				
.875	−.144	.975	.049				
.975	−.112						

Table D-19

MINF = .866
HP= 20583
PSINF = 949.0
PRI = 871.5
QBAR = 498.2
ALPHA = 1.6

Upper surface

X/C	CP	X/C	CP	X/C	CP	X/C	CP
η = 0.25		η = 0.47		η = 0.64		η = 0.78	
.025	−.385	.040	−.607	.050	−.648	.050	−.800
.120	−.608	.140	−.943	.200	−.701	.220	−.501
.200	−.555	.200	−.545	.300	−.849	.300	−.877
.250	−.517	.300	−.551	.400	−.514	.400	−.515
.300	−.527	.400	−.526	.450	−.466	.450	−.453
.400	−.550	.500	−.582	.500	−.554	.500	−.382
.500	−.515	.550	−.462	.550	−.371	.550	−.382
.550	−.401	.600	−.367	.600	−.417	.600	−.338
.600	−.373	.650	−.362	.650	−.380	.650	−.312
.650	−.379	.700	−.362	.700	−.476	.700	−.575
.700	−.363	.750	−.353	.740	−.368	.750	−.505
.750	−.448	.800	−.353				
.850	−.203	.850	−.213				
.900	−.132	.900	−.138				
.984	−.048	1.000	.050				

Lower surface

X/C	CP	X/C	CP	X/C	CP	X/C	CP
η = 0.25		η = 0.47		η = 0.64		η = 0.78	
.075	.069	.075	−.247	.075	−.381	.075	−.454
.125	.054	.125	−.196	.125	−.308	.125	−.566
.175	−.060	.175	−.391	.225	−.538	.225	−.633
.225	−.034	.225	−.387	.325	−.654	.325	−.716
.325	−.281	.325	−.304	.425	−.643	.425	−.561
.425	−.385	.425	−.600	.525	−.686	.525	−.693
.525	−.472	.525	−.625	.575	−.730	.575	−.814
.575	−.550	.575	−.539	.675	−.358	.675	−.188
.625	−.535	.625	−.697	.725	−.239		
.675	−.603	.725	−.279				
.725	−.478	.775	−.182				
.775	−.413	.825	−.124				
.825	−.272	.875	−.063				
.875	−.132	.975	.071				
.975	−.097						

Table D-20

MINF = .866
HP= 20765
PSINF = 941.7
PRI = 864.3
QBAR = 494.7
ALPHA = 1.7

Upper surface

X/C	CP	X/C	CP	X/C	CP	X/C	CP
η = 0.25		η = 0.47		η = 0.64		η = 0.78	
.025	−.394	.040	−.686	.050	−.675	.050	−.838
.120	−.616	.140	−.967	.200	−.716	.220	−.683
.200	−.578	.200	−.572	.300	−.798	.300	−.855
.250	−.508	.300	−.568	.400	−.547	.400	−.490
.300	−.532	.400	−.536	.450	−.478	.450	−.339
.400	−.553	.500	−.583	.500	−.539	.500	−.334
.500	−.525	.550	−.460	.550	−.352	.550	−.404
.550	−.416	.600	−.334	.600	−.377	.600	−.368
.600	−.328	.650	−.345	.650	−.378	.650	−.312
.650	−.417	.700	−.345	.700	−.478	.700	−.571
.700	−.506	.750	−.316	.740	−.368	.750	−.532
.750	−.387	.800	−.316				
.850	−.193	.850	−.207				
.900	−.125	.900	−.146				
.984	−.044	1.000	.046				

Lower surface

X/C	CP	X/C	CP	X/C	CP	X/C	CP
η = 0.25		η = 0.47		η = 0.64		η = 0.78	
.075	.081	.075	−.239	.075	−.373	.075	−.450
.125	.069	.125	−.188	.125	−.301	.125	−.555
.175	−.049	.175	−.383	.225	−.535	.225	−.632
.225	−.022	.225	−.384	.325	−.645	.325	−.708
.325	−.263	.325	−.299	.425	−.643	.425	−.560
.425	−.389	.425	−.595	.525	−.685	.525	−.680
.525	−.471	.525	−.615	.575	−.726	.575	−.794
.575	−.553	.575	−.536	.675	−.378	.675	−.181
.625	−.533	.625	−.696	.725	−.241		
.675	−.495	.725	−.265				
.725	−.642	.775	−.180				
.775	−.414	.825	−.148				
.825	−.270	.875	−.111				
.875	−.129	.975	.047				
.975	−.087						

Table D-21

MINF =	.876
HP=	20688
PSINF =	944.8
PRI =	869.6
QBAR =	507.1
ALPHA =	1.4

Upper surface

X/C	CP	X/C	CP	X/C	CP	X/C	CP
η = 0.25		η = 0.47		η = 0.64		η = 0.78	
.025	−.348	.040	−.620	.050	−.198	.050	−.719
.120	−.585	.140	−.849	.200	−.198	.220	−.484
.200	−.535	.200	−.523	.300	−.850	.300	−.876
.250	−.489	.300	−.539	.400	−.550	.400	−.578
.300	−.510	.400	−.531	.450	−.493	.450	−.551
.400	−.534	.500	−.594	.500	−.600	.500	−.530
.500	−.534	.550	−.588	.550	−.539	.550	−.580
.550	−.466	.600	−.561	.600	−.564	.600	−.582
.600	−.450	.650	−.459	.650	−.593	.650	−.317
.650	−.324	.700	−.459	.700	−.485	.700	−.491
.700	−.198	.750	−.392	.740	−.319	.750	−.371
.750	−.198	.800	−.392				
.850	−.241	.850	−.215				
.900	−.159	.900	−.198				
.984	−.050	1.000	.043				

Lower surface

X/C	CP	X/C	CP	X/C	CP	X/C	CP
η = 0.25		η = 0.47		η = 0.64		η = 0.78	
.075	.030	.075	−.258	.075	−.373	.075	−.198
.125	.060	.125	−.196	.125	−.311	.125	−.568
.175	−.035	.175	−.387	.225	−.503	.225	−.618
.225	−.091	.225	−.373	.325	−.732	.325	−.737
.325	−.206	.325	−.317	.425	−.662	.425	−.589
.425	−.400	.425	−.614	.525	−.697	.525	−.711
.525	−.538	.525	−.652	.575	−.732	.575	−.198
.575	−.422	.575	−.579	.675	−.396	.675	−.176
.625	−.599	.625	−.706	.725	−.251		
.675	−.198	.725	−.198				
.725	−.404	.775	−.228				
.775	−.342	.825	−.163				
.825	−.270	.875	−.103				
.875	−.198	.975	.039				
.975	−.160						

APPENDIX E
SURFACE PRESSURE COEFFICIENTS, PYLONS OFF, HP ≈ 30,000 FT

	M	α, deg
1	.630	10.5
2	.649	7.0
3	.650	6.3
4	.739	4.6
5	.747	5.0
6	.752	6.1
7	.793	7.1
8	.800	3.7
9	.800	4.0
10	.841	5.2
11	.845	3.1
12	.847	3.3
13	.873	2.7
14	.873	2.7
15	.875	4.0

Table E-1

MINF =	.630
HP=	30032
PSINF =	627.5
PRI =	615.0
QBAR =	174.3
ALPHA =	10.5

Upper surface

X/C	CP	X/C	CP	X/C	CP	X/C	CP
η = 0.25		η = 0.47		η = 0.64		η = 0.78	
.025	−1.436	.040	−1.659	.050	−2.471	.050	−2.230
.120	−.954	.140	−1.306	.200	−.973	.220	−.883
.200	−.789	.200	−1.053	.300	−.812	.300	−.757
.250	−.754	.300	−.888	.400	−.560	.400	−.574
.300	−.660	.400	−.677	.450	−.507	.450	−.497
.400	−.597	.500	−.525	.500	−.487	.500	−.466
.500	−.521	.550	−.469	.550	−.439	.550	−.443
.550	−.464	.600	−.438	.600	−.368	.600	−.413
.600	−.416	.650	−.388	.650	−.357	.650	−.378
.650	−.382	.700	−.388	.700	−.348	.700	−.394
.700	−.348	.750	−.258	.740	−.282	.750	−.322
.750	−.318	.800	−.258				
.850	−.195	.850	−.206				
.900	−.135	.900	−.175				
.984	−.058	1.000	−.123				

Lower surface

X/C	CP	X/C	CP	X/C	CP	X/C	CP
η = 0.25		η = 0.47		η = 0.64		η = 0.78	
.075	.273	.075	.307	.075	.269	.075	.252
.125	.257	.125	.253	.125	.197	.125	.133
.175	.191	.175	.099	.225	−.001	.225	−.018
.225	.128	.225	.037	.325	−.079	.325	−.065
.325	.014	.325	−.002	.425	−.115	.425	−.174
.425	−.156	.425	−.160	.525	−.204	.525	−.197
.525	−.363	.525	−.223	.575	−.294	.575	−.208
.575	−.397	.575	−.289	.675	−.182	.675	−.110
.625	−.472	.625	−.325	.725	−.140		
.675	−.392	.725	−.329				
.725	−.341	.775	−.052				
.775	−.210	.825	.086				
.825	−.082	.875	.189				
.875	.046	.975	.115				
.975	.003						

Table E-2

MINF =	.649
HP=	30291
PSINF =	620.2
PRI =	603.9
QBAR =	183.0
ALPHA =	7.0

Upper surface

X/C	CP	X/C	CP	X/C	CP	X/C	CP
η = 0.25		η = 0.47		η = 0.64		η = 0.78	
.025	−1.083	.040	−1.892	.050	−1.958	.050	−2.003
.120	−.752	.140	−.894	.200	−.705	.220	−.627
.200	−.641	.200	−.723	.300	−.738	.300	−.673
.250	−.579	.300	−.632	.400	−.499	.400	−.508
.300	−.529	.400	−.517	.450	−.453	.450	−.435
.400	−.472	.500	−.448	.500	−.467	.500	−.420
.500	−.414	.550	−.411	.550	−.423	.550	−.411
.550	−.369	.600	−.396	.600	−.359	.600	−.391
.600	−.372	.650	−.356	.650	−.374	.650	−.372
.650	−.336	.700	−.356	.700	−.392	.700	−.492
.700	−.263	.750	−.252	.740	−.316	.750	−.384
.750	−.286	.800	−.252				
.850	−.141	.850	−.176				
.900	−.063	.900	−.126				
.984	−.038	1.000	.003				

Lower surface

X/C	CP	X/C	CP	X/C	CP	X/C	CP
η = 0.25		η = 0.47		η = 0.64		η = 0.78	
.075	.246	.075	.135	.075	.081	.075	.069
.125	.246	.125	.102	.125	.041	.125	−.029
.175	.154	.175	−.049	.225	−.135	.225	−.140
.225	.102	.225	−.103	.325	−.183	.325	−.155
.325	−.012	.325	−.120	.425	−.191	.425	−.238
.425	−.204	.425	−.254	.525	−.266	.525	−.237
.525	−.413	.525	−.298	.575	−.341	.575	−.235
.575	−.426	.575	−.344	.675	−.193	.675	−.106
.625	−.496	.625	−.370	.725	−.136		
.675	−.438	.725	−.170				
.725	−.346	.775	−.040				
.775	−.181	.825	.093				
.825	−.057	.875	.197				
.875	.067	.975	.182				
.975	.046						

Table E-3

MINF = .649
HP= 30183
PSINF = 623.2
PRI = 605.0
QBAR = 184.2
ALPHA = 6.3

Upper surface

X/C	CP	X/C	CP	X/C	CP	X/C	CP
$\eta = 0.25$		$\eta = 0.47$		$\eta = 0.64$		$\eta = 0.78$	
.025	−1.086	.040	−1.835	.050	−1.305	.050	−1.130
.120	−.711	.140	−.747	.200	−.668	.220	−.587
.200	−.614	.200	−.696	.300	−.719	.300	−.656
.250	−.588	.300	−.587	.400	−.482	.400	−.495
.300	−.503	.400	−.499	.450	−.430	.450	−.423
.400	−.468	.500	−.436	.500	−.449	.500	−.408
.500	−.407	.550	−.407	.550	−.415	.550	−.403
.550	−.377	.600	−.383	.600	−.350	.600	−.383
.600	−.344	.650	−.346	.650	−.362	.650	−.362
.650	−.304	.700	−.346	.700	−.388	.700	−.492
.700	−.264	.750	−.243	.740	−.300	.750	−.372
.750	−.291	.800	−.243				
.850	−.158	.850	−.183				
.900	−.092	.900	−.141				
.984	−.055	1.000	.013				

Lower surface

X/C	CP	X/C	CP	X/C	CP	X/C	CP
$\eta = 0.25$		$\eta = 0.47$		$\eta = 0.64$		$\eta = 0.78$	
.075	.199	.075	.077	.075	.021	.075	−.004
.125	.173	.125	.063	.125	−.010	.125	−.097
.175	.096	.175	−.096	.225	−.182	.225	−.195
.225	.034	.225	−.149	.325	−.229	.325	−.206
.325	−.082	.325	−.165	.425	−.227	.425	−.281
.425	−.241	.425	−.292	.525	−.302	.525	−.277
.525	−.414	.525	−.324	.575	−.376	.575	−.267
.575	−.447	.575	−.373	.675	−.222	.675	−.133
.625	−.475	.625	−.393	.725	−.170		
.675	−.379	.725	−.337				
.725	−.380	.775	−.060				
.775	−.217	.825	.077				
.825	−.089	.875	.177				
.875	.034	.975	.174				
.975	.025						

Table E-4

MINF = .739
HP= 30307
PSINF = 619.7
PRI = 590.9
QBAR = 236.9
ALPHA = 4.6

Upper surface

X/C	CP	X/C	CP	X/C	CP	X/C	CP
η = 0.25		η = 0.47		η = 0.64		η = 0.78	
.025	−.817	.040	−1.285	.050	−1.321	.050	−1.514
.120	−.678	.140	−.719	.200	−.601	.220	−.538
.200	−.579	.200	−.618	.300	−.717	.300	−.633
.250	−.554	.300	−.561	.400	−.461	.400	−.470
.300	−.485	.400	−.481	.450	−.421	.450	−.400
.400	−.451	.500	−.431	.500	−.447	.500	−.389
.500	−.399	.550	−.414	.550	−.407	.550	−.392
.550	−.361	.600	−.386	.600	−.359	.600	−.367
.600	−.329	.650	−.355	.650	−.361	.650	−.347
.650	−.318	.700	−.355	.700	−.393	.700	−.500
.700	−.306	.750	−.261	.740	−.294	.750	−.358
.750	−.310	.800	−.261				
.850	−.172	.850	−.197				
.900	−.105	.900	−.153				
.984	−.052	1.000	.031				

Lower surface

X/C	CP	X/C	CP	X/C	CP	X/C	CP
η = 0.25		η = 0.47		η = 0.64		η = 0.78	
.075	.145	.075	−.050	.075	−.143	.075	−.174
.125	.122	.125	−.040	.125	−.132	.125	−.242
.175	.042	.175	−.202	.225	−.302	.225	−.316
.225	−.020	.225	−.249	.325	−.335	.325	−.303
.325	−.142	.325	−.244	.425	−.316	.425	−.384
.425	−.294	.425	−.388	.525	−.405	.525	−.357
.525	−.449	.525	−.410	.575	−.494	.575	−.356
.575	−.541	.575	−.465	.675	−.275	.675	−.180
.625	−.495	.625	−.484	.725	−.198		
.675	−.405	.725	−.355				
.725	−.458	.775	−.083				
.775	−.261	.825	.043				
.825	−.136	.875	.139				
.875	−.008	.975	.178				
.975	.008						

Table E-5

MINF = .747
HP= 30342
PSINF = 618.7
PRI = 591.0
QBAR = 241.4
ALPHA = 5.0

Upper surface

X/C	CP	X/C	CP	X/C	CP	X/C	CP
η = 0.25		η = 0.47		η = 0.64		η = 0.78	
.025	−.799	.040	−1.343	.050	−1.364	.050	−1.649
.120	−.741	.140	−.941	.200	−.582	.220	−.556
.200	−.598	.200	−.602	.300	−.725	.300	−.646
.250	−.559	.300	−.545	.400	−.477	.400	−.485
.300	−.504	.400	−.489	.450	−.431	.450	−.414
.400	−.464	.500	−.453	.500	−.465	.500	−.405
.500	−.408	.550	−.415	.550	−.421	.550	−.405
.550	−.371	.600	−.396	.600	−.365	.600	−.377
.600	−.352	.650	−.367	.650	−.372	.650	−.357
.650	−.349	.700	−.367	.700	−.400	.700	−.508
.700	−.290	.750	−.285	.740	−.306	.750	−.372
.750	−.328	.800	−.285				
.850	−.168	.850	−.203				
.900	−.095	.900	−.157				
.984	−.051	1.000	.037				

Lower surface

X/C	CP	X/C	CP	X/C	CP	X/C	CP
η = 0.25		η = 0.47		η = 0.64		η = 0.78	
.075	.176	.075	−.009	.075	−.105	.075	−.129
.125	.165	.125	−.014	.125	−.104	.125	−.209
.175	.080	.175	−.179	.225	−.280	.225	−.283
.225	.016	.225	−.223	.325	−.311	.325	−.283
.325	−.107	.325	−.222	.425	−.298	.425	−.363
.425	−.263	.425	−.374	.525	−.389	.525	−.342
.525	−.429	.525	−.395	.575	−.479	.575	−.339
.575	−.546	.575	−.449	.675	−.265	.675	−.165
.625	−.521	.625	−.474	.725	−.191		
.675	−.484	.725	−.194				
.725	−.378	.775	−.066				
.775	−.259	.825	.060				
.825	−.124	.875	.160				
.875	.011	.975	.196				
.975	.022						

Table E-6

MINF =	.752
HP=	30405
PSINF =	616.9
PRI =	590.3
QBAR =	244.3
ALPHA =	6.1

Upper surface

X/C	CP	X/C	CP	X/C	CP	X/C	CP
η = 0.25		η = 0.47		η = 0.64		η = 0.78	
.025	−.891	.040	−1.448	.050	−1.473	.050	−1.784
.120	−.943	.140	−1.467	.200	−.917	.220	−.638
.200	−.687	.200	−.800	.300	−.679	.300	−.603
.250	−.619	.300	−.557	.400	−.457	.400	−.476
.300	−.543	.400	−.488	.450	−.421	.450	−.413
.400	−.488	.500	−.439	.500	−.452	.500	−.409
.500	−.420	.550	−.413	.550	−.410	.550	−.409
.550	−.386	.600	−.391	.600	−.359	.600	−.378
.600	−.351	.650	−.359	.650	−.361	.650	−.359
.650	−.328	.700	−.359	.700	−.383	.700	−.494
.700	−.306	.750	−.247	.740	−.294	.750	−.359
.750	−.319	.800	−.247				
.850	−.172	.850	−.179				
.900	−.102	.900	−.144				
.984	−.057	1.000	.028				

Lower surface

X/C	CP	X/C	CP	X/C	CP	X/C	CP
η = 0.25		η = 0.47		η = 0.64		η = 0.78	
.075	.201	.075	.050	.075	−.021	.075	−.051
.125	.178	.125	.040	.125	−.045	.125	−.143
.175	.103	.175	−.124	.225	−.227	.225	−.239
.225	.037	.225	−.173	.325	−.273	.325	−.248
.325	−.071	.325	−.180	.425	−.272	.425	−.339
.425	−.253	.425	−.335	.525	−.368	.525	−.333
.525	−.402	.525	−.374	.575	−.463	.575	−.334
.575	−.494	.575	−.446	.675	−.262	.675	−.164
.625	−.510	.625	−.476	.725	−.192		
.675	−.423	.725	−.351				
.725	−.543	.775	−.069				
.775	−.261	.825	.063				
.825	−.130	.875	.161				
.875	.002	.975	.187				
.975	.014						

Table E-7

MINF = .793
HP= 30457
PSINF = 615.5
PRI = 586.3
QBAR = 270.6
ALPHA = 7.1

Upper surface

X/C	CP	X/C	CP	X/C	CP	X/C	CP
$\eta = 0.25$		$\eta = 0.47$		$\eta = 0.64$		$\eta = 0.78$	
.025	−.895	.040	−1.392	.050	−1.405	.050	−1.681
.120	−1.121	.140	−1.623	.200	−1.453	.220	−1.499
.200	−.983	.200	−1.453	.300	−1.478	.300	−1.234
.250	−.877	.300	−1.197	.400	−.764	.400	−.670
.300	−.792	.400	−.727	.450	−.639	.450	−.479
.400	−.555	.500	−.369	.500	−.457	.500	−.338
.500	−.417	.550	−.341	.550	−.366	.550	−.299
.550	−.385	.600	−.330	.600	−.289	.600	−.285
.600	−.348	.650	−.315	.650	−.284	.650	−.279
.650	−.316	.700	−.315	.700	−.294	.700	−.355
.700	−.283	.750	−.209	.740	−.246	.750	−.283
.750	−.322	.800	−.209				
.850	−.163	.850	−.157				
.900	−.087	.900	−.138				
.984	−.051	1.000	.026				

Lower surface

X/C	CP	X/C	CP	X/C	CP	X/C	CP
$\eta = 0.25$		$\eta = 0.47$		$\eta = 0.64$		$\eta = 0.78$	
.075	.241	.075	.107	.075	.030	.075	.005
.125	.211	.125	.099	.125	−.001	.125	−.098
.175	.142	.175	−.072	.225	−.188	.225	−.203
.225	.093	.225	−.118	.325	−.251	.325	−.232
.325	−.029	.325	−.143	.425	−.253	.425	−.336
.425	−.217	.425	−.311	.525	−.368	.525	−.331
.525	−.360	.525	−.352	.575	−.483	.575	−.348
.575	−.415	.575	−.440	.675	−.257	.675	−.164
.625	−.530	.625	−.494	.725	−.183		
.675	−.600	.725	−.315				
.725	−.498	.775	−.054				
.775	−.286	.825	.077				
.825	−.140	.875	.176				
.875	.010	.975	.206				
.975	.024						

Table E-8

MINF =	.800
HP=	30425
PSINF =	616.4
PRI =	581.0
QBAR =	276.0
ALPHA =	3.7

Upper surface

X/C	CP	X/C	CP	X/C	CP	X/C	CP
$\eta = 0.25$		$\eta = 0.47$		$\eta = 0.64$		$\eta = 0.78$	
.025	−.668	.040	−1.035	.050	−1.049	.050	−1.271
.120	−.771	.140	−1.229	.200	−.574	.220	−.504
.200	−.662	.200	−.628	.300	−.754	.300	−.689
.250	−.584	.300	−.484	.400	−.465	.400	−.487
.300	−.509	.400	−.473	.450	−.428	.450	−.405
.400	−.473	.500	−.455	.500	−.470	.500	−.404
.500	−.413	.550	−.427	.550	−.427	.550	−.405
.550	−.377	.600	−.399	.600	−.372	.600	−.368
.600	−.349	.650	−.375	.650	−.375	.650	−.352
.650	−.312	.700	−.375	.700	−.416	.700	−.540
.700	−.274	.750	−.281	.740	−.309	.750	−.366
.750	−.343	.800	−.281				
.850	−.178	.850	−.206				
.900	−.119	.900	−.164				
.984	−.052	1.000	.040				

Lower surface

X/C	CP	X/C	CP	X/C	CP	X/C	CP
$\eta = 0.25$		$\eta = 0.47$		$\eta = 0.64$		$\eta = 0.78$	
.075	.113	.075	−.118	.075	−.232	.075	−.279
.125	.098	.125	−.089	.125	−.199	.125	−.350
.175	.020	.175	−.265	.225	−.393	.225	−.411
.225	−.051	.225	−.296	.325	−.421	.325	−.373
.325	−.144	.325	−.290	.425	−.378	.425	−.493
.425	−.337	.425	−.467	.525	−.539	.525	−.421
.525	−.438	.525	−.463	.575	−.699	.575	−.431
.575	−.525	.575	−.528	.675	−.306	.675	−.205
.625	−.631	.625	−.586	.725	−.221		
.675	−.497	.725	−.316				
.725	−.413	.775	−.094				
.775	−.303	.825	.012				
.825	−.190	.875	.098				
.875	−.071	.975	.178				
.975	−.032						

Table E-9

MINF = .800
HP= 30423
PSINF = 616.4
PRI = 580.6
QBAR = 276.4
ALPHA = 4.1

Upper surface

X/C	CP	X/C	CP	X/C	CP	X/C	CP
η = 0.25		η = 0.47		η = 0.64		η = 0.78	
.025	−.644	.040	−1.131	.050	−1.093	.050	−1.320
.120	−.831	.140	−1.256	.200	−.876	.220	−.444
.200	−.686	.200	−.728	.300	−.611	.300	−.608
.250	−.607	.300	−.461	.400	−.444	.400	−.485
.300	−.518	.400	−.461	.450	−.412	.450	−.402
.400	−.468	.500	−.448	.500	−.467	.500	−.405
.500	−.411	.550	−.423	.550	−.422	.550	−.409
.550	−.374	.600	−.401	.600	−.370	.600	−.375
.600	−.357	.650	−.377	.650	−.375	.650	−.354
.650	−.357	.700	−.377	.700	−.414	.700	−.548
.700	−.302	.750	−.300	.740	−.309	.750	−.376
.750	−.349	.800	−.300				
.850	−.173	.850	−.204				
.900	−.106	.900	−.159				
.984	−.048	1.000	.048				

Lower surface

X/C	CP	X/C	CP	X/C	CP	X/C	CP
η = 0.25		η = 0.47		η = 0.64		η = 0.78	
.075	.145	.075	−.083	.075	−.197	.075	−.240
.125	.133	.125	−.066	.125	−.177	.125	−.310
.175	.051	.175	−.240	.225	−.362	.225	−.379
.225	−.016	.225	−.279	.325	−.397	.325	−.351
.325	−.113	.325	−.269	.425	−.358	.425	−.469
.425	−.340	.425	−.447	.525	−.516	.525	−.403
.525	−.426	.525	−.455	.575	−.673	.575	−.416
.575	−.509	.575	−.521	.675	−.297	.675	−.195
.625	−.672	.625	−.582	.725	−.209		
.675	−.459	.725	−.205				
.725	−.400	.775	−.080				
.775	−.289	.825	.028				
.825	−.164	.875	.115				
.875	−.040	.975	.194				
.975	−.006						

Table E-10

MINF = .841
HP= 30486
PSINF = 614.7
PRI = 578.3
QBAR = 304.2
ALPHA = 5.2

Upper surface

X/C	CP	X/C	CP	X/C	CP	X/C	CP
$\eta = 0.25$		$\eta = 0.47$		$\eta = 0.64$		$\eta = 0.78$	
.025	−.656	.040	−1.023	.050	−1.081	.050	−1.306
.120	−.875	.140	−1.280	.200	−1.179	.220	−1.179
.200	−.839	.200	−1.176	.300	−1.218	.300	−1.281
.250	−.771	.300	−1.232	.400	−1.167	.400	−1.112
.300	−.721	.400	−.801	.450	−1.079	.450	−.871
.400	−.732	.500	−.769	.500	−.667	.500	−.612
.500	−.738	.550	−.488	.550	−.485	.550	−.474
.550	−.597	.600	−.312	.600	−.307	.600	−.294
.600	−.344	.650	−.273	.650	−.224	.650	−.192
.650	−.295	.700	−.273	.700	−.216	.700	−.240
.700	−.247	.750	−.201	.740	−.190	.750	−.211
.750	−.296	.800	−.201				
.850	−.139	.850	−.147				
.900	−.082	.900	−.111				
.984	−.043	1.000	.068				

Lower surface

X/C	CP	X/C	CP	X/C	CP	X/C	CP
$\eta = 0.25$		$\eta = 0.47$		$\eta = 0.64$		$\eta = 0.78$	
.075	.197	.075	−.012	.075	−.114	.075	−.167
.125	.165	.125	.003	.125	−.113	.125	−.258
.175	.085	.175	−.171	.225	−.318	.225	−.341
.225	.052	.225	−.215	.325	−.357	.325	−.326
.325	−.124	.325	−.212	.425	−.327	.425	−.512
.425	−.173	.425	−.421	.525	−.514	.525	−.382
.525	−.558	.525	−.408	.575	−.701	.575	−.427
.575	−.403	.575	−.457	.675	−.259	.675	−.196
.625	−.502	.625	−.648	.725	−.182		
.675	−.554	.725	−.281				
.725	−.528	.775	−.104				
.775	−.387	.825	−.013				
.825	−.203	.875	.066				
.875	−.017	.975	.181				
.975	−.005						

Table E-11

MINF = .845
HP= 30472
PSINF = 615.1
PRI = 572.7
QBAR = 307.3
ALPHA = 3.1

Upper surface

X/C	CP	X/C	CP	X/C	CP	X/C	CP
$\eta = 0.25$		$\eta = 0.47$		$\eta = 0.64$		$\eta = 0.78$	
.025	−.547	.040	−.864	.050	−.878	.050	−1.079
.120	−.719	.140	−1.110	.200	−.912	.220	−.909
.200	−.674	.200	−.957	.300	−1.107	.300	−.846
.250	−.621	.300	−.638	.400	−.346	.400	−.336
.300	−.601	.400	−.593	.450	−.327	.450	−.326
.400	−.623	.500	−.394	.500	−.392	.500	−.367
.500	−.407	.550	−.391	.550	−.385	.550	−.400
.550	−.365	.600	−.387	.600	−.354	.600	−.356
.600	−.348	.650	−.372	.650	−.358	.650	−.339
.650	−.321	.700	−.372	.700	−.419	.700	−.589
.700	−.294	.750	−.287	.740	−.310	.750	−.351
.750	−.373	.800	−.287				
.850	−.188	.850	−.204				
.900	−.127	.900	−.146				
.984	−.042	1.000	.055				

Lower surface

X/C	CP	X/C	CP	X/C	CP	X/C	CP
$\eta = 0.25$		$\eta = 0.47$		$\eta = 0.64$		$\eta = 0.78$	
.075	.105	.075	−.164	.075	−.281	.075	−.347
.125	.080	.125	−.121	.125	−.237	.125	−.400
.175	−.005	.175	−.291	.225	−.470	.225	−.658
.225	−.029	.225	−.321	.325	−.392	.325	−.366
.325	−.240	.325	−.289	.425	−.558	.425	−.546
.425	−.223	.425	−.604	.525	−.633	.525	−.648
.525	−.618	.525	−.437	.575	−.708	.575	−.455
.575	−.567	.575	−.483	.675	−.337	.675	−.209
.625	−.523	.625	−.665	.725	−.212		
.675	−.537	.725	−.280				
.725	−.468	.775	−.140				
.775	−.380	.825	−.059				
.825	−.237	.875	.013				
.875	−.093	.975	.115				
.975	−.059						

Table E-12

MINF = .846
HP= 30511
PSINF = 613.9
PRI = 572.1
QBAR = 308.0
ALPHA = 3.3

Upper surface

X/C	CP	X/C	CP	X/C	CP	X/C	CP
η = 0.25		η = 0.47		η = 0.64		η = 0.78	
.025	−.531	.040	−.919	.050	−.893	.050	−1.086
.120	−.735	.140	−1.108	.200	−.956	.220	−.919
.200	−.682	.200	−.983	.300	−1.106	.300	−1.190
.250	−.623	.300	−.662	.400	−.443	.400	−.337
.300	−.604	.400	−.634	.450	−.323	.450	−.268
.400	−.632	.500	−.372	.500	−.342	.500	−.296
.500	−.483	.550	−.355	.550	−.341	.550	−.343
.550	−.355	.600	−.371	.600	−.319	.600	−.331
.600	−.341	.650	−.360	.650	−.338	.650	−.325
.650	−.364	.700	−.360	.700	−.401	.700	−.578
.700	−.321	.750	−.308	.740	−.308	.750	−.361
.750	−.380	.800	−.308				
.850	−.180	.850	−.203				
.900	−.110	.900	−.143				
.984	−.037	1.000	.061				

Lower surface

X/C	CP	X/C	CP	X/C	CP	X/C	CP
η = 0.25		η = 0.47		η = 0.64		η = 0.78	
.075	.128	.075	−.137	.075	−.268	.075	−.328
.125	.112	.125	−.106	.125	−.227	.125	−.381
.175	.020	.175	−.276	.225	−.448	.225	−.650
.225	−.004	.225	−.308	.325	−.381	.325	−.356
.325	−.202	.325	−.279	.425	−.556	.425	−.533
.425	−.215	.425	−.593	.525	−.630	.525	−.639
.525	−.618	.525	−.430	.575	−.704	.575	−.458
.575	−.573	.575	−.486	.675	−.328	.675	−.202
.625	−.526	.625	−.660	.725	−.200		
.675	−.546	.725	−.221				
.725	−.452	.775	−.130				
.775	−.365	.825	−.050				
.825	−.218	.875	.021				
.875	−.072	.975	.135				
.975	−.046						

Table E-13

MINF =	.873
HP=	30556
PSINF =	612.7
PRI =	567.0
QBAR =	326.7
ALPHA =	2.7

Upper surface

X/C	CP	X/C	CP	X/C	CP	X/C	CP
η = 0.25		η = 0.47		η = 0.64		η = 0.78	
.025	−.466	.040	−.752	.050	−.759	.050	−.952
.120	−.666	.140	−1.027	.200	−.831	.220	−.856
.200	−.646	.200	−.877	.300	−1.035	.300	−1.150
.250	−.615	.300	−.618	.400	−.609	.400	−.806
.300	−.578	.400	−.601	.450	−.552	.450	−.809
.400	−.610	.500	−.667	.500	−.653	.500	−.574
.500	−.609	.550	−.666	.550	−.595	.550	−.354
.550	−.596	.600	−.655	.600	−.648	.600	−.252
.600	−.536	.650	−.631	.650	−.353	.650	−.229
.650	−.445	.700	−.631	.700	−.290	.700	−.435
.700	−.354	.750	−.232	.740	−.219	.750	−.285
.750	−.358	.800	−.232				
.850	−.178	.850	−.165				
.900	−.118	.900	−.124				
.984	−.039	1.000	.065				

Lower surface

X/C	CP	X/C	CP	X/C	CP	X/C	CP
η = 0.25		η = 0.47		η = 0.64		η = 0.78	
.075	.101	.075	−.193	.075	−.321	.075	−.375
.125	.069	.125	−.148	.125	−.248	.125	−.506
.175	−.036	.175	−.336	.225	−.490	.225	−.620
.225	−.023	.225	−.354	.325	−.588	.325	−.613
.325	−.258	.325	−.271	.425	−.633	.425	−.554
.425	−.344	.425	−.575	.525	−.666	.525	−.675
.525	−.423	.525	−.578	.575	−.699	.575	−.745
.575	−.543	.575	−.519	.675	−.429	.675	−.192
.625	−.528	.625	−.675	.725	−.267		
.675	−.690	.725	−.235				
.725	−.529	.775	−.158				
.775	−.448	.825	−.122				
.825	−.273	.875	−.097				
.875	−.096	.975	.061				
.975	−.057						

Table E-14

MINF = .873
HP= 30644
PSINF = 610.2
PRI = 565.8
QBAR = 325.9
ALPHA = 2.7

Upper surface

X/C	CP	X/C	CP	X/C	CP	X/C	CP
η = 0.25		η = 0.47		η = 0.64		η = 0.78	
.025	−.443	.040	−.767	.050	−.761	.050	−.957
.120	−.671	.140	−1.026	.200	−.833	.220	−.846
.200	−.647	.200	−.885	.300	−1.029	.300	−1.142
.250	−.601	.300	−.666	.400	−.658	.400	−.808
.300	−.584	.400	−.606	.450	−.560	.450	−.818
.400	−.601	.500	−.666	.500	−.650	.500	−.703
.500	−.613	.550	−.668	.550	−.605	.550	−.458
.550	−.593	.600	−.664	.600	−.647	.600	−.272
.600	−.552	.650	−.644	.650	−.506	.650	−.231
.650	−.533	.700	−.644	.700	−.301	.700	−.416
.700	−.452	.750	−.245	.740	−.221	.750	−.305
.750	−.374	.800	−.245				
.850	−.168	.850	−.158				
.900	−.122	.900	−.099				
.984	−.032	1.000	.069				

Lower surface

X/C	CP	X/C	CP	X/C	CP	X/C	CP
η = 0.25		η = 0.47		η = 0.64		η = 0.78	
.075	.113	.075	−.176	.075	−.304	.075	−.364
.125	.094	.125	−.142	.125	−.247	.125	−.486
.175	−.017	.175	−.324	.225	−.463	.225	−.612
.225	.001	.225	−.344	.325	−.574	.325	−.587
.325	−.247	.325	−.267	.425	−.627	.425	−.539
.425	−.313	.425	−.568	.525	−.660	.525	−.675
.525	−.443	.525	−.575	.575	−.693	.575	−.746
.575	−.554	.575	−.518	.675	−.357	.675	−.194
.625	−.535	.625	−.676	.725	−.238		
.675	−.629	.725	−.250				
.725	−.467	.775	−.156				
.775	−.436	.825	−.097				
.825	−.268	.875	−.048				
.875	−.102	.975	.080				
.975	−.051						

Table E-15

MINF = .875
HP= 31192
PSINF = 595.1
PRI = 555.4
QBAR = 318.6
ALPHA = 4.0

Upper surface

X/C	CP	X/C	CP	X/C	CP	X/C	CP
$\eta = 0.25$		$\eta = 0.47$		$\eta = 0.64$		$\eta = 0.78$	
.025	−.518	.040	−.850	.050	−.874	.050	−1.082
.120	−.737	.140	−1.075	.200	−1.033	.220	−.978
.200	−.737	.200	−1.005	.300	−1.072	.300	−1.172
.250	−.681	.300	−1.022	.400	−1.017	.400	−.992
.300	−.638	.400	−.707	.450	−.970	.450	−.979
.400	−.680	.500	−.726	.500	−.943	.500	−.995
.500	−.678	.550	−.745	.550	−.789	.550	−.856
.550	−.656	.600	−.751	.600	−.727	.600	−.681
.600	−.648	.650	−.757	.650	−.649	.650	−.555
.650	−.566	.700	−.757	.700	−.420	.700	−.401
.700	−.484	.750	−.216	.740	−.250	.750	−.238
.750	−.406	.800	−.216				
.850	−.153	.850	−.133				
.900	−.089	.900	−.073				
.984	−.035	1.000	.022				

Lower surface

X/C	CP	X/C	CP	X/C	CP	X/C	CP
$\eta = 0.25$		$\eta = 0.47$		$\eta = 0.64$		$\eta = 0.78$	
.075	.155	.075	−.093	.075	−.204	.075	−.266
.125	.123	.125	−.067	.125	−.173	.125	−.320
.175	.025	.175	−.248	.225	−.403	.225	−.587
.225	.027	.225	−.283	.325	−.351	.325	−.407
.325	−.187	.325	−.233	.425	−.499	.425	−.493
.425	−.297	.425	−.513	.525	−.573	.525	−.655
.525	−.363	.525	−.418	.575	−.646	.575	−.717
.575	−.354	.575	−.485	.675	−.478	.675	−.189
.625	−.511	.625	−.618	.725	−.241		
.675	−.705	.725	−.301				
.725	−.532	.775	−.184				
.775	−.562	.825	−.095				
.825	−.312	.875	−.022				
.875	−.062	.975	.078				
.975	−.009						

APPENDIX F
SURFACE PRESSURE COEFFICIENTS, PYLONS OFF, HP $\approx$ 40,000 FT

	M	α, deg
1	.734	7.9
2	.799	6.1
3	.853	4.7

Table F-1

MINF = .734
HP= 40164
PSINF = 388.6
PRI = 375.7
QBAR = 146.7
ALPHA = 7.9

Upper surface

X/C	CP	X/C	CP	X/C	CP	X/C	CP
η = 0.25		η = 0.47		η = 0.64		η = 0.78	
.025	−1.126	.040	−1.655	.050	−1.714	.050	−2.021
.120	−1.131	.140	−1.284	.200	−1.253	.220	−1.018
.200	−.759	.200	−.989	.300	−.765	.300	−.643
.250	−.674	.300	−.795	.400	−.484	.400	−.472
.300	−.578	.400	−.591	.450	−.457	.450	−.412
.400	−.537	.500	−.479	.500	−.448	.500	−.403
.500	−.463	.550	−.425	.550	−.424	.550	−.401
.550	−.433	.600	−.406	.600	−.350	.600	−.378
.600	−.390	.650	−.375	.650	−.360	.650	−.360
.650	−.396	.700	−.375	.700	−.367	.700	−.439
.700	−.322	.750	−.261	.740	−.297	.750	−.338
.750	−.362	.800	−.261				
.850	−.178	.850	−.197				
.900	−.106	.900	−.155				
.984	−.070	1.000	−.025				

Lower surface

X/C	CP	X/C	CP	X/C	CP	X/C	CP
η = 0.25		η = 0.47		η = 0.64		η = 0.78	
.075	.225	.075	.160	.075	.089	.075	.072
.125	.207	.125	.126	.125	.035	.125	−.030
.175	.140	.175	−.040	.225	−.149	.225	−.165
.225	.074	.225	−.082	.325	−.202	.325	−.180
.325	−.039	.325	−.115	.425	−.216	.425	−.285
.425	−.194	.425	−.269	.525	−.310	.525	−.292
.525	−.382	.525	−.304	.575	−.404	.575	−.295
.575	−.454	.575	−.371	.675	−.242	.675	−.157
.625	−.495	.625	−.408	.725	−.184		
.675	−.495	.725	−.166				
.725	−.345	.775	−.047				
.775	−.251	.825	.087				
.825	−.140	.875	.187				
.875	−.029	.975	.184				
.975	.032						

Table F-2

MINF =	.799
HP=	40334
PSINF =	385.5
PRI =	366.5
QBAR =	172.3
ALPHA =	6.1

Upper surface

X/C	CP	X/C	CP	X/C	CP	X/C	CP
$\eta = 0.25$		$\eta = 0.47$		$\eta = 0.64$		$\eta = 0.78$	
.025	−.796	.040	−1.224	.050	−1.289	.050	−1.548
.120	−1.012	.140	−1.502	.200	−1.352	.220	−1.365
.200	−.883	.200	−1.346	.300	−1.324	.300	−.965
.250	−.811	.300	−.959	.400	−.546	.400	−.477
.300	−.729	.400	−.482	.450	−.377	.450	−.318
.400	−.518	.500	−.375	.500	−.350	.500	−.282
.500	−.423	.550	−.365	.550	−.323	.550	−.306
.550	−.401	.600	−.366	.600	−.281	.600	−.312
.600	−.351	.650	−.348	.650	−.309	.650	−.310
.650	−.373	.700	−.348	.700	−.341	.700	−.437
.700	−.315	.750	−.262	.740	−.272	.750	−.324
.750	−.358	.800	−.262				
.850	−.174	.850	−.183				
.900	−.105	.900	−.145				
.984	−.059	1.000	.042				

Lower surface

X/C	CP	X/C	CP	X/C	CP	X/C	CP
$\eta = 0.25$		$\eta = 0.47$		$\eta = 0.64$		$\eta = 0.78$	
.075	.201	.075	.045	.075	−.046	.075	−.081
.125	.173	.125	.036	.125	−.072	.125	−.177
.175	.107	.175	−.131	.225	−.261	.225	−.279
.225	.039	.225	−.176	.325	−.308	.325	−.275
.325	−.066	.325	−.181	.425	−.298	.425	−.390
.425	−.271	.425	−.360	.525	−.421	.525	−.369
.525	−.384	.525	−.390	.575	−.544	.575	−.376
.575	−.480	.575	−.474	.675	−.284	.675	−.186
.625	−.572	.625	−.513	.725	−.206		
.675	−.505	.725	−.184				
.725	−.420	.775	−.053				
.775	−.296	.825	.060				
.825	−.177	.875	.149				
.875	−.058	.975	.209				
.975	.037						

Table F-3

MINF =	.853
HP=	40492
PSINF =	382.5
PRI =	360.7
QBAR =	195.0
ALPHA =	4.7

Upper surface

X/C	CP	X/C	CP	X/C	CP	X/C	CP
η = 0.25		η = 0.47		η = 0.64		η = 0.78	
.025	−.589	.040	−.919	.050	−.992	.050	−1.212
.120	−.824	.140	−1.205	.200	−1.117	.220	−1.110
.200	−.793	.200	−1.108	.300	−1.163	.300	−1.218
.250	−.745	.300	−1.150	.400	−1.102	.400	−1.064
.300	−.691	.400	−.764	.450	−1.076	.450	−1.052
.400	−.713	.500	−.767	.500	−.949	.500	−.681
.500	−.720	.550	−.760	.550	−.649	.550	−.596
.550	−.689	.600	−.646	.600	−.378	.600	−.476
.600	−.629	.650	−.320	.650	−.251	.650	−.253
.650	−.388	.700	−.320	.700	−.219	.700	−.210
.700	−.286	.750	−.213	.740	−.170	.750	−.175
.750	−.315	.800	−.213				
.850	−.198	.850	−.144				
.900	−.158	.900	−.092				
.984	−.042	1.000	.063				

Lower surface

X/C	CP	X/C	CP	X/C	CP	X/C	CP
η = 0.25		η = 0.47		η = 0.64		η = 0.78	
.075	.176	.075	−.042	.075	−.155	.075	−.212
.125	.143	.125	−.027	.125	−.150	.125	−.300
.175	.060	.175	−.202	.225	−.365	.225	−.395
.225	.034	.225	−.232	.325	−.378	.325	−.344
.325	−.176	.325	−.220	.425	−.330	.425	−.522
.425	−.174	.425	−.488	.525	−.510	.525	−.635
.525	−.515	.525	−.423	.575	−.690	.575	−.402
.575	−.491	.575	−.453	.675	−.305	.675	−.212
.625	−.489	.625	−.633	.725	−.197		
.675	−.511	.725	−.212				
.725	−.455	.775	−.119				
.775	−.495	.825	−.036				
.825	−.290	.875	.033				
.875	−.086	.975	.155				
.975	.007						

APPENDIX G
INTEGRATED SECTION QUANTITIES, c_n and c_m, PYLONS ON, HP ≈ 20,000 FT

			C_n	C_m	C_n	C_m	C_n	C_m	C_n	C_m
M	α, deg	Run no.	η = 0.25		η = 0.47		η = 0.64		η = 0.78	
0.456	8.8	65T16	0.387	0.005	0.501	−0.047	0.432	−0.012	0.459	−0.034
0.504	8.2	65T1	0.357	0.007	0.469	−0.046	0.398	−0.011	0.408	−0.031
0.640	5.1	65T2	0.244	0.011	0.307	−0.036	0.204	−0.004	0.207	−0.022
0.747	3.3	66T14	0.173	0.016	0.210	−0.028	0.073	0.002	0.090	−0.023
0.800	2.7	66T15	0.155	0.021	0.162	−0.023	0.060	0.010	0.088	−0.022
0.803	2.9	65T3	0.162	0.024	0.183	−0.019	0.077	0.009	0.135	−0.023
0.805	2.7	65T15	0.156	0.027	0.168	−0.020	0.071	0.006	0.130	−0.030
0.842	2.3	65T13	0.154	0.027	0.124	0.008	0.034	0.018	0.112	−0.035
0.859	2.2	65T4	0.129	0.031	0.127	0.018	0.044	0.016	0.155	−0.042

APPENDIX II

INTEGRATED SECTION QUANTITIES, c_n and c_m, PYLONS ON, HP ≈ 30,000 FT

			C_n	C_m	C_n	C_m	C_n	C_m	C_n	C_m
M	α, deg	Run no.	$\eta = 0.25$		$\eta = 0.47$		$\eta = 0.64$		$\eta = 0.78$	
0.642	7.0	66T8	0.334	0.000	0.437	−0.030	0.375	0.014	0.337	−0.015
0.747	5.0	66T12	0.255	0.008	0.315	−0.027	0.211	0.013	0.265	−0.006
0.796	4.2	66T9	0.239	0.016	0.280	−0.017	0.185	0.016	0.186	−0.013
0.841	5.2	66T11T	0.348	0.012	0.446	−0.019	0.318	0.019	0.393	−0.008
0.843	3.4	66T11	0.225	0.020	0.230	0.002	0.103	0.029	0.206	−0.018
0.874	4.0	66T10MT	0.272	0.009	0.344	−0.013	0.278	−0.006	0.343	−0.041
0.876	3.5	66T10T	0.249	0.010	0.293	−0.007	0.235	−0.004	0.295	−0.034
0.877	2.7	66T10	0.207	0.012	0.224	−0.001	0.160	−0.002	0.209	−0.023

APPENDIX I
INTEGRATED SECTION QUANTITIES, c_n and c_m, PYLONS ON, HP ≈ 40,000 FT

			C_n	C_m	C_n	C_m	C_n	C_m	C_n	C_m
M	α, deg	Run no.	$\eta = 0.25$		$\eta = 0.47$		$\eta = 0.64$		$\eta = 0.78$	
0.754	7.6	66T5	0.401	0.016	0.530	−0.019	0.386	0.026	0.400	0.010
0.818	5.9	66T6	0.361	0.019	0.463	−0.011	0.348	0.030	0.372	0.010
0.843	5.2	66T7	0.345	0.012	0.440	−0.016	0.317	0.021	0.391	−0.008

APPENDIX J
INTEGRATED SECTION QUANTITIES, c_n and c_m, PYLONS OFF, HP ≈ 20,000 FT

			C_n	C_m	C_n	C_m	C_n	C_m	C_n	C_m
M	α, deg	Run no.	η = 0.25		η = 0.47		η = 0.64		η = 0.78	
0.486	7.4	612T1	0.333	0.009	0.422	−0.038	0.393	−0.020	0.419	−0.039
0.495	8.1	610T1	0.337	0.016	0.429	−0.029	0.427	−0.020	0.460	−0.038
0.500	7.6	612T19F	0.344	0.008	0.430	−0.036	0.401	−0.020	0.434	−0.038
0.642	4.3	612T2	0.240	0.010	0.263	−0.031	0.211	−0.010	0.224	−0.028
0.647	4.7	610T2	0.222	0.018	0.254	−0.019	0.219	−0.007	0.235	−0.026
0.651	4.3	612T19E	0.242	0.008	0.266	−0.029	0.211	−0.009	0.237	−0.031
0.725	5.0	612T14	0.250	0.012	0.321	−0.022	0.277	−0.004	0.248	−0.030
0.742	3.3	610T14	0.163	0.026	0.193	−0.010	0.128	−0.003	0.143	−0.022
0.750	2.6	612T19D	0.176	0.013	0.193	−0.021	0.107	−0.008	0.116	−0.030
0.767	2.7	612T18	0.091	0.054	0.203	−0.021	0.130	−0.011	0.142	−0.030
0.799	2.4	69T15	0.142	0.023	0.154	−0.013	0.093	0.007	0.096	−0.014
0.799	2.7	610T3	0.147	0.029	0.144	−0.003	0.128	0.008	0.126	−0.018
0.800	1.9	612T19C	0.156	0.015	0.150	−0.019	0.075	−0.004	0.065	−0.029
0.801	4.8	612T3	0.269	0.022	0.352	−0.010	0.297	0.011	0.315	−0.013
0.820	5.2	612T13	0.274	0.021	0.299	−0.003	0.292	0.019	0.154	−0.015
0.845	1.9	69T13	0.147	0.025	0.153	−0.002	0.072	0.002	0.085	−0.015
0.848	2.0	610T13	0.148	0.029	0.141	0.007	0.087	0.007	0.084	−0.016
0.851	1.0	612T19B	0.119	0.019	0.087	−0.011	0.011	−0.005	0.012	−0.041
0.866	1.6	69T4	0.146	0.023	0.127	0.006	0.074	0.006	0.068	−0.018
0.866	1.7	610T4	0.153	0.024	0.131	0.013	0.073	0.008	0.096	−0.019
0.876	1.4	612T19A	0.139	0.025	0.144	−0.006	−0.020	−0.008	0.123	−0.030

APPENDIX K
INTEGRATED SECTION QUANTITIES, c_n and c_m, PYLONS OFF, HP ≈ 30,000 FT

			C_n	C_m	C_n	C_m	C_n	C_m	C_n	C_m
M	α, deg	Run no.	η = 0.25		η = 0.47		η = 0.64		η = 0.78	
0.630	10.5	610T8T	0.444	0.003	0.595	−0.028	0.586	0.011	0.582	−0.008
0.649	7.0	69T8	0.316	0.012	0.439	−0.020	0.436	−0.001	0.469	−0.019
0.650	6.3	610T8	0.281	0.014	0.373	−0.012	0.326	−0.003	0.329	−0.027
0.739	4.6	610T12	0.215	0.019	0.262	−0.011	0.246	0.006	0.285	−0.010
0.747	5.0	69T12	0.244	0.016	0.316	−0.019	0.269	0.003	0.327	−0.013
0.752	6.1	610T12T	0.290	0.021	0.383	−0.003	0.331	0.010	0.363	−0.008
0.793	7.1	611TT9	0.375	0.025	0.534	−0.002	0.498	0.015	0.508	0.010
0.800	3.7	611TP9	0.200	0.027	0.245	−0.004	0.164	0.010	0.212	−0.011
0.800	4.0	69T9	0.227	0.022	0.281	−0.009	0.205	0.012	0.221	−0.013
0.841	5.2	611TT11	0.325	0.020	0.428	0.000	0.390	0.011	0.412	0.004
0.845	3.1	611TP11	0.193	0.028	0.234	0.005	0.168	0.017	0.182	−0.003
0.847	3.3	69T11	0.216	0.024	0.256	0.002	0.181	0.018	0.212	−0.003
0.873	2.7	611TP10	0.205	0.020	0.248	−0.006	0.139	0.020	0.178	0.003
0.873	2.7	69T10	0.226	0.013	0.264	−0.009	0.168	0.011	0.198	−0.002
0.875	4.0	611TT10	0.295	0.008	0.387	−0.020	0.351	−0.010	0.358	−0.021

APPENDIX L

INTEGRATED SECTION QUANTITIES, c_n and c_m, PYLONS OFF, HP ≈ 40,000 FT

			C_n	C_m	C_n	C_m	C_n	C_m	C_n	C_m
M	α, deg	Run no.	$\eta = 0.25$		$\eta = 0.47$		$\eta = 0.64$		$\eta = 0.78$	
0.734	7.9	69T5	0.377	0.014	0.507	−0.023	0.450	0.013	0.472	0.001
0.799	6.1	69T6	0.329	0.021	0.450	−0.008	0.389	0.021	0.405	0.009
0.853	4.7	69T7	0.325	0.010	0.419	−0.012	0.371	0.006	0.374	0.003

REFERENCES

1. Taylor, John W.R., ed., "Jane's All The World's Aircraft," B.P.C. Publishing Limited, London, W.I., England, 1968–1969, pp. 178–180.
2. Taylor, John W.R. and Kenneth Munson, eds., "Jane's All The World's Aircraft," Jane's Yearbooks, Franklin Watts Inc., New York, NY,1979–1980, pp. 235–237 and 384–385.
3. Lacey, T.R. and K. Miller, "The AV-8B Wing: Aerodynamic Concept and Design," AIAA-77-607, V/STOL Conference, Palo Alto, CA, June 6–8, 1977.
4. Berger, Roger L., James S. Crupper, and Donald L. Mosier, *Engineering and Technical Support for the NASA YAV-8B Research Aircraft*, NASA CR-166527, 1984.
5. McDonnell Douglas Corporation, *YAV-8B Simulation and Modeling, Vol. I: Aircraft Description and Program Summary*, NASA CR-170397, 1983.
6. Montoya, Lawrence C. and David P. Lux, *Comparisons of Wing Pressure Distribution From Flight Tests of Flush and External Orifices for Mach Numbers From 0.50 to 0.97*, NASA TM X-56032, 1975.
7. Gracey, William, *Measurement of Aircraft Speed and Altitude*, NASA RP-1046, 1980.
8. Crowder, James P. and Paul E. Robertson, "Flow Cones for Flight Test Flow Visualization," Flow Visualization III, edited by W.J. Yang, Proceedings of the Third International Symposium on Flow Visualization, University of Michigan, Ann Arbor, MI, Sept. 6–9, 1983, pp. 60–64.
9. Staff of NASA Flight Research Center, *Supercritical Wing Technology, A Progress Report on Flight Evaluations*, Supercritical Wing Symposium proceedings, NASA Flight Research Center, Edwards, CA, NASA SP-301, 1972.
10. Lock, R.C. and J.L. Fulker, "Design of Supercritical Aerofoils," *Aeronautical Quarterly*, Vol. 25, Royal Aircraft Establishment, Farnborough, England, Nov. 1974, pp. 245–265.
11. McDonnell Douglas Corporation, "YAV-8B, 15% Scale Powered Aerodynamic Test in the NASA-Ames 14 Foot (ARC) Transonic Wind Tunnel," Vol. I, Report MDC A5138, Mar. 1978.
12. McDonnell Douglas Corporation, "AV-8B/GR Mk.5, 15% Scale Model AV-8B/GR Mk.5 Aerodynamic and Loads Test in the ARA 9 Foot x 8 Foot Transonic Wind Tunnel," Report MDC A7540, May 1982.
13. Diederich, Franklin W., *A Plan-Form Parameter for Correlating Certain Aerodynamic Characteristics of Swept Wings*, NACA TN-2335, 1951.
14. Hoerner, Sighard F. and Henry V. Borst, "Fluid-Dynamic Lift," published by Mrs. Liselotte A. Hoerner, Brick Town, NJ, 1975.
15. Moes, Timothy R. and Robert R. Meyer, Jr., *In-Flight Wing Pressure Distributions for the F-14A Aircraft*, NASA TM-85921, 1985.

REPORT DOCUMENTATION PAGE

Form Approved
OMB No. 0704-0188

1. AGENCY USE ONLY *(Leave blank)*

2. REPORT DATE
November 1992

3. REPORT TYPE AND DATES COVERED
Technical Memorandum

4. TITLE AND SUBTITLE
Pressure Distribution for the Wing of the YAV-8B Airplane; With and Without Pylons

5. FUNDING NUMBERS
RTOP 505-59-53

6. AUTHOR(S)
Edwin J. Saltzman, John H. Del Frate, Catherine M. Sabsay, and Jill M. Yarger

7. PERFORMING ORGANIZATION NAME(S) AND ADDRESS(ES)
NASA Dryden Flight Research Facility
P.O. Box 273
Edwards, CA 93523-0273

8. PERFORMING ORGANIZATION REPORT NUMBER
H-1708

9. SPONSORING/MONITORING AGENCY NAME(S) AND ADDRESS(ES)
National Aeronautics and Space Administration
Washington, DC 20546-0001

10. SPONSORING/MONITORING AGENCY REPORT NUMBER
NASA TM-4429

11. SUPPLEMENTARY NOTES
Edwin J. Saltzman: PRC Inc., Edwards, CA; John H. Del Frate, Catherine M. Sabsay, and Jill M. Yarger: NASA Dryden Flight Research Facility, Edwards, CA.

12a. DISTRIBUTION/AVAILABILITY STATEMENT
Unclassified — Unlimited
Subject Category 02

12b. DISTRIBUTION CODE

13. ABSTRACT *(Maximum 200 words)*

Pressure distribution data have been obtained in flight at four span stations on the wing panel of the YAV-8B airplane. Data obtained for the supercritical profiled wing, with and without pylons installed, ranged from Mach 0.46 to 0.88. The altitude ranged from approximately 20,000 to 40,000 ft and the resultant Reynolds numbers varied from approximately 7.2 million to 28.7 million based on the mean aerodynamic chord.

Pressure distribution data and flow visualization results show that the full-scale flight wing performance is compromised because the lower surface cusp region experiences flow separation for some important transonic flight conditions. This condition is aggravated when local shocks occur on the lower surface of the wing (mostly between 20- and 35-percent chord) when the pylons are installed for Mach 0.8 and above. There is evidence that convex fairings, which cover the pylon attachment flanges, cause these local shocks. Pressure coefficients significantly more negative than those for sonic flow also occur farther aft on the lower surface (near 60-percent chord) whether or not the pylons are installed for Mach numbers 0.8. These negative pressure coefficient peaks and associated local shocks would be expected to cause increasing wave and separation drag as transonic Mach number increases.

14. SUBJECT TERMS
Supercritical wing aerodynamics; Wing pressure distribution; Wing–pylon interaction; YAV-8B

15. NUMBER OF PAGES
140

16. PRICE CODE
A07

17. SECURITY CLASSIFICATION OF REPORT	18. SECURITY CLASSIFICATION OF THIS PAGE	19. SECURITY CLASSIFICATION OF ABSTRACT	20. LIMITATION OF ABSTRACT
Unclassified	Unclassified	Unclassified	Unlimited